UNIVERSIDADE FEDERAL DO RIO GRANDE DO NORTE
CENTRO DE TECNOLOGIA (CT)
CENTRO DE CIÊNCIAS EXATAS E DA TERRA (CCET)

PROGRAMA DE PÓS-GRADUAÇÃO EM CIÊNCIA E ENGENHARIA DE MATERIAIS

MASTER THESIS

Study of the addition of poly(ethylene-co-methyl acrylate-co-glycidyl methacrylate) thermoplastic to epoxy resin for use in self-healing composites

Érick Stéfano Silveira Guerra

Academic Advisor:
Prof. Dr. Ana Paula Cysne Barbosa
Academic Co-Advisor:
Prof. Dr. José Daniel Diniz Melo

Dissertation number _____ /PPGCEM

2017 April
Natal – RN – Brazil

ÉRICK STÉFANO SILVEIRA GUERRA

STUDY OF THE ADDITION OF POLY(ETHYLENE-CO-METHYL ACRYLATE-CO-GLYCIDYL METHACRYLATE) THERMOPLASTIC TO EPOXY RESIN FOR USE IN SELF-HEALING COMPOSITES

Master thesis presented to the Federal University of Rio Grande do Norte, in partial fulfillment of the requirements for the Degree of Master of Science in Materials Science and Engineering.

Academic Advisor:
Prof. Dr. Ana Paula Cysne Barbosa

_____

Academic co-Advisor:
Prof. Dr. José Daniel Diniz Melo

_____

2017 April
Natal – RN – Brazil

Dedicatory

To my grandmother,

Maria Pompeia.

Universidade Federal do Rio Grande do Norte – UFRN
Sistema de Bibliotecas – SISBI
Catalogação da Publicação na Fonte - Biblioteca Central Zila Mamede

Guerra, Erick Stefano Silveira.
Study of the addition of poly(ethylene-co-methyl acrylate-co-glycidyl methacrylate) thermoplastic to epoxy resin for use in self-healing composites / Erick Stefano Silveira Guerra. - 2017.
96 f. : il.

Dissertação (mestrado) - Universidade Federal do Rio Grande do Norte, Centro de Ciências Exatas e da Terra, Programa de Pós-Graduação em Ciência e Engenharia de Materiais. Natal. RN, 2017.
Orientadora: Prof.ª Dr.ª Ana Paula Cysne Barbosa.
Coorientador: José Daniel Diniz Melo.

1. Materiais compósitos - Dissertação. 2.Auto-reparo - Dissertação. 3. Termoplástico-termofixo - Dissertação. I. Barbosa, Ana Paula Cysne. II. Melo, José Daniel Diniz. III. Título.

RN/UFRN/BCZM CDU 620.1

Acknowledgments

I would like to thank my academic advisor, professor Ana Paula Cysne Barbosa, for her support, outstanding dedication and comprehension on obstacles I have faced through my research process.

I also would like to thank my academic co-advisor, professor José Daniel Diniz Melo for the experienced advice, which guided me in the realization of this work.

I would like to thank to all academic crew from Laboratory of Composites, especially Professor Maria Carolina and Professor Evans Paiva, who assisted discussing and advising me during all the crucial parts on the construction of this work.

I also would to thank all the partner students from Laboratory of Composites, especially Natalia Praxedes, who effortlessly helped me in the conduction of the experiments realized in this work, and the PhD students Ana Paula Fulco and Ana Cláudia Medeiros, whose daily instructions were fundamental on the realization of this study.

I would like to thank the Embraer engineers Fernando Fernandes and Fábio Silva for the helpful and providential discussions.

I would like to thank Coordenação de Aperfeiçoamento de Pessoal de Nível Superior – CAPES, for the financial support on the realization of this study.

I would like to thank all my colleagues, professors and technician crew of PPgCEM, especially professor Edson Noriyuki Ito, who truly helped me on the realization of atomic force microscope characterization, and the technicians José Roberto and Igor Zumba for the readiness on the realization of other crucial characterizations.

I would like to thank my friends and family for supporting me spiritually throughout the process of writing this thesis and in my life in general.

ABSTRACT

Repair of damaged composite structural elements to restore pristine conditions and meet regulatory requirements can be a great challenge. Thus, materials capable of self-healing when damaged are of great interest. In one of the self-healing approaches studied in the literature, thermoplastic is added to a thermosetting matrix and the damaged material partially recovers its mechanical properties after a healing cycle. This technique employs heat to trigger the healing process and partially re-establish the mechanical properties of the composite material. In the present study, poly(ethylene-co-methyl acrylate-co-glycidyl methacrylate) (E-MA-GMA) thermoplastic was added to epoxy matrix and evaluated as a self-healing agent. The influence of the type of hardener employed (anhydride or amine) on the properties of the material was also investigated. Dynamic mechanical thermal analysis (DMTA) was performed to evaluate changes in viscoelastic properties due to the addition of thermoplastic. Fourier transform infrared (FTIR) spectroscopy was used to evaluate chemical alterations in thermoplastic-epoxy systems. Atomic force microscopy (AFM) was employed to examine the role of thermoplastic addition on epoxy network structure. Healing ability was assessed by comparison of areas damaged by indentations on the surface of samples before and after a healing cycle for materials with and without E-MA-GMA addition. Results suggest the presence of a E-MA-GMA second phase after curing, an increase in glass transition temperature (Tg) for all thermoplastic blended samples as compared to neat epoxy, the presence of one single Tg for epoxy anhydride hardened E-MA-GMA mixtures and chemical and structural alterations on the epoxy network due to addition of E-MA-GMA. Further, the elimination of visible damage areas of the material modified with thermoplastic after a heating cycle supports the potential use of E-MA-GMA as healing agent.

Key words: self-healing, thermoplastic-thermoset, DMTA, FTIR, AFM.

RESUMO

O reparo de estruturas compósitas danificadas a fim de recuperar condições iniciais e atender requisitos regulatórios pode ser um grande desafio. Assim, materiais capazes de se auto-reparar quando danificados são de grande interesse. Em uma das abordagens de auto-reparo estudada na literatura, um material termoplástico é adicionado à matriz termofixa e o material danificado é capaz de parcialmente recuperar suas propriedades mecânicas depois de um ciclo de reparo. Essa técnica usa calor para reestabelecer parcialmente as propriedades mecânicas do material compósito. No presente estudo, a modificação de resina epóxi com a adição de poli(etileno-co-metil acrilato-co-glicidil metacrilato) (E-MA-GMA) foi avaliada. A influência do tipo de endurecedor (anidrido e amina) empregado nas propriedades do material também foi investigada. Análises dinâmico-mecânicas (DMA) foram realizadas para averiguar mudanças nas propriedades viscoelásticas devido a adição do termoplástico. Mudanças químicas nas misturas termoplástico-epóxi foram avaliadas por espectroscopia de infravermelho por transformada de Fourier (FTIR). Microscopia de força atômica (AFM) foi empregada para examinar o papel da adição de termoplástico na estrutura da rede do epóxi.

A habilidade de reparo foi avaliada comparando áreas danificadas por uma indentação padrão na superfície das amostras antes e depois do ciclo de reparo para amostras com e sem a adição de E-MA-GMA. Os resultados sugerem a presença de uma segunda fase de E-MA-GMA após a cura, um aumento na temperatura de transição vítrea (Tg) para todas as misturas com termoplástico quando comparadas à epóxi pura, a presença de uma única Tg para misturas E-MA-GMA-epóxi curadas com anidrido e mudanças químicas e estruturais na rede epóxi devido à adição de E-MA-GMA. Além disso, o desaparecimento de danos causados por indentações em áreas do material modificado com o termoplástico depois do ciclo de aquecimento confirmam o potencial no uso de E-MA-GMA como agente de reparo.

Palavras-chave: auto-reparo, termoplástico-termofixo, DMA, FTIR, AFM.

List of Figures

List of Tables

List of abbreviations

ABS – Acrylonitrile butadiene styrene copolymer

AFM – Atomic force microscopy

BDMA – Benzyl dimethylamine

DCB – Double cantilever beam

DDS – Diaminodiphenylsulfone

DEB – Differential expansive bleeding

DETDA – Diethyltoluenediamine

DGEBA – Diglycidyl ether of bisphenol-A

DMTA – Dynamic mechanical thermal analysis

DSC – Differential scanning calorimetry

E-GMA – Poly(ethylene-co-glycidyl methacrylate)

E-MA – Poly(ethylene-co-methyl acrylate)

E-MAA – Poly(ethylene-co-methacrylic acid)

E-MA-GMA – Poly(ethylene-co-methyl acrylate-co-glycidyl methacrylate)

EVA – ethylene vinyl acetate copolymer

FTIR – Fourier transform infrared

ILSS – Interlaminar shear strength

MTHPA – Methyl tetrahydrophthalic anhydride

NMA – Nadic methylene anhydride

PBE – Poly(bisphenol-A-co-epichlorohydrin)

PBT – Poly(butylene terephthalate)

PCL – Poly(ε-caprolactone)

PIPS – Polymerization-induced phase separation

PMC – Polymer matrix composite

POM – Polarized optical microscopy

PVB – Poly(vynil-butyral)

SEBS - Styrene ethylene butadiene styrene copolymer

SENB – Single edge notched beam

SEM – Scanning electron microscopy

Tg – Glass transition temperature

Table of contents

1 Introduction

Composite materials are composed of two or more different materials that act synergistically allying properties of each constituent individually. For this reason, it is widely known that composite materials are an excellent alternative to other classes of monolithic materials [1-7]. Moreover, when reinforced with fibers, composite materials often exhibit high mechanical properties and low density, which are attractive qualities for more fuel-efficient devices [1-7].

Polymers are undoubtedly the most broadly material used as matrices in composite materials. Further, inexpensive costs, good processability and low-density, among other relevant advantages, make thermosetting polymers the most useful matrix constituent in the design for structural applications [1-7].

However, this class of materials also presents some limitations. Low thermal stability, for instance, does not allow these materials to be used at high temperatures [1-7]. Other serious drawback consists on the low interlaminar fracture toughness and impact resistance due to low ductility and strength of thermoset polymer matrices [8-9]. This may lead composite materials to delamination or matrix cracks. Other factors such as continuous fatigue loads and environmental aging may also contribute to the formation of those cracks, which can affect both fiber and matrix dominated properties of composites.

Traditional repair techniques of composite materials include patches of plies or, depending on the level of damage, removal of the damaged region and surrounding material, followed by replacement with new material [14]. However, these conventional repair methods are not effective for healing invisible microcracks. In this context, special attention is given to materials capable of self-repair, evidenced by the increase number of researches conducted in the area.

Currently, there are several techniques of self-healing for composite materials, which may be divided into extrinsic or intrinsic groups [18]. Extrinsic techniques utilize reservoirs of a chemically active agent placed into the material that, once broken, release contents that fulfill the crack surface and subsequently solidify it. Finally, the crack surface is shut and the mechanical properties of the composite are partially restored. On the other hand, intrinsic techniques cover the use of modified resin systems, in which the polymer itself has mechanisms of self-

repair, whether by formation of new covalent bonds (thermally reversible reactions) or by re-mending throughout non-covalent bonds.

One of these intrinsic techniques is the use of modified thermosetting matrices in which portions of thermoplastic polymers are utilized as healing agents [18]. This technique employs heat to partially re-establish the mechanical properties of the composite material. When heated above the melting temperature, the thermoplastic gains mobility and is allowed to migrate and fill in the open cracks. Once the thermoplastic is solidified, the crack is closed and the composite recovers part of its mechanical properties.

Depending on the employed thermoplastic, three different mechanisms of self-healing may occur: (i) viscous flow mechanism [25], where embedded particles of thermoplastic are heated above its melting point and flow in order to fill nearby open cracks; (ii) molecular dissolution mechanism [13], where the thermoplastic is dissolved within the matrix and then migrates when heated up and; (iii) thermal interactions mechanism [29,31] in which a thermoplastic healing agent reacts with the matrix in some level and triggers different manners to fill in the fractured surface.

For this study, thermosetting epoxy modified matrices with the copolymer poly(ethylene-co-methyl acrylate-co-glycidyl methacrylate) (E-MA-GMA) were evaluated. This material has never been employed as thermoplastic additive for self-healing purposes before. However, as previously reported in literature, other glycidyl methacrylate copolymer, poly(ethylene-co-glycidyl methacrylate) (E-GMA) [32,34,35], which chemical structure is very similar to E-MA-GMA, has also exhibited healing capabilities.

The goal of this work is to study the effects of the addition of E-MA-GMA to epoxy resin, in order to evaluate this thermoplastic material as a healing agent in polymer matrix composites. The influence of the addition of the thermoplastic on thermo-mechanical, chemical and microstructural properties of epoxy was evaluated. Finally, the healing effect was assessed by comparing changes on areas of damaged surfaces before and after a healing cycle.

2 Literature Review

2.1 Self-healing in Polymer Matrix Composites (PMCs)

The definition of composite materials is not yet a consensus in academia. For most authors, a composite material consists of two or more separated materials, which are combined within a structural unity in a macroscopic level [1] – excluding from this concept metal alloys and polymer blends. However, in general, composite materials are defined as those materials in which two or more materials (or phases) with distinct chemical and physical nature are arranged together to create an unique material whose properties are different from the properties of the originals in separate [1–5]. Other definitions also suggest that composites are made up of at least two components not soluble in each other that act synergistically in order to obtain improved properties as compared to its constituents individually [2,3]. Another criterion of definition lies on the ratio of a component present in the composite material, which should be greater than 5% [6]. As a result, commercial plastics, for example, although they normally have small quantities of additives (as lubricants and ultra-violet absorbers), do not satisfy this condition and consequently are not classified as composite materials.

Composite materials are multiphase systems constituted by matrix and reinforcing phases. The matrix phase is continuous and surrounds the reinforcement [1–6]. On the other hand, the reinforcing phase, or just reinforcement, enhances suitable properties of the matrix.

Polymers are undoubtedly the most broadly material used as matrices in composite materials [1–7]. Moreover, thermoset polymers present superior properties as high modulus, high fracture strength and solvent resistance if compared to thermoplastics due to its highly cross-linked network. These properties justify the use of thermoset polymers as the major class of materials in composite matrices [1–7]. Still, mechanical properties of polymers are typically inadequate for many structural applications. Its Young's modulus and strength are too low if compared to metals or ceramics. For this reason, reinforcing polymer matrices is important, once they do not have exceptional mechanical properties. Furthermore, the following reasons can be cited to support the use of polymers as matrices [5,7]:

- Processing facility, since usually there is no need for high temperatures and pressures;
- Simple fabrication equipments, in general;
- Low density;
- More researches on development and improvement technologies;
- High availability in the market and relatively lower costs;
- Great diversity of mechanical behaviors, ranging among rigid, ductile and rubbery;
- Good chemical stability.

As a consequence, polymer matrix composites (PMCs) have been playing important role in structural components in high technology industries, such as aerospace, military, wind energy, high performance sports goods and transport vehicles [1–7].

Nevertheless, PMCs have also some limitations. One of the these problems is its low thermal stability [6], as they cannot withstand temperatures higher than 300˚C without significant loss of properties or even degradation. Other problematic issues are concerned to its long-term durability, as polymer matrices undergo thermo-oxidative degradation when exposed to service conditions [8–10]. Further, due to its brittle behavior, PMCs are highly susceptible to the appearance of matrix microcracks when exposed to impact, mechanical stresses and/or thermal cycles [11–14].

> "*Microcracks also instigate other forms of damage through coalescence, including fiber/matrix de-bond, ply delamination, and fiber break, or provide pathways for entry of corrosive liquids*" [14].

Under these conditions, such materials can be irreversibly damaged due to the formation and propagation of cracks, where detection and external intervention are difficult or even impossible of being held [15–18]. Conventional repair methods are not effective for healing invisible microcracks within the structure during service life. As a result, PMCs still face considerable constraints regarding to its reliability. In this context, special attention has been given to materials capable of self-repair, to

address the problem of rehabilitation of PMCs as shown in the increasing number of researches on polymer and polymer composites with self-healing properties in the last ten years (Figure 2. 1).

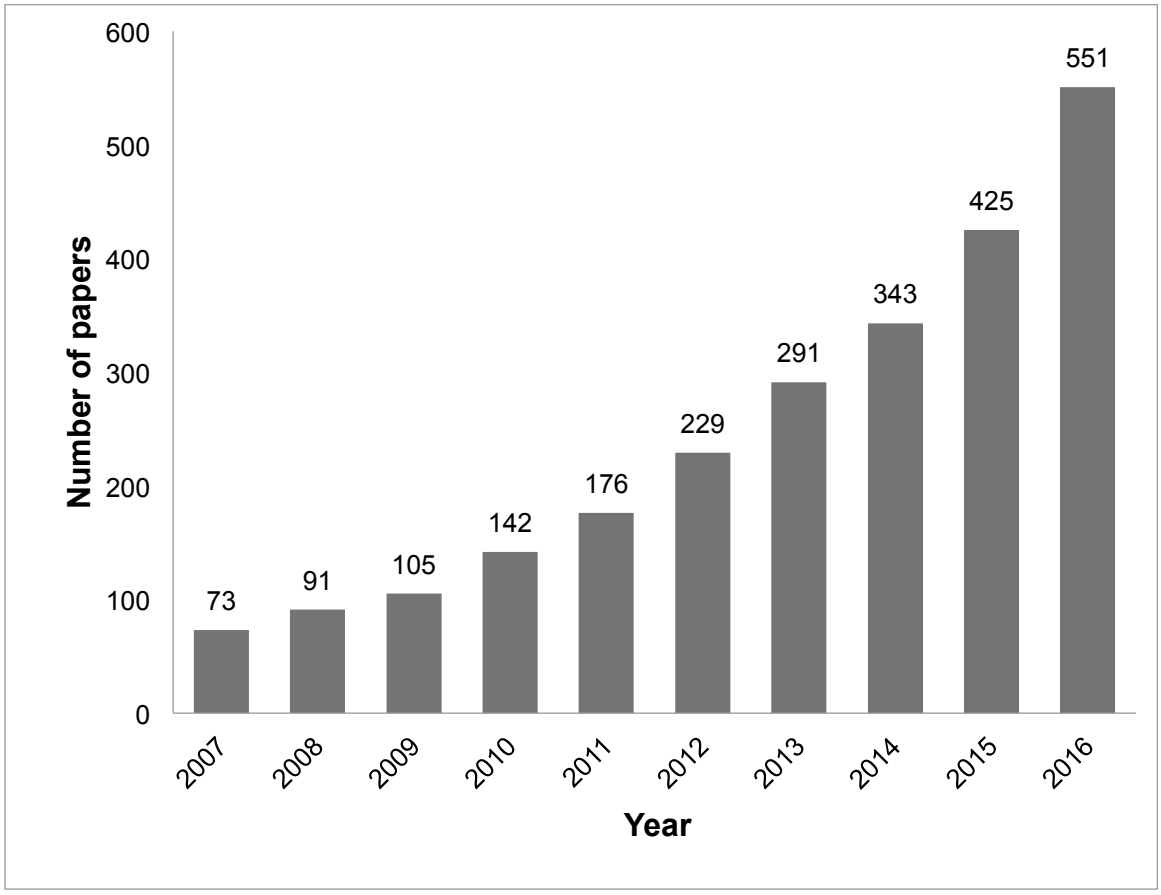

Figure 2. 1 – Number of research papers containing the topics "self-healing polymers" or "self-healing composites" according to the database Web of Science in the period from 2007 to 2016.

The preconceptions of the self-healing materials have firstly appeared based on biological mimetic processes [11,19,20]. In this regard, a damage inflicted on the skin, for example, initiates a complex path of chemical reactions that culminates in the creation of a fibrin clot, which subsequently will trigger others reactions, usually called fibrin polymerization [15,17,21] , resulting in a new structure that will as much close the wound in the skin as eventually reconstruct the damaged area. While this sequence of events practically describes the healing process in humans, it is not to be completely reproduced in the design of healing mechanisms for synthetic materials. Therefore, inspired by this concept, researchers have begun to integrate aspects of biological healing into synthetic materials, proposing the creation of the

term “self-healing” materials in the 1970’s [19]. Table 2. 1 summarizes the biomimetic self-healing inspiration in advanced composites.

Table 2. 1 - Biomimetic self-healing inspiration in advanced composites [11].

Biological attribute	Composite/polymer engineering	Biomimetic self-healing or repair strategy
‘Concept of self-healing’	Remendable polymers	Bioinspired healing requiring external intervention to initiate repair
Bleeding	Capsules	Action of bleeding from a storage medium housed within the structure. 2-phase polymeric cure process rather than enzyme ‘waterfall’ reaction
Bleeding	Hollow fibres	Action of bleeding from a storage medium housed within the structure. 2-phase polymeric cure process rather than enzyme ‘waterfall’ reaction
Blood cells	Nano-particles	Artificial cells that deposit nano-particles into regions of damage
Blood flow vascular network	Hollow fibres	2D or 3D network would permit the healing agent to be replenished and renewed during the life of the structure
Blood clotting	Healing resin	Synthetic self-healing resin systems designed to clot locally to the damage site. Remote from the damage site clotting is inhibited and the network remains flowing.
Skeleton/bone healing	Reinforcing fibres	Deposition, resorption, and remodelling of fractured reinforcing fibres
Elastic/plastic behaviour in reinforcing fibres	Reinforcing fibres	Repair strategy, similar to byssal thread, where repeated breaking and reforming of sacrificial bonds ca occur for multiple loading cycles
Tree bark healing – compartmentalization	–	Formation of internal impervious boundary walls to protect the damaged structure from environmental attack

> “*Conceptually, self-healing polymeric materials have the built-in capability to substantially recover their load transferring ability after damage. Such recovery can occur autonomously or be activated after an application of a specific stimulus (e.g. heat, radiation)*” [20].

Therefore, according to the way of repair self-healing, PMCs may be classified as **autonomic**, which does not need any intervention to occur; or **non-autonomic**, which needs intervention to trigger the healing ability [17].

Nevertheless, self-healing PMCs may also be classified into **extrinsic** and **intrinsic**. Thus,

> *"Intrinsic self-healing are those where the chemistry of the material is designed to direct the mechanical energy from the damage to latent functionalities that lead to healing without the need for external materials, while extrinsic self-healing, where the healing chemicals are separated from the matrix and delivered upon damage"* [21].

The extrinsic approach, also called as "sequestered" [18,19], utilizes reservoirs of a chemically active agent placed into the material. Once damage, such as microcracks, reaches and breaks these reservoirs the content is released, fulfilling the created voids activating consequently the healing agent. The healing agent will then bridge the two halves repairing the damage. The extrinsic approach embodies the vascular (hollow fibers) and microcapsule based self-healing agent, which are schematically shown in Figure 2. 2 (a) and (b), respectively.

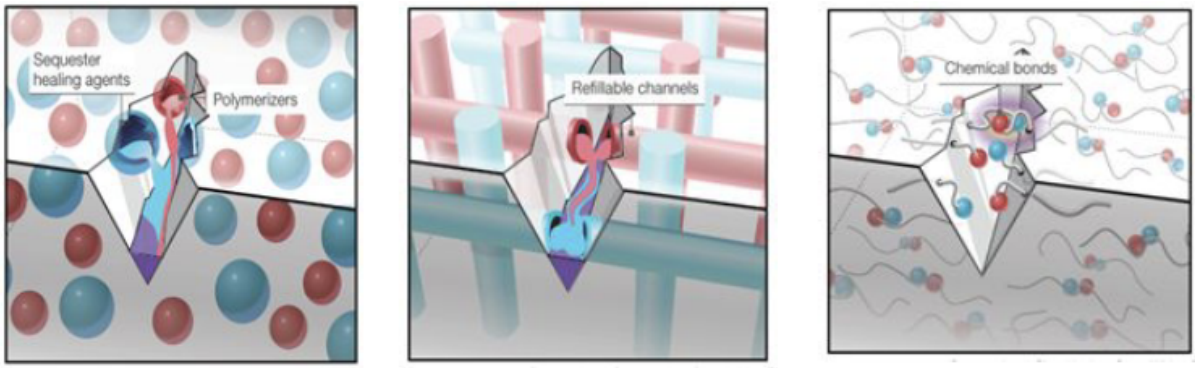

Figure 2. 2 – Schematics showing the main approaches of self-healing technology in PMCs: (a) microencapsulated healing system; (b) vascular healing system and; (c) intrinsic healing system [14].

Intrinsic self-healing systems (Figure 2. 2 (c)) do not present a partitioned healing agent but carry itself a self-healing mechanism which can be autonomously activated by a damage or non-autonomously triggered by an external stimulus.

> *"Intrinsic self-healing materials rely on chain mobility and entanglement, reversible polymerizations, melting of thermoplastic*

phases, hydrogen bonding, or ionic interactions to start with the self-healing process. Because each of these reactions is reversible, multiple healing events are possible" [14].

The present study will focus on the use of thermoplastic additives as healing agents to PMCs, which is classified into an intrinsic self-healing approach as much as a non-autonomous healing process.

2.2 Self-healing in PMCs using thermoplastic additives

The use of thermoplastic additives in PMCs as healing agents shows relevant advantages over others approaches. The incorporation of resin-filled hollow fibers, for example, may undergo problems of filling and sealing of fibers in practice [22]. The use of microencapsulated healing agents into a composite structure may also be difficult, since the dimension of the microcapsules will distort the fiber architecture [22]. The most problematic issue, however, presented by extrinsic techniques is the inability of repeated healing cycles, once it is not possible to predict when the liquid healing agents will be completely consumed [18,22,23]. Another potential factors such as high costs healing agents, difficult processing conditions due to required fragility of the containers of healing agent and short in-use lifespan present relevant constraints to the application of these self-healing approaches [18,22,23].

Regarding the intrinsic technique of thermally reversible approach, in spite of being a monolithic material and the fact that the matrix can be repeatedly healed, this technique will require completely new matrix systems and processing technologies, which may be challenging [22]. Besides, it has also to be proved that these new matrix systems have similar mechanical properties in order to replace the current matrix systems used in industry.

Hence, considering the disadvantages mentioned, the mechanism of self-healing with addition of thermoplastics is a promising approach. The use of thermoplastic modifiers in cross-linked matrices (specially in epoxy networks) is an intrinsic healing mechanism, which permits latent repeatability of healing multiple times once stimulus is applied [15,20]. In this approach, a thermoplastic solid-state healing agent is incorporated into a thermosetting matrix system. Besides, "this

thermoplastic healing agent may prove to be an attractive alternative to the more traditional healing agents as it is relatively inexpensive and does not require the encapsulation/infiltration processing stages that are currently used to produce many of the existing self-healing epoxy resins" [24].

In general, the basic mechanism of the inclusion of thermoplastics consists on a thermoset matrix in which a thermo-sensitive polymer is incorporated that at a stipulated temperature will migrate and fill eventual cracks, solidifying when the temperature is reestablished, then bridging the fracture surface as it is shown schematically in Figure 2. 3. In this case, the weak non-covalent bonds of thermoplastic within the matrix will break and reorganize upon heating, enabling the matrix to be repaired after damage [13,16]. Other criteria for selection of a thermoplastic are the low melt point, low glass transition temperature and low viscosity, so that it migrates to the cracks while the thermosetting matrix remains in the solid state, as well as good adhesion properties (such as hydrogen bonds) that will act bridging crack planes [16].

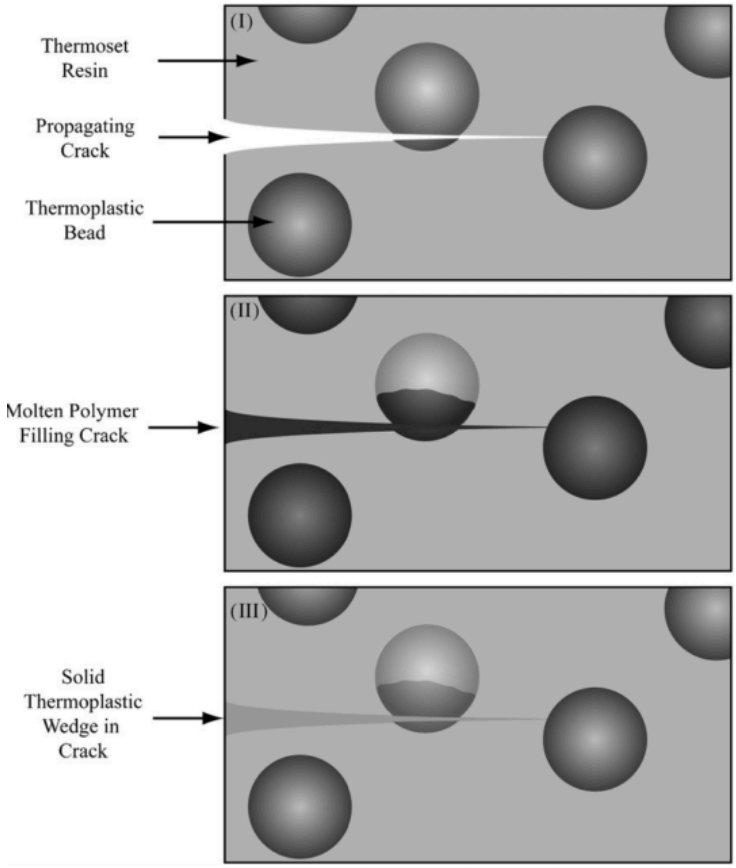

Figure 2. 3 - Representative schema of healing process using the addition of thermoplastic healing agent [20].

Depending on the thermoplastic used, three different mechanisms of self-healing can occur. The first self-healing mechanism was proposed by Zako and Tanako [25],who utilized the **viscous flow** of a polymer based material when heated above its melting point. Secondly, Hayes et al. [22,26,27] have proposed a **molecular dissolution** mechanism where the thermoplastic is dissolved within the matrix and then migrates when heated up. Later, other authors [24,28–31] have proposed the **thermal interactions** mechanism in which a thermoplastic healing agent reacts with the matrix and triggers different manners to fill in the fractured surface. Other authors [21,30,31] also suggest the concepts of **miscible** and **immiscible** blends of thermoplastic and thermosetting matrix. For this reason, distinct requirements of the polymer are necessary for each of these healing mechanisms, which are described in the following sections.

2.2.1 Viscous flow mechanism

A thermoplastic additive was first reported as self-healing agent by Zako and Takano [25] in 1999. In their work, a resin system was proposed in which micrometric particles of epoxy (with mean diameter of 109 μm) were embedded in the matrix. Two types of epoxy were utilized: the coldsetting (acting as the matrix) and the thermosetting (as the pre-polymer thermal melting particles embedded in the matrix). During all the manufacturing process, the epoxy pre-polymer remains as solid particles, while the coldsetting epoxy resin cross-links and finally cures. Once damages such as matrix cracks or delamination arise, the material is heated up and the pre-polymer particles melt and flow, filling the cracks. When the composite is cooled down the epoxy pre-polymer is cured, repairing the damage. Figure 2. 4 illustrates the schematic mechanism of healing on a $[0/90]_s$ laminated system according to this self-healing technique. Factors such as diameter of the particles to be embedded are important in the design and manufacturing of this material system, once the smaller the diameter of the particles, the more uniformly they can be dispersed in the matrix, and the less they affect the mechanical properties of the composite.

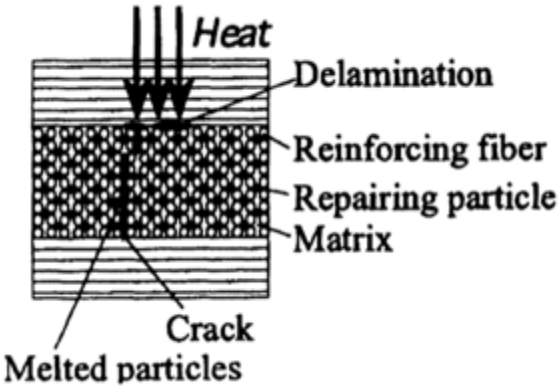

Figure 2. 4 - Schema of thermoplastic particles acting as healing agent in a composite laminate [25].

The melting point of the pre-polymer epoxy particles used in the cited work [25] was about to 110-140 ˚C. The matrix and particles were mixed while heated to 37-47 ˚C. Regarding to the quantity of healing agent particles in the matrix, Zako and Tanako suggest a maximum of 40% volume fraction for particles to be contained in the matrix. According to them, this percentage allows better productivity and minimum decrease of strength. In order to assess the healing effect on the polymer matrix, Zako and Tanako developed a test of mending two broken pieces of the matrix with thermosetting epoxy particles embedded. In this test, the two parts were put in contact with each other and heated up. After 5 minutes, the crack between the two parts disappeared, and indeed the two broken pieces were bonded to each other.

Mechanical tests were also used to evaluate the healing ability of this particle system [25]. Both tensile and three-point bending tests demonstrate that a 100% recovery of stiffness was reached when samples were heated up at 120˚C for 10 minutes.

Others works [32,33] also employed the viscous flow mechanism concept using different thermoplastic healing agents, once no chemical interaction were observed between matrix reactants and healing agents. Copolymers as ethylene vinyl acetate (EVA), acrylonitrile budatiene styrene (ABS), Poly(vynil-butyral) (PVB) and styrene ethylene butadiene (SEBS), which have not demonstrated egligible chemical interaction with epoxy matrix, also revealed mendable behavior, recovering mechanical properties in healed samples test specimens [32,33].

2.2.2 Molecular dissolution mechanism

The second approach of healing mechanism with thermoplastic addition was proposed by Jones and Hayes [22,26,27]. According to them, the polymer should be compatible with the matrix by terms of solubility parameters, thus the thermoplastic healing agent should be miscible within the thermoset polymer, but does not chemically react with it, remaining dissolved in the matrix – in contrast to the conventional matrices toughened with thermoplastic. This means that the thermoplastic preferably forms a homogeneous solution with the thermoset matrix both before and after cure. Another criterion for the thermoplastic healing agent is that the addition of the linear chain molecule should not considerably diminish the thermomechanical properties of the resin matrix. Therefore, upon heating the thermoplastic would gain mobility and diffuse through the thermosetting matrix, with some chains bridging closed cracks and then repairing the composite.

It is well understood that the contact between two identical or compatible polymer surfaces above the glass transition temperatures drives to molecular diffusion through their interface [19,20]. The polymer-polymer interface increasingly disappears as much as molecules diffuse across the interface, thus allowing to fill and heal cracks. The time dependence of healing is leaded by the following sequential stages: (A) surface rearrangement, (B) surface approach, (C) wetting, (D) diffusion, and (E) randomization, which are described in Figure 2. 5.

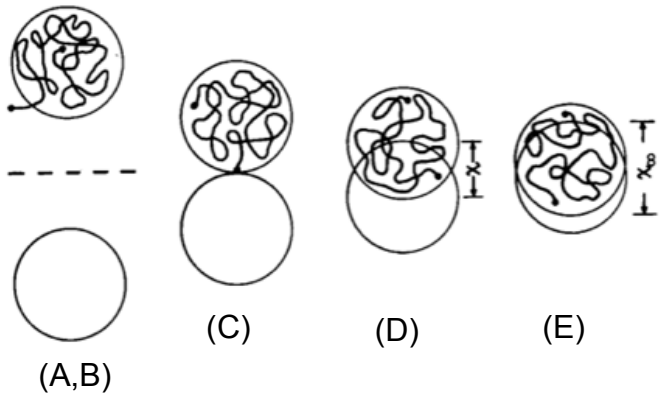

Figure 2. 5 - Schematic diagram showing two random-coil chains on opposite crack surface during the five stages of crack healing: (A) rearrangement, (B) surface approaching, (C) wetting, (D) diffusion to a distance χ and (E) diffusion to an equilibrium distance χ_∞ and randomization. The dashed line represents the original crack plane [34].

In their works [22,26,27] , Jones and Hayes used the linear copolymer poly(bisphenol-A-*co*-epichlorohydrin) (PBE), which is highly compatible with the diglycidyl ether of bisphenol-A (DGEBA) epoxy based resin. Thus, they have developed a one-phase solid-state semi-interpenatrated polymer blend by mixing the thermoplastic healing agent into a thermosetting epoxy to produce the homogeneous matrix. For this, they have used two epoxy DGEBA based resins, which were mixed and cured with nadic methylene anhydride (NMA) and a mercaptan terminated curing agent that, in this case, acts as an accelerator for the anhydride.

In Jones and Hayes works' [22,26,27] the copolymer was added to the resin in different proportions. DGEBA resins and PBE were blended using an overhead stirrer at 80 °C until the mixture was homogeneous (at least 24 h). Once blended, the resin was cured at 80˚C for 4 h followed by a postcure at 130˚C for 3 h. It was observed that this material was compatible with the resin system both before and after cure, as it continued in solution during the whole processing time.

Mechanical tests showed that the modified resin system has the ability to recover its mechanical properties when healing cycle is carried out [22,26,27]. Further, each specimen was repeatedly tested (at least 10 times) proving its latent healing functionality over multiple healing cycles. Furthermore, it was verified that the proportion of added thermoplastic affects the resin recovery, showing that 7.5 % of PBE added obtained the higher mechanical recover. However it is important to notice that the viscosity of the resin system is also impacted by the content of healing agent, which at the high concentration may lead to a phase separation [27]. Thus it is preferable to choose the quantity of additive that better balance processability and healing efficiency.

Dynamic mechanical thermal analysis (DMTA) was also performed in order to verify the changes in thermomechanical properties and subsequently the phase behavior of the blend system. Table 2. 2 summarizes the obtained data from DMTA made in a range from 0 to 15 wt% of PBE.

Table 2. 2 - The effect of the healing agent on the dynamic thermomechanical properties of the epoxy resin [26].

Concentration of healing agent (%)	Onset of modulus drop (˚C)	log (E') (Pa)	tan δ peak (˚C)
0	76.2	8.98	88.7
2.5	75.6	8.97	89.5
5	74.1	8.99	89.9
7.5	74.2	8.97	91.4
10	74.1	9.03	90.2
12.5	73.1	8.99	91.3
15	73.5	8.98	90.6

The results showed that the addition of the PBE healing agent over the range of addition (2.5 to 15 wt%) does not affect significantly the thermomechanical properties of the epoxy resin. These results also suggest that PBE is miscible in the epoxy resin, although some broadening of tan δ peaks was also observed.

Regarding the effect of the thermoplastic content in composite materials, Jones and Hayes performed two experiments [22,26] in which samples with two different contents of PBE healing agent were subjected to impact tests. In both cases, glass-fibers were used to create $[0/90_2/0]$ crossply laminates, which were vaccum bagged in order to produce square panels. The panels were then subjected to a falling-dart impact tower with a 10 mm diameter hemispherical tup. The resultant delaminated area was photographed using transmitted light at a fixed camera position. The same area was then photographed after subjected to a healing cycle. All images were taken at the same magnification.

In the first study [22] glass-fiber composites square panels with 10 x 10 mm were produced using a resin system containing 10 wt% of healing agent. After the impact damage of 2.7 J, samples were healed at 130˚C for 1h. The healing cycle occurred into an oven and no constraints were applied. The resulting images reveal a recover greater than 30% of the damage area as shown in Figure 2. 6.

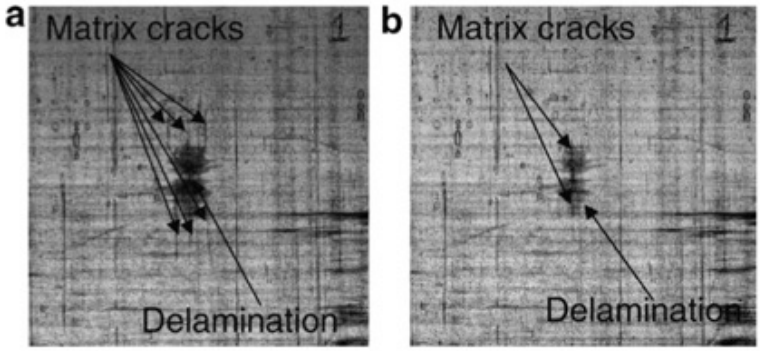

Figure 2. 6 - Photographs showing an example of a glass-fiber composite panel impacted at 2.7 J (a) before and (b) after a healing cycle [22].

In the second work [26], a similar procedure was carried out to produce crossply [0/90$_2$/0] composite square samples in 200 x 200 mm dimensions containing optimum concentration of 7.5 wt% of PBE healing agent. The specimens were then subjected to 2.6 J falling-dart impact test. Photographs of the damaged area were also compared to samples with unmodified resin systems. The healing cycle occurred at 130˚C for 2 h and it was repeated three times for each specimen to quantify the healing response after successive 2.6 J impacts and thermal healing cycles. Results show that a reduction of up to 30% of the damage area was also accomplished. Concerning to the multiple impact-healing cycles, results showed that the samples produced with the healing system appeared to exhibit less damage after three impacts than samples produced with non-healable systems. This suggests that the unmodified resin system tends to fragilize the composite leading to a larger damage area after successive impacts. Other consideration is that the normalized damage area of the healable system has more damage tolerance, i.e. it presents smaller variations than its non-healable equivalent, as shown in Figure 2. 7.

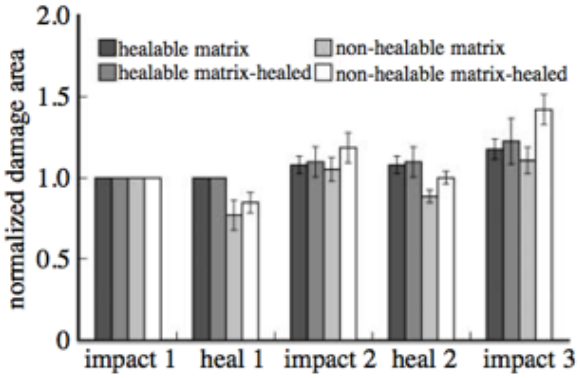

Figure 2. 7 - The rate of growth of damage area under impact in healed and non-healed composite specimens prepared from healable or non-healable resin [26].

2.2.3 Thermally reactive mechanism

Poly(ε-caprolactone) (PCL)

This approach was first introduced by Luo et al. [31] who demonstrated a thermoplastic-thermosetting blend of poly(ε-caprolactone) (PCL) and DGEBA based epoxy resin exhibiting thermal healing capabilities. In their work the concept of polymerization-induced phase separation (PIPS) was employed to produce a biphasic structure capable of self-healing. The morphology of PIPS in epoxy is usually obtained from an initially miscible blend of a thermoplastic and the uncured thermoset resin, differently from the morphology obtained through the mechanical mixing of fully immiscible system (like those cited in *viscous flow mechanism* section). Thus, as the resin crosslinks, the polymerization-induced phase separation occurs. Several of others thermoplastics such as poly(ether sulfone), polyetherimide, poly(methyl methacrylate) and polystyrene have also been demonstrated to show this type of morphology when mixed with epoxy resins [35].

The biphasic morphology obtained from PIPS consists of a (i) major load-bearing phase that has good mechanical properties and structural functions and (ii) a healing phase composed by a thermoplastic which involves the load-bearing phase, acting as a “brick” and “mortar” structures, respectively. Then, it is important to mention that the mechanical properties of this structure may vary significantly depending on the content of the isolated (brick) and continuous (mortar) phases in the blend.

In this regard, although various thermoplastic additives have shown to form PIPS structure, some criteria are required to employ them in self-healing matrix systems. Then, to be able to heal, the thermoplastic phase created by PIPS should present the following requirements [35]:

- Melting and consequent volume expansion of the thermoplastic;
- Flow of the thermoplastic melt into the damage zone;
- Physical healing at the molecular level.

PCL has demonstrated to be a potential candidate for self-healing purposes because of its low melting point (55˚C) and high degree of thermal expansion (an increase in volume by up to 14% between room temperature and 150˚C). Figure 2. 8 suggest a schematic mechanism of self-healing in epoxy/PCL blends, which will be further discussed.

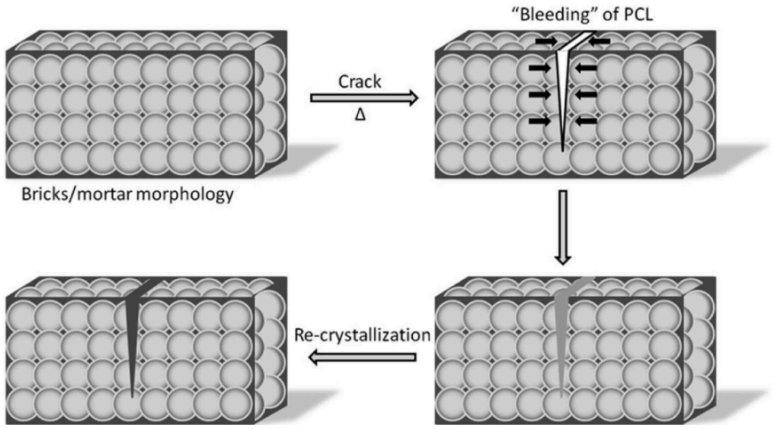

Figure 2. 8 - Schematic illustration of the overall mechanism of thermal crack healing [31].

In their work, Luo et al. [31] have blended DGEBA liquid resin with PCL pellets in different mass ratios (Table 2. 3), which were melt-mixed at 120˚C for 1-2 h by continuous stirring. The temperature was set to 140˚C and then the curing agent, 4,4'-diaminodiphenylsulfone (DDS) was added in ratio DGEBA:DDS = 2:1. The mechanical agitation remained until the blend became clear and transparent, indicating a single phase. After degasing, the mixture was cured at 180˚C for 3 h. Chemical structures of the reactants are given in Figure 2. 9.

Table 2. 3 - Summary of blend epoxy-PCL compositions studied [31].

Sample name[a]	m_{DGEBA}:m_{PCL}
epoxy/PCL(4.3)	90:10
epoxy/PCL(11.5)	85:15
epoxy/PCL(15.5)	80:20
epoxy/PCL(27.0)	70:30
epoxy/PCL(34.9)	60:40

[a] The numbers in parentheses indicate the percentage weight fractions of PCL in the blend (DGEBA + DDS + PCL).

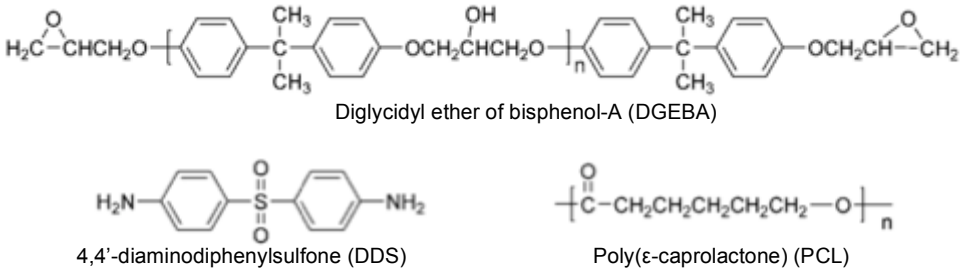

Figure 2. 9 - Chemical structures of DGEBA, DDS and PCL.

Thermal analysis of the blends show that no exothermic peak was observed in the differential scanning calorimetry (DSC) heating runs, indicating that all epoxy/PCL were fully cured at the cure cycle. Dynamic mechanical thermo analyses (DMTA) were also carried out in order to assess the temperature-dependent viscoelasticity of selected samples, determining also values for melting temperature, T_m, and glass transition temperature, T_g. The DMTA curves of pure epoxy, PCL and epoxy/PCL systems are given in Figure 2. 10.

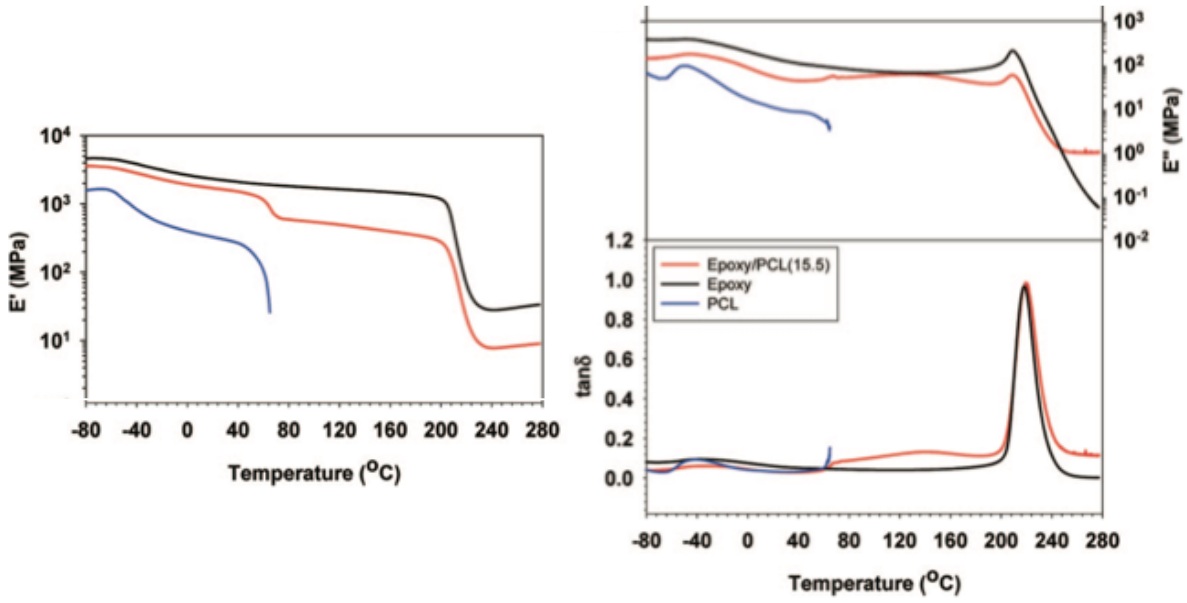

Figure 2. 10 - DMTA results (3˚C/min; 1Hz) of pure epoxy and PCL and epoxy/PCL(15.5) [31].

According to the graph, T_m of thermoplastic is 59˚C given by the storage modulus (*E'* trace) onset and the T_g of the epoxy is around 203˚C. Other relevant information given by the curve is that the storage modulus (E') of pure epoxy resin is very close to the epoxy/PCL blend. This implies that even above the melting

temperature of PCL, the blend still presents good mechanical properties, likewise evidenced by the relatively small loss modulus (E'') and tanδ differences.

Images of the morphological blend structures were obtained using scanning electron microscopy (SEM) and polarized optical microscopy (POM). For SEM, samples were submerged in liquid nitrogen and then immediately fractured. The fractured surface was then etched with chloroform solution, which attacks preferentially the PCL phase. Finally a thin sputter-coating layer of gold was applied on samples, resulting that only epoxy phase is allowed to be observed. For POM images, a thin layer of epoxy/PCL was prepared sandwiching two coverslips and then curing at 180˚C for 3h. SEM images are shown in Figure 2. 11 for all compositions studied, while POM images are given in Figure 2. 12 for only two formulations (epoxy/PCL(11.5) and (15.5)).

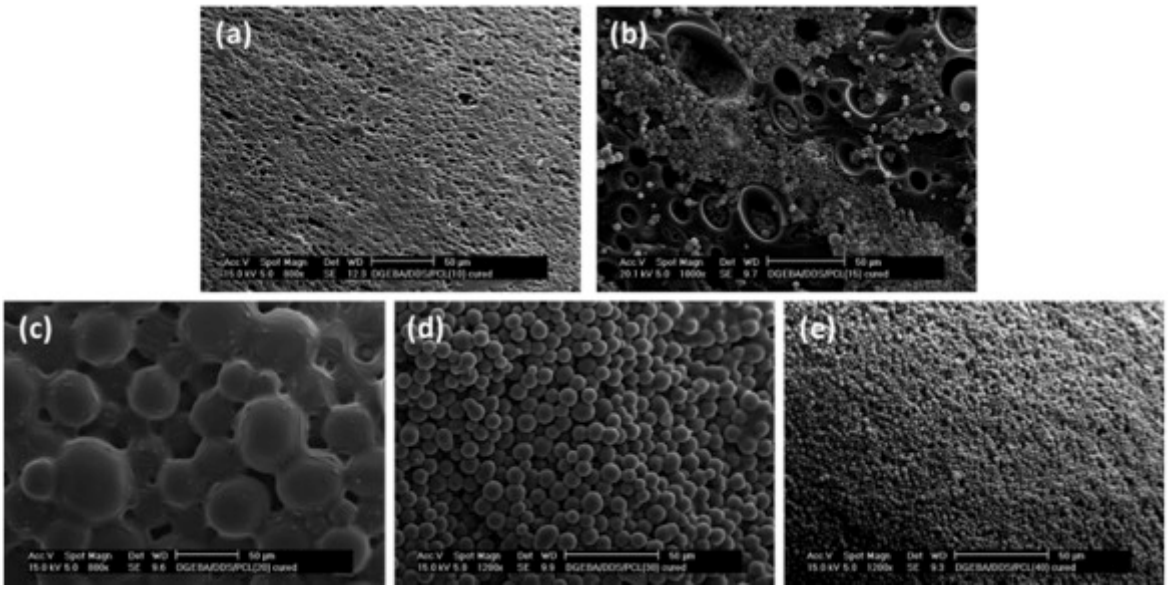

Figure 2. 11 - SEM images exhibiting the morphologies of epoxy/PCL blends in different compositions: (a) epoxy/PCL(4.3), (b) epoxy/PCL(11.5), (c) epoxy/PCL(15.5), (d) epoxy/PCL(27.0) and (e) epoxy/PCL(34.9) [31].

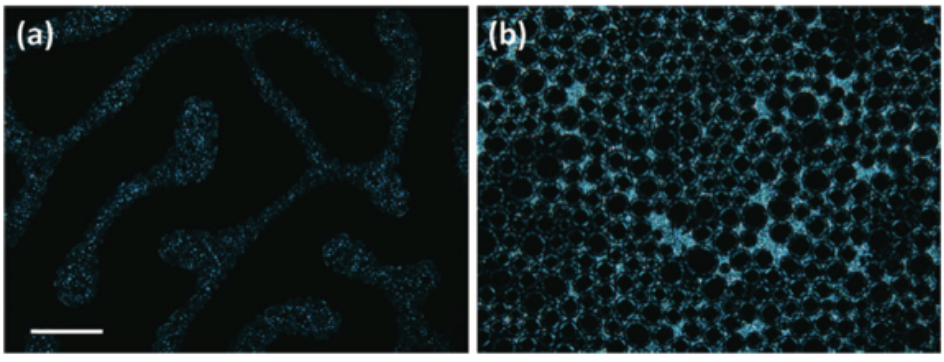

Figure 2. 12 - POM images for (a) epoxy/PCL (11.5) and (b) epoxy/PCL(15.5) [31].

The images show that at low PCL content (epoxy/PCL(4.3)), epoxy forms the matrix (primary) phase with randomly dispersed PCL particles (Figure 2. 11(a)). As the PCL content increases, however, a quite complex structure is formed. This is due to the secondary and tertiary phase separation events occurring within the primary phase [36]. The inversion phase is emerged from epoxy/PCL(27.7) and further concentrations.

Therefore, it was established that among all compositions, epoxy/PCL(15.5) presented the most promising morphology for self-healing application. The first reason is that the PCL forms a continuous phase highly interpenetrated with the epoxy phase, which can guarantee its presence and delivery in any damage position. Secondly, since the epoxy is presented in greater quantity, the mechanical properties should be governed by its highly interconnected sphere structures, which can effectively bear loads as a unique entity.

Using hot-stage microscopy it was possible to observe the microstructural changes that occur during thermo cycles of epoxy/PCL blends. For better resolution images, epoxy/PCL bar samples were sputter-coated with a thin layer (1-3 nm) of gold and placed in a heated plate while undergo to microscope observation, under constant thermal monitoring with a thermocouple. A typical morphology of an epoxy/PCL blend schematically exhibited in terms of temperature and time is given in Figure 2. 13.

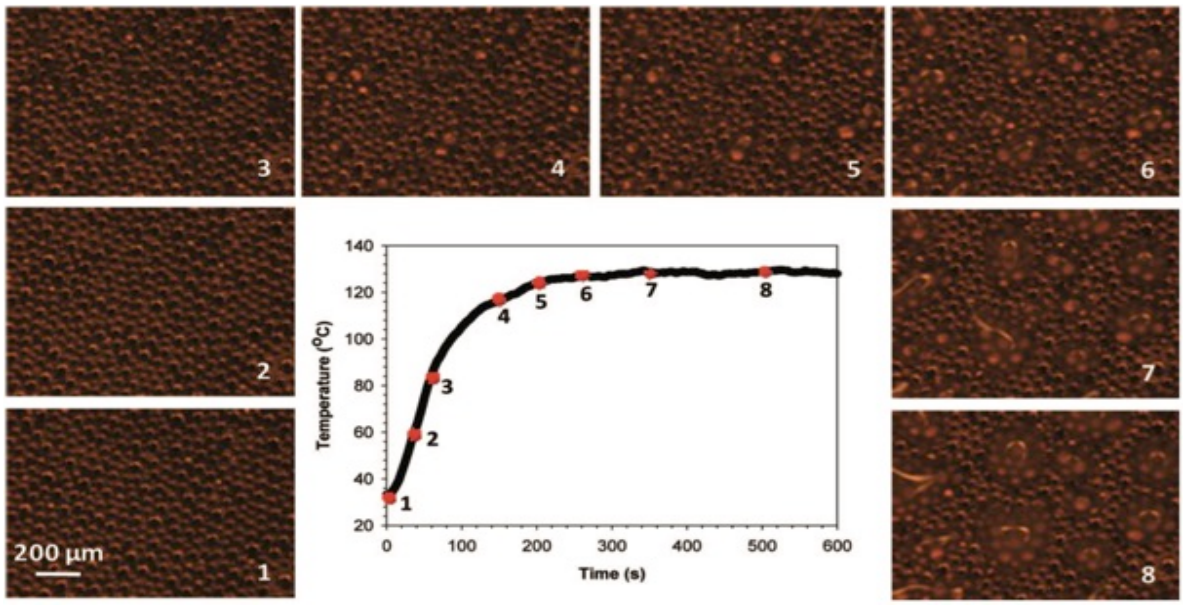

Figure 2. 13 - Monitoring of heat-induced morphology behaviour of an epoxy/PCL blend across the time [31].

According to the images it was observed that the morphological changes initiated as the temperature exceed the PCL melting temperature (approximately after 1 min), evidenced by the formation of droplets in Figure 2. 13 (3). Afterwards, the droplets grow and coalesce by contact motion of adjacent growing droplets, as a "bleeding" mechanism. "We interpret the bleeding phenomenon to be a consequence of differential thermal expansion between the two interpenetrating phases, with the minor (but continuous) PCL phase expanding at least 10% more than the epoxy phase because of the melting transition itself and the large expansivity of the fluid phase" [31]. This mechanism is shown schematically in Figure 2. 14. The authors termed this phenomenon as "**differential expansive bleeding** (DEB)".

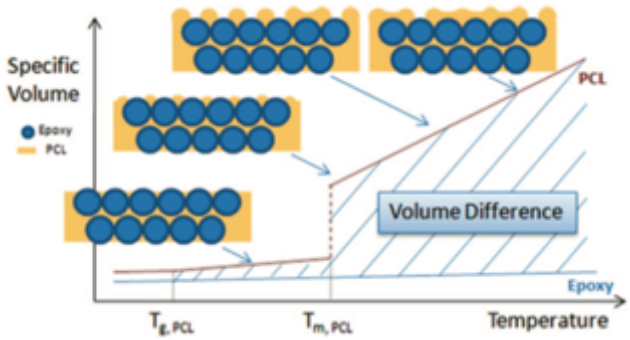

Figure 2. 14 - Schematic illustration of DEB indicating its origin in differential thermal expansion between PCL and epoxy [31].

Experiments were also performed to observe microstructural changes at the crack surface of fractured samples containing 15 wt% of PCL [31] both before and after healing cycle (Figure 2. 15). In the first fracture (Figure 2. 15(a) and (b)) it can be noticed that the specimen has fractured in a "hybrid" mode, where the crack propagated plastically (ductile fracture) throughout the PCL fibrils, and in a brittle way at the connecting epoxy sphere planes (dotted area in Figure 2. 15(b)).

Moreover, after thermal mending cycle at 180 ˚C for 8 min, the aspect of the fractured site changed considerably (Figure 2. 15(c) and (d)). Instead of the hybrid crack surface, a continuous "scar" formation took place, which the authors reasoned to the PCL bleeding process responsible to bridge the two crack surfaces. Furthermore, once the self-healed specimen was loaded again, the crack propagation occurred by deforming plastically the PCL scar (Figure 2. 15(e)). This result is consistent to the fracture experiments, in which all thermal mended samples presented larger deformations when compared to the virgin ones.

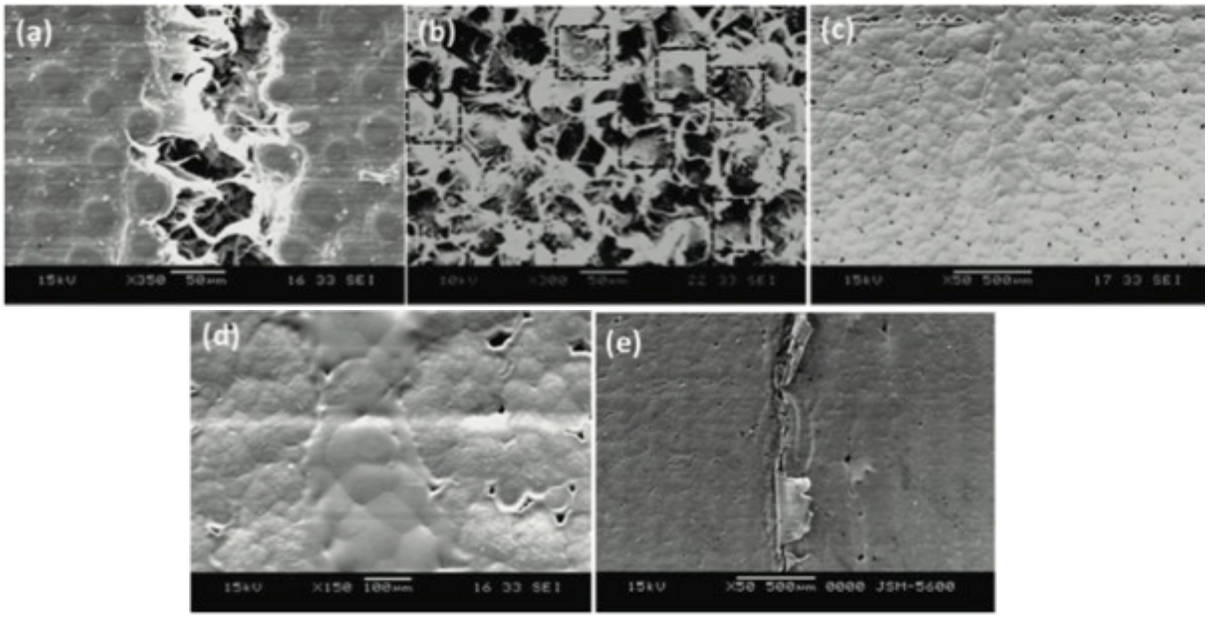

Figure 2. 15 - SEM images of (a) the crack on a completely fractured sample, (b) the fracture surface, (c and d) the cracked surface after thermal mending and (e) the reopened crack after the fracturing of a thermally mended sample [31].

In other relevant PCL-epoxy study [35], Fourier Transform Infrared (FTIR) microscopy was used to examine the phase composition of specimens containing 17.7 and 25 vol% PCL. In that case, the absorption spectra in the wavelength range 1680-1780 cm^{-1} was chosen in order to characterize the composition of the phase by the presence of carbonyl stretch band characteristic of PCL. Figure 2. 16 shows the absorption spectra for the two PCL-epoxy samples compositions, along with spectra for the pure epoxy and PCL.

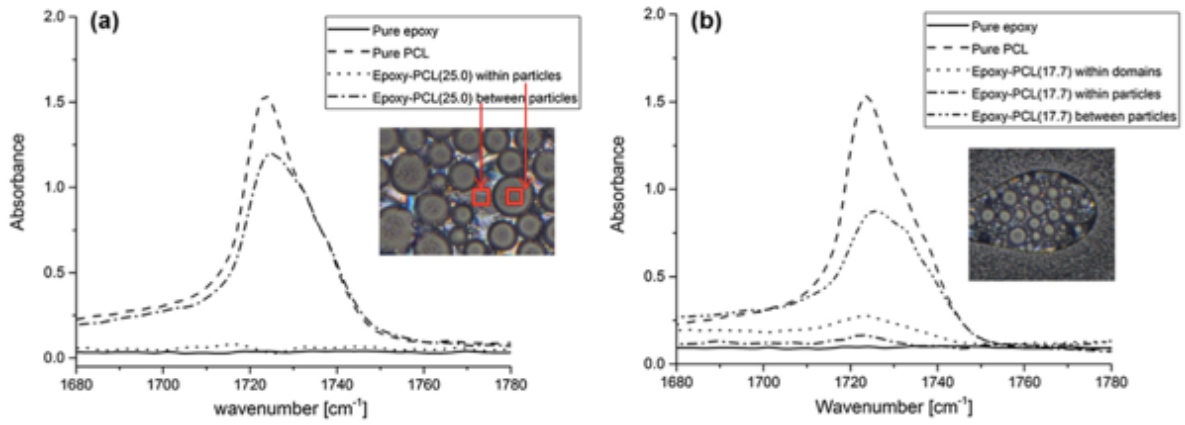

Figure 2. 16 - FTIR spectra in the carbonyl stretch band (wavelenght range 1680-1780 cm-1) from selected regions of (a) Epoxy-PCL (25 vol%) and (b) Epoxy-PCL (17.7 vol%) blends. Spectra for the pure epoxy and pure PCL are also shown [35].

This result indicated that the discrete particles present at both sample blends (25 and 17.7 vol% PCL) were confirmed as epoxy rich phase, once no absorption in this range were noticed. In contrast, strong carbonyl peaks were observed from the surrounding area indicating a PCL rich phase. “Even so, the carbonyl peaks tended to be weaker than those obtained from the pure PCL reference specimens, presumably because of the limited lateral and vertical resolution of the FTIR microscope” [35].

Poly(ethylene-co-methacrylic acid) (E-MAA)

Poly(ethylene-co-methacrylic acid) (E-MAA) is undoubtedly the most studied thermoplastic healing agent in literature [24,28–30,32,33,37–42]. Its use was firstly reported by Meure et al. [28], who pointed out the limitations previous thermoplastic healing agents presented concerning the need for high temperatures and clamping loads during the healing cycle, as well as losses of healing efficiency at the expense of resin properties. For this reason, a new material capable of forming a discrete phase within the matrix that can react with the resin during healing was proposed. Further, they have also suggested a **pressure delivery mechanism** in which the healing agent is driven into the matrix by the thermal expansion of embedded bubbles.

Samples were prepared mixing E-MAA particles directly into a triethyltetramine (TETA) cured diglycidyl ether of bisphenol A (DGEBA) resin, which chemical structures are given in Figure 2. 17.

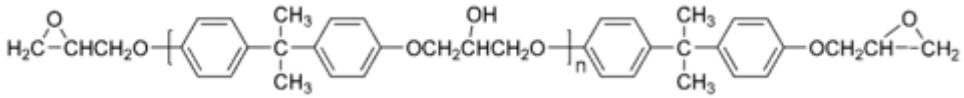

Diglycidil ether of bisphenol A (DGEBA)

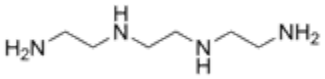

Triethyltetramine (TETA)

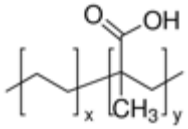

Poly(ethylene-co-methacrylic acid) (E-MAA)

Figure 2. 17 - Chemical structures of DGEBA, TETA and E-MAA.

Test specimens were produced by curing DGEBA with TETA amine hardener at stoichiometric mass ratio of 100:13 (epoxy:amine). Test pieces were cured at 50 ˚C for 90 min in silicone mold and then post-cured at 150 ˚C for 30 min. E-MAA pellets were cryogenically ground and sieved and a particle size range of 250-425 μm was obtained. The blend was produced by heating up the DGEBA monomer to 70 ˚C, to which 15 vol% E-MAA particles were added. Finally, the TETA hardener was added to the mixture.

Meure et al. [28] have evaluated the effect of inclusion of E-MAA on the resin properties, once “the incorporation of healing agents should not have a detrimental effect on the material’s original physical properties” [28]. Thus, neat epoxy resin (without any addition of E-MAA) and mendable resin (containing 15 vol% of E-MAA) were compared by both tapered double cantilever beam (TDCB) and single-edge-notched beam (SENB) tests. Typical load-extension curves for both tests demonstrated that the addition of 15 vol% E-MAA have resulted in a slight increase in the peak load. The authors attribute this small change due to particulate-base toughening of the resin, which reduce or even eliminate crack growth during loading. They also mentioned that the mendable resin has a smaller load-extension gradient than that of the unmodified resin, which consequently implies a drop in elastic modulus [28]. Therefore, both SENB and TDCB testing demonstrated that the addition of the E-MAA healing agent has increased the fracture strength of the resin.

Healing of fractured test pieces was performed at 150 ˚C for 30 min in an oven and it was observed using optical microscopy (Figure 2. 18). During the crack growth, it can be observed that E-MAA particles also fracture, resulting in E-MAA particles in both sides of the fracture surface (Figure 2. 18(a)). When the test piece is subjected to the healing cycle at 150 ˚C, the E-MAA particles undergo thermal expansion and viscous flow, which contribute to heal through diffusion and entanglement of the E-MAA chains between the fractured parts (Figure 2. 18(b) and (c)). Evidences of the particle-epoxy interface force can be observed when sample is reloaded and the stress transfer occurs at the E-MAA fracture plane (Figure 2. 18(d)).

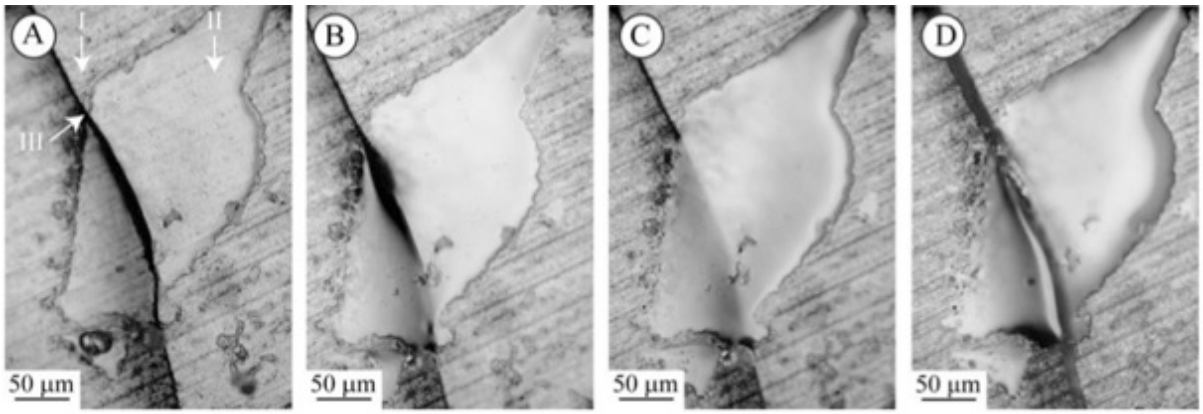

Figure 2. 18 - Optical microscopy image showing (I) epoxy resin, (II) E-MAA particle and (III) a crack after: (a) 2 min at 150 ˚C, (b) 5 min at 150 ˚C, (c) 9 min at 150 ˚C and (d) 30 min at 150 ˚C and then being stressed to reopen the crack [**Error! Bookmark not defined.**].

Meure et al. [28] also pointed out the development of an adhesive layer reuniting contiguous epoxy fracture surfaces using optical microscopy (Figure 2. 36). In this case, it is possible to identify the healing agent filling the adjacent fracture plane of epoxy matrix surrounding one E-MAA particle, binding the crack surfaces. Thus, “the resulting reduction in the cracked area of the epoxy resin results in the restoration of the resin’s initial strength as the stress is transferred through the adhesive layer on reloading of the healed resin” [28].

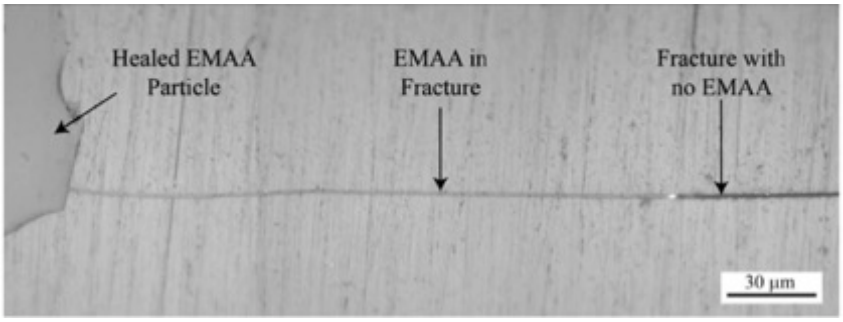

Figure 2. 19 - Optical microscopy image of the cross-section of a healed SENB showing the fracture plane surrounding an E-MAA particle [28].

Meure et al. [28] also mentioned the formation of an adhesive layer from the E-MAA particle in a SENB fracture surface after healing cycle. Scanning electron microscope images (Figure 2. 20) show that the layer has been ruptured and stretched during reloading of the healed SENB, proving that the stress was transferred to the adhesive layer during reload of the healed SENB test piece.

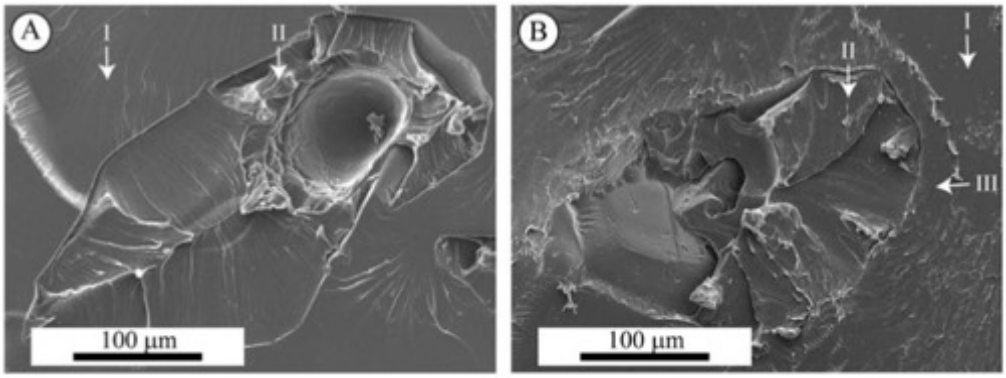

Figure 2. 20 - SEM image showing (I) epoxy matrix, (II) an E-MAA particle and (III) the adhesive layer on the resin surrounding the particle of (a) a damaged SENB and (b) a healed SENB [28].

Still in the same study [28], authors suggested, by comparing thermal expansion coefficients of E-MAA and epoxy resin (approximated as 7–11 x 10^{-4} K^{-1} and 0.6–1.6 x 10^{-4} K^{-1}, respectively), that the effect of "differential bleeding expansion" (DEB) also contribute to the delivery of E-MAA through open cracks. Furthermore, they also proposed that the formation of the adhesive layer was facilitated by a pressure difference created during the expansion of small bubbles embedded in the E-MAA particles, as shown in Figure 2. 21 and in the schema of Figure 2. 22.

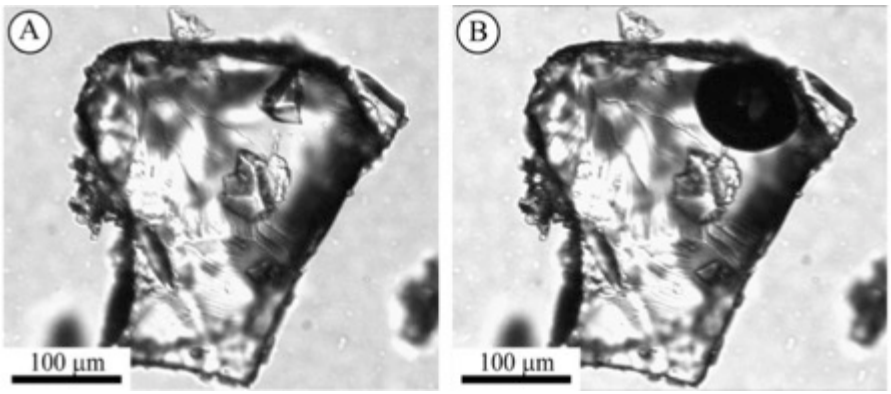

Figure 2. 21 - Transmission optical microscopy images of the E-MAA particle embedded in epoxy resin (a) prior to post-curing at 150˚C and (b) after 5 min at 150˚C [28].

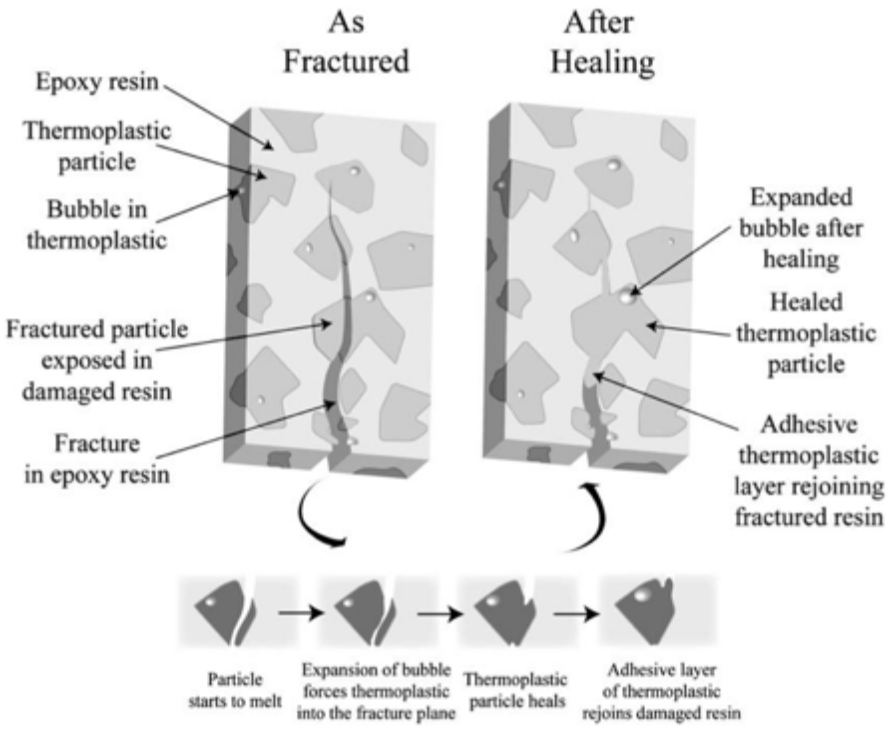

Figure 2. 22 - Schema of the healing agent delivery mechanism utilized by epoxy resin containing E-MAA particles [28].

Authors suggest that “these bubbles were likely to have formed due to a phase separation of volatile products formed during reactions between the E-MAA particles and the epoxy system reactants” [28]. Thus, in other study [24], Meure et al. has investigated the chemical reactions/interactions between E-MAA, DGEBA and TETA hardener using attenuated total reflectance Fourier transformed infrared (ATR-FTIR) spectroscopy. Authors also highlighted that those chemical reactions/interactions are crucial to better understand the interfacial strength between the E-MAA and the epoxy matrix.

In order to inspect chemical interaction between E-MAA and epoxy resin reactants (DGEBA and TETA), in the cited study [24], authors have produced E-MAA films, which were exposed systematically to DGEBA, to TETA and to DGEBA + TETA at two different temperatures, 50 ˚C and 150 ˚C. After treatment E-MAA films were thoroughly washed with a solvent in order to remove any material that was not bound to the film surface. They also mentioned that “this production method provides a route for the E-MAA to react with the DGEBA, TETA or the DGEBA-TETA reaction products that are present during curing, post-cure and healing processes” [24]. A schematic of DGEBA-TETA reaction products is shown in Figure 2. 23, in which its main reactive chemical sites are highlighted. Authors also mentioned that “the

existence of six available bonding sites on the TETA molecule prevents complete consumption of the epoxide/amine groups during curing such that even when the epoxy is post-cured there will still be unreacted amine and oxirane groups within the epoxy network" [24].

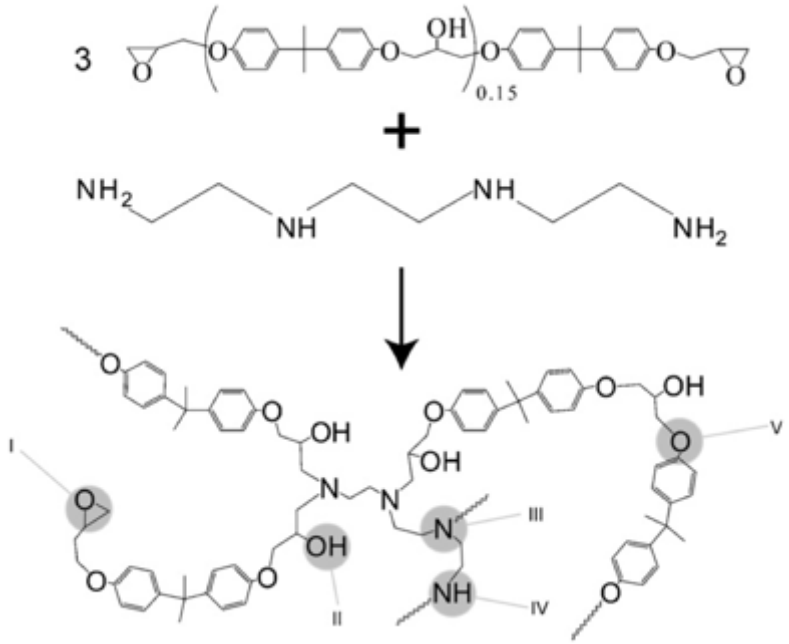

Figure 2. 23 - Schema of DGEBA-TETA reaction showing (I) epoxide ring, (II) hydroxyl, (III) tertiary amine, (IV) secondary amine and (V) ether groups incorporated into the cured epoxy resin's polymer network [24].

Therefore, considering the available chemical sites cited above, Figure 2. 24 outlines the most likely chemical reactions occurring between the carboxylic acid from E-MAA particles and the chemical sites from DGEBA-TETA reaction. The type of chemical bond (ionic, covalent and/or hydrogen bond) between E-MAA particles and the epoxy resin are directly related to the interfacial strength, once primary bonds (ionic and covalent) gives much stronger interfacial strengths than secondary ones (hydrogen bonds). It is important to observe that acid concentration does not change when secondary bonds are promoted, as it is shown in Figure 2. 24. Thus, in the cited study [24] changes in acid concentration and, consequently, the appearance of new functional groups was monitored using ATR-FTIR spectroscopy. Table 2. 4 summarizes the FTIR peak assignments of the functional groups used to assess the chemical changes in the E-MAA films.

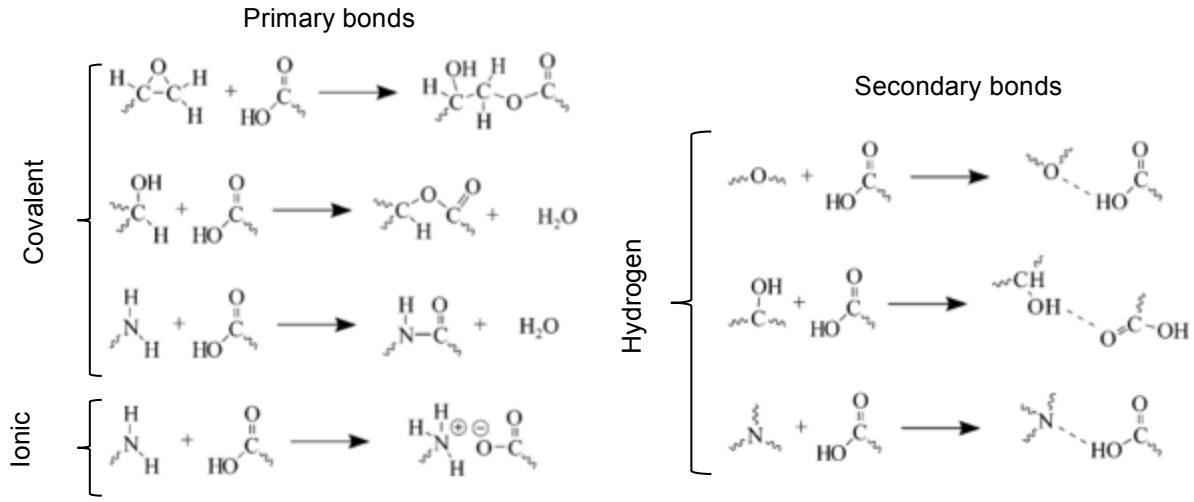

Figure 2. 24 - Main chemical reactions/interactions between E-MAA and DGEBA, TETA and DGEBA+TETA reactants (Adapted from [24]).

Table 2. 4 - Band assignments of FTIR spectra for the main functional groups from DGEBA, TETA and E-MAA [24].

Material type	Bond type	Peak location (cm^{-1})
EMAA, DGEBA, TETA	Alkane	720
DGEBA	Aromatic carbons	830
DGEBA	Oxirane	915
EMAA	Acid dimer	930
DGEBA	Aromatic carbon and aliphatic ether	1035
DGEBA	Aromatic carbon	1180
DGEBA	Carbon-hydrogen or aromatic ether	1230–1250
EMAA	Carboxylic acid	1255
EMAA	Ketone	1365
EMAA	Ketone	1435
EMAA, DGEBA, TETA	Alkane	1430–1470
Ionomer	Amide	1500
DGEBA	Aromatic carbon	1505
Ionomer	Amine salt of carboxylic acid	1500–1570
TETA	Amine	1580
DGEBA	Aromatic carbon	1605
Ionomer	Amine salt of carboxylic acid	1620–1650
Ionomer	Amide	1650
EMAA	Acid dimer	1700
EMAA	Ketone	1727
EMAA	Ester	1735
EMAA	Free carboxylic acid	1750
EMAA, DGEBA, TETA	Alkane	2850–2960

Figure 2. 25 shows FTIR spectra of E-MAA films exposed to DGEBA at 50˚C (ED-50) and 150 ˚C (ED-150), exposed to TETA at 50 ˚C (ET-50) and 150 ˚C (ET-150), along with FTIR spectrum of E-MAA pure film.

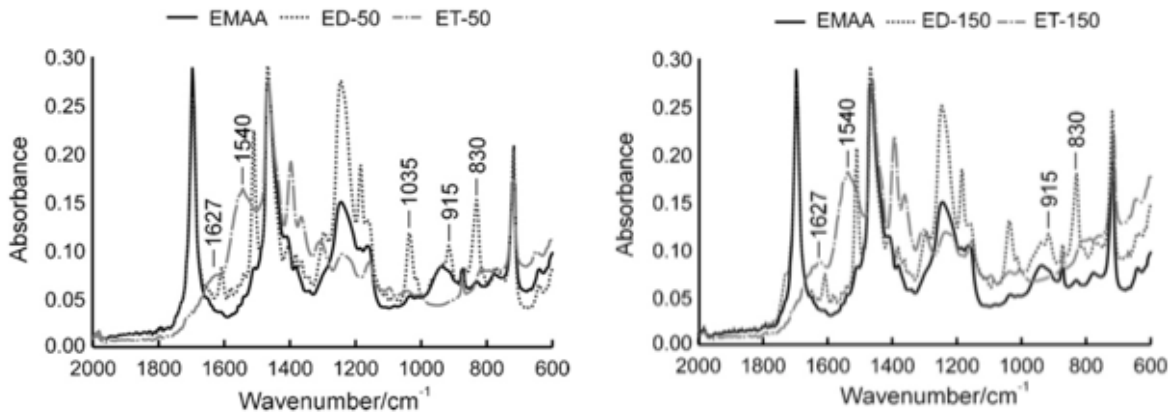

(a) (b)

Figure 2. 25 - FTIR spectra of E-MAA pure film along with (a) E-MAA exposed to DGEBA at 50 ˚C (ED-50) and exposed to TETA at 50 ˚C (ET-50) and (b) E-MAA film exposed to DGEBA at 150 ˚C (ED-150) and to TETA at 150 ˚C (ET-150) [24].

Spectrum of E-MAA film exposed to DGEBA (ED-50) presented characteristic bands from the aromatic structures of DGEBA (830, 1030, 1180, 1225, 1510 and 1610 cm^{-1} peaks), aliphatic ether (1035 cm^{-1} peak) and epoxide group (915 cm^{-1} peak), which indicates that DGEBA molecules have been adsorbed onto E-MAA film surface [24]. Nevertheless, no significant changes were observed in acid dimer peaks (920 and 1700cm^{-1}) and, consequently, in the functionality of ED-50, which suggests that only hydrogen based-bonds were performed [24]. Spectrum of E-MAA film exposed to TETA at 50 ˚C (ET-50), however, reveals the appearance of two peaks (1540 and 1627 cm^{-1}), which are related to the salt formation, at the expense in intensity of acid dimer peaks [24]. Furthermore, authors also compared the changes in spectra of E-MAA film exposed to DGEBA at 150 ˚C (ED-150) and exposed to TETA at 150 ˚C (ET-150) (Figure 2. 25(b)), which showed the same trend observed for 50 ˚C experiments (Figure 2. 25(a)). In this case, however, an increase in all peaks associated to a large adsorption of DGEBA chemical structures and associated to an outstanding formation of ionic salts was observed [24]. The appearance of a new shoulder peak at 1710 cm^{-1} for ET-150 spectrum (Figure 2. 25(b)) was also noticed and it was attributed to the formation of an ester, which has likewise appeared in E-MAA films exposed to DGEBA-TETA at 150 ˚C (EDT-150), as exhibited in Figure 2. 26.

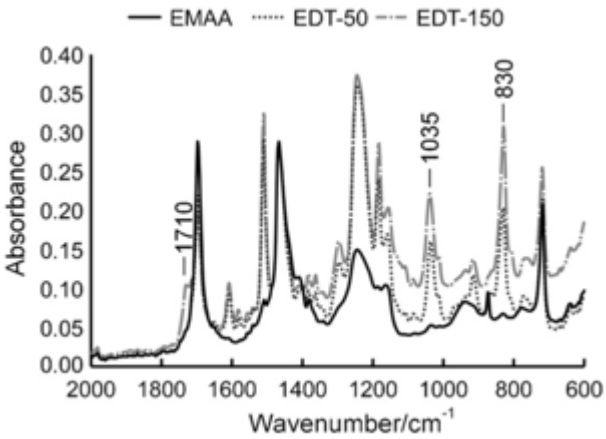

Figure 2. 26 - FTIR spectra of pure E-MAA film, E-MAA exposed to the DGEBA-TETA mixture at 50 ˚C (EDT-50) and E-MAA exposed to DGEBA-TETA mixture at 150 ˚C (EDT-150) [24].

Meure et al. [24] also observed changes in the surface of the E-MAA films in contact with DGEBA-TETA mixtures at 150 ˚C (EDT-150), which has exhibited a rippled appearance and possessed small voids where bubbles have formed (Figure 2. 27(left)). Authors attributed these distortions to the boiling and loss of water that was formed subsequent to the acid-hydroxyl reaction (Figure 2. 24). Such surface changes were not observed in any other condition, which indicates that a similar reaction had not taken place to an appreciable extent under these conditions [24].

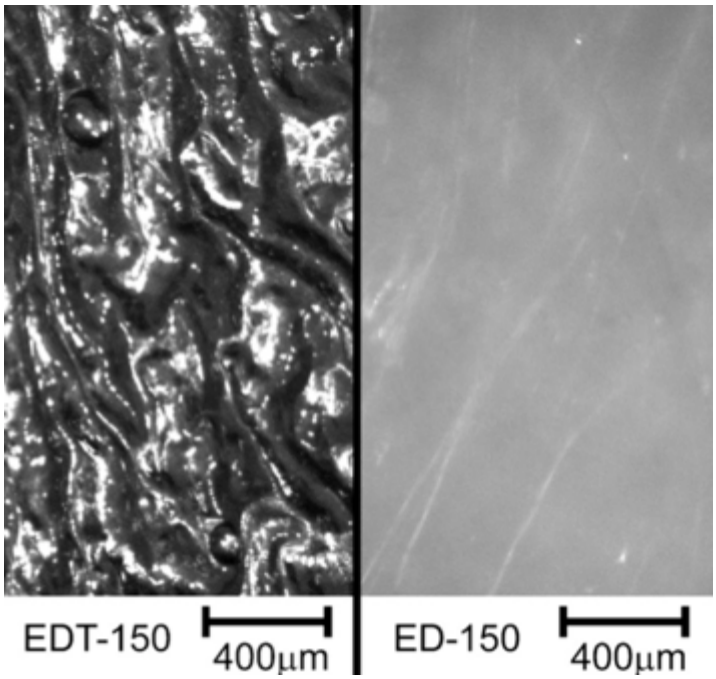

Figure 2. 27 - Optical microscope images of the surface of E-MAA film exposed to a DGEBA-TETA mixture at 150 ˚C (EDT-150) and DGEBA at 150 ˚C (ED-150) [24].

As mentioned before, E-MAA is the thermoplastic healing agent most studied in literature. Table 2. 5 summarizes some examples of the use of E-MAA healing agents found in literature, which includes the physical form E-MAA is disposed, the substrate used and the main results on healing efficiency.

Table 2. 5 - Main characteristics of E-MAA healing agent studied in literature.

E-MAA physical structure	Resin reactants	Substrate	Healing efficiency (Γ)	Ref
Particles	DGEBA + TETA	Base resin	• Up to 140% in fracture peak load (TDCB and SENB test) • Up to 85% in K_{IC} (fracture toughness) (TDCB and SENB test)	[28]
		Carbon fiber laminate	• Up to 309% in K_{IC} (mode I interlaminar opening crack using DCB test)	[37]
Films	-	Prepreg	• Up to 88% in K_{IC} (mode I interlaminar opening crack using DCB test) • Up to 36% peak load (ILSS test)	[39]
Fibers	DGEBA + TETA	Carbon fiber laminate	• Up to 185% in G_{IC} (mode I interlaminar opening crack using DCB test) • Up to 121 % peak load (ILSS test).	[29]
			• Up to 290% in K_{IC} (mode I interlaminar opening crack using DCB test)	[37]
	-	Prepreg	• Up to 120% in K_{IC} (mode I interlaminar opening crack using DCB test)	[39]
Encapsulated fibers	DGEBA + DETDA	Carbon fiber laminates	• Up to 100% in peak load (mode I interlaminar opening crack using DCB test) • 50-60% peak loads (ILSS test).	[41]
	DGEBA + TETA			

DETDA – Diethyltoluenediamine, ILSS – interlaminar shear strength, DCB – Double Cantilever Beam, K_{IC} – fracture toughness, G_{IC} – critic fracture energy.

Poly(ethylene-co-methyl acrylate) (E-MA)

In other study [39], the acrylate thermoplastic copolymer poly(ethylene-co-methyl acrylate) (E-MA) (Figure 2. 28) was employed as healing agent in prepreg laminates. In this work [39], films of 0.15 mm thickness of E-MA and E-MAA were produced by hot pressing thermoplastics pellets. The thin films were placed between carbon fiber prepreg layers and were regularly cured in autoclave at 75 ˚C for 5 h with a pressure of 830 kPa and post-cured at 150 ˚C for 1 h in an oven. Samples were subjected to interlaminar fracture tests followed by healing cycle in order to assess healing efficiency.

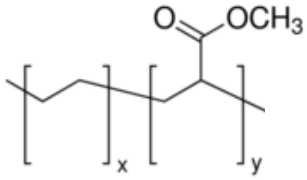

Figure 2. 28 - Chemical structure of poly(ethylene-co-methyl acrylate) (E-MA).

Results showed that both E-MAA and E-MA enhanced the interlaminar fracture toughness [39]. Figure 2. 29 exhibits SEM images of the morphology of the interlaminar fracture of tested with no healing agent addition (Figure 2. 29(a)) and samples with EMA (Figure 2. 29 (b)), EMAA (Figure 2. 29 (c)).

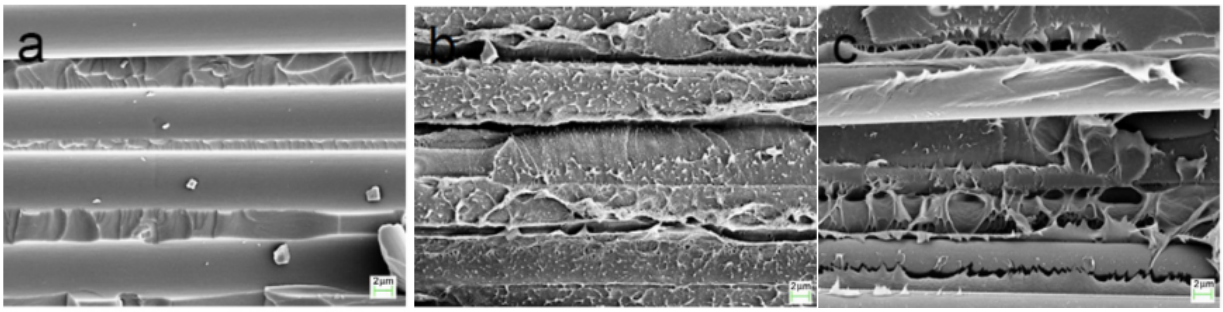

Figure 2. 29 - SEM images of the effect of healing agent on interlaminar fracture of carbon fiber prepreg laminates: (a) with no healing agent addition, (b) with E-MA and (c) with E-MAA [39].

Compared with the unmodified system (Figure 2. 29(a)), the interlaminar fracture surface showed ductile tearing in the thermoplastic copolymers (Figure 2. 29(b) and (c)), revealing that the healing agents melted after the heating treatment. Further, authors also pointed the nanoscale biphasic structure presented in samples with E-MA addition. Therefore, it has been proposed that “ionic aggregation created a physically cross-linked, though thermally reversible structure that retained mechanical properties at both room temperature and in the melt state” [39]. This result is consistent to others works [43–45] , which studied the miscibility and the formation of nanoporous structure in consequence of the addition of other acrylate polymer, poly(methyl methacrylate) (PMMA), to epoxy resin. Figure 2. 30 show the morphologies of epoxy/PMMA blends with different molecular weights of PMMA, where the nanoporous structure can also be observed.

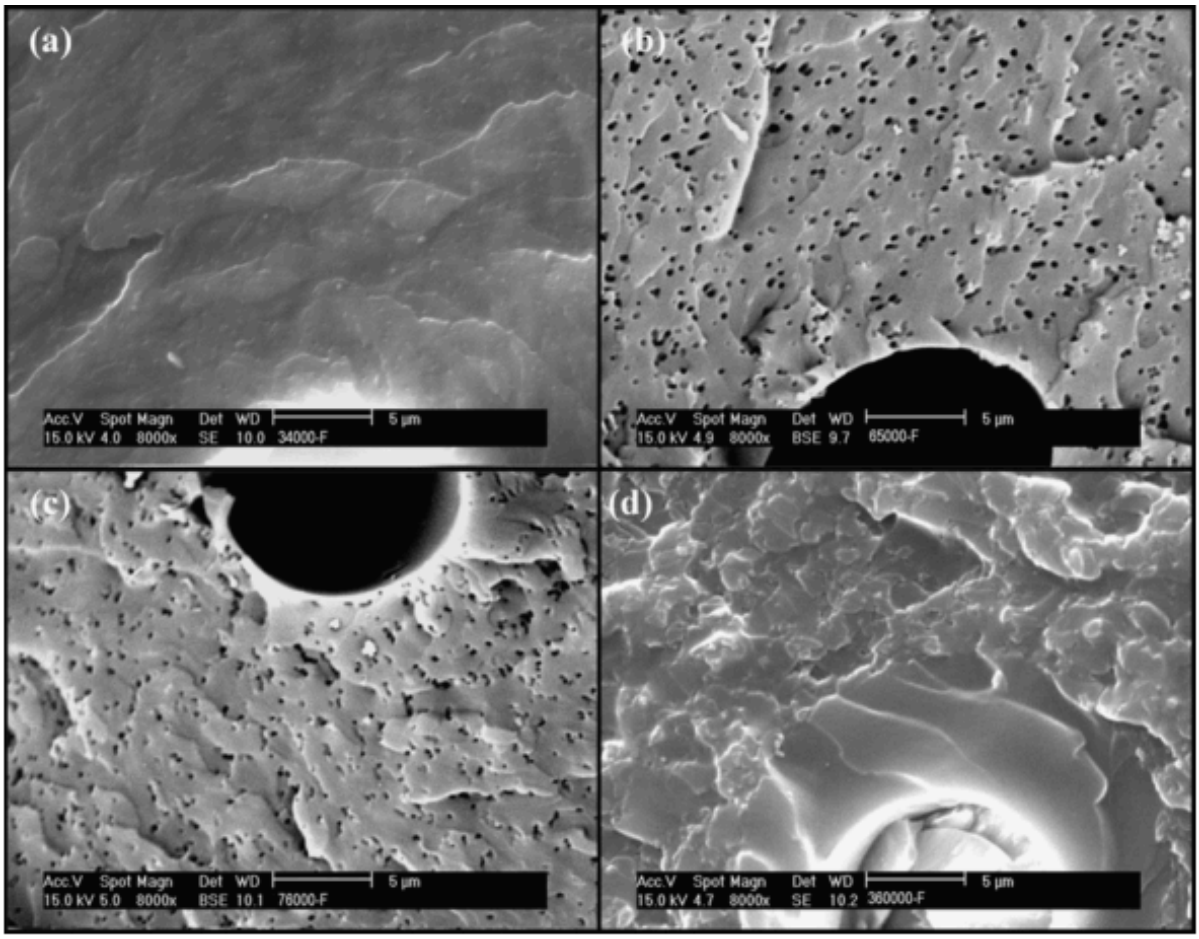

Figure 2. 30 - SEM images taken from the fractured surface of glass fiber reinforced epoxy/PMMA samples: (a) EP/PMMA 34.000 M_w; (b) EP/PMMA 65.000 M_w; (c) EP/PMMA 76.000 M_w and (d) EP/PMMA 360.000 M_w [45].

In the cited study [39], however, E-MAA healing agent demonstrated better results than E-MA in terms of healing efficiency. Authors remembered that the effective healing depends on several factors such recover mechanical properties before and after melting and flow sufficiently to infill damaged regions [39]. Further, authors also mentioned that one possible reason to the lower performance of E-MA healing agent is due the extensive nanoporous structure that may have restricted toughening and consequently its healing effect, as it can be observed in Figure 2. 31. Moreover, the pressure delivery mechanism from E-MAA healing agent has also played a determining role to enhance its healing efficiency over E-MA thermoplastic.

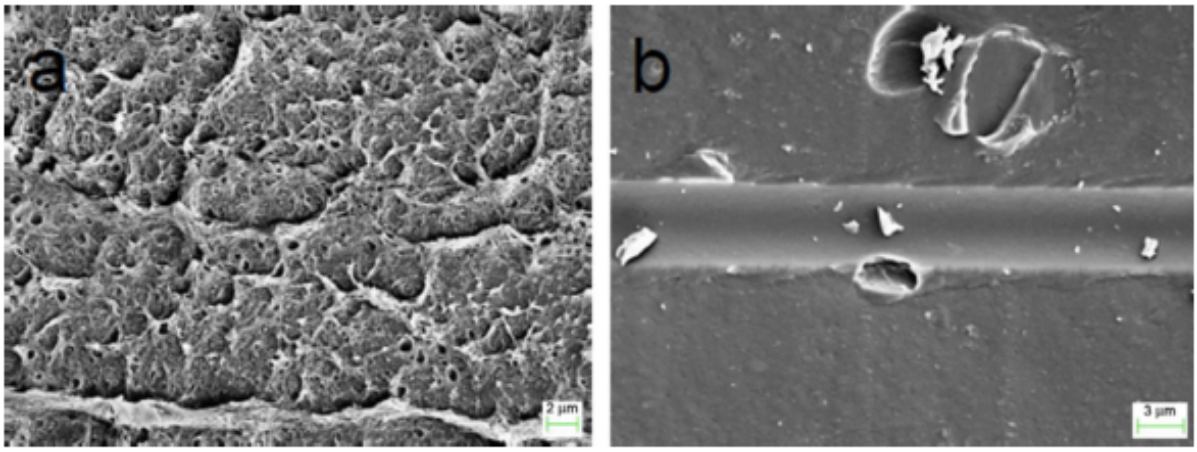

Figure 2. 31 - SEM images from the morphology of delaminated surface containing (a) E-MA and (b) E-MAA healing agents after healing cycle [39].

As it has been demonstrated, chemical changes are crucial to better understand interaction between acrylic polymers and epoxy.

Poly(ethylene-co-glycidyl methacrylate) (E-GMA)

In other studies [32,33,38] the copolymer poly(ethylene-co-glycidyl methacrylate) (E-GMA) was used as healing agent. One of the main reason of E-GMA has been chosen as healing agent was the glycidyl pendant group that “could enable interfacial reactions with the residual amine from the epoxy matrix and exhibit a similar healing mechanism as E-MAA” [33]. Chemical structure of E-GMA is given in Figure 2. 32.

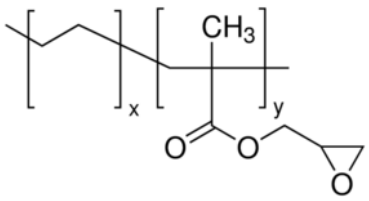

Figure 2. 32 - Chemical structure of poly(ethylene-co-glycidyl methacrylate).

In all studies [32,33,38] pellets of E-GMA were cryogenically ground and sieved to obtain a particle size in a range of 149-425 µm. Similar processing route for E-MAA studies was adopted, that is stirring the thermoplastic particles with DGEBA monomer at 65 ˚C for 30 min. After mixing, the blend was degassed for 25 min in a vaccum oven at 50 ˚C and allowed to cool down until room temperature. Then TETA hardener was added in a proportion of 13 to 100 g of DGEBA monomer,

producing a 1 : 1 stoichiometric network. E-GMA particles were added to the resin at weight fraction of 5, 10 or 15 % and remained immiscible during all the processing route. The blend mixture was allowed to cure at room temperature during approximately 15 h and then post cured at 50 ˚C for 90 min and 150 ˚C for 30 min.

Carbon fiber laminates [32,38] and polymeric SENB samples [33] were produced in order to assess the healing efficiency of the particles. In all cases, E-GMA particles revealed excellent healing ability. Fracture surface of E-GMA and others thermoplastic healing agents after one healing cycle are shown in Figure 2. 33. It was observed that E-GMA (Figure 2. 33(c)) presented very similar behavior to E-MAA (Figure 2. 33(a)) and EVA (Figure 2. 33(e)) thermoplastic healing agents, which reveals an extensive flow and large plastic deformation, indicating an excellent adhesion between epoxy matrix and the thermoplastic. In contrast, other thermoplastics as ABS (Figure 2. 33(b)), PVB (Figure 2. 33(d)) and SEBS (Figure 2. 33(f)) showed a brittle fracture characterized by the well-defined boundaries between particles and epoxy matrix and also by no indication of flow of particles.

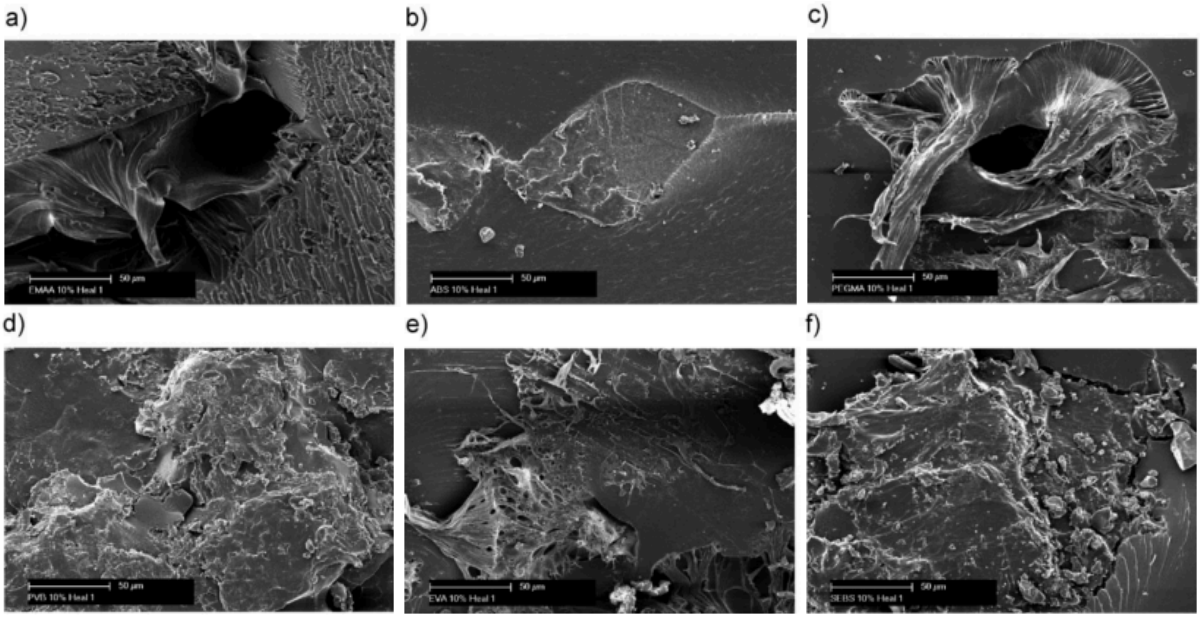

Figure 2. 33 - SEM images of the SENB fracture surfaces of the 10wt% thermoplastic modified samples after one healing cycle for each thermoplastic healing agent: (a) E-MAA, (b) ABS, (c) E-GMA, (d) PVB, (e) EVA and (f) SEBS [33].

Further, authors [33] also suggest that the healing mechanism of E-GMA particles appears to be a hybrid of the pressure delivery mechanism from E-MAA particles and elastomeric tearing from EVA. The explanation to the similarity to the

E-MAA pressure delivery mechanism relies on the bubbles existing in the fracture surface, which most likely appeared from condensation chemical reactions between E-GMA particles and epoxy matrix [33]. Figure 2. 34 show more SEM images of the crack area at distinct magnifications of one and four healing cycles for the E-GMA modified epoxy system.

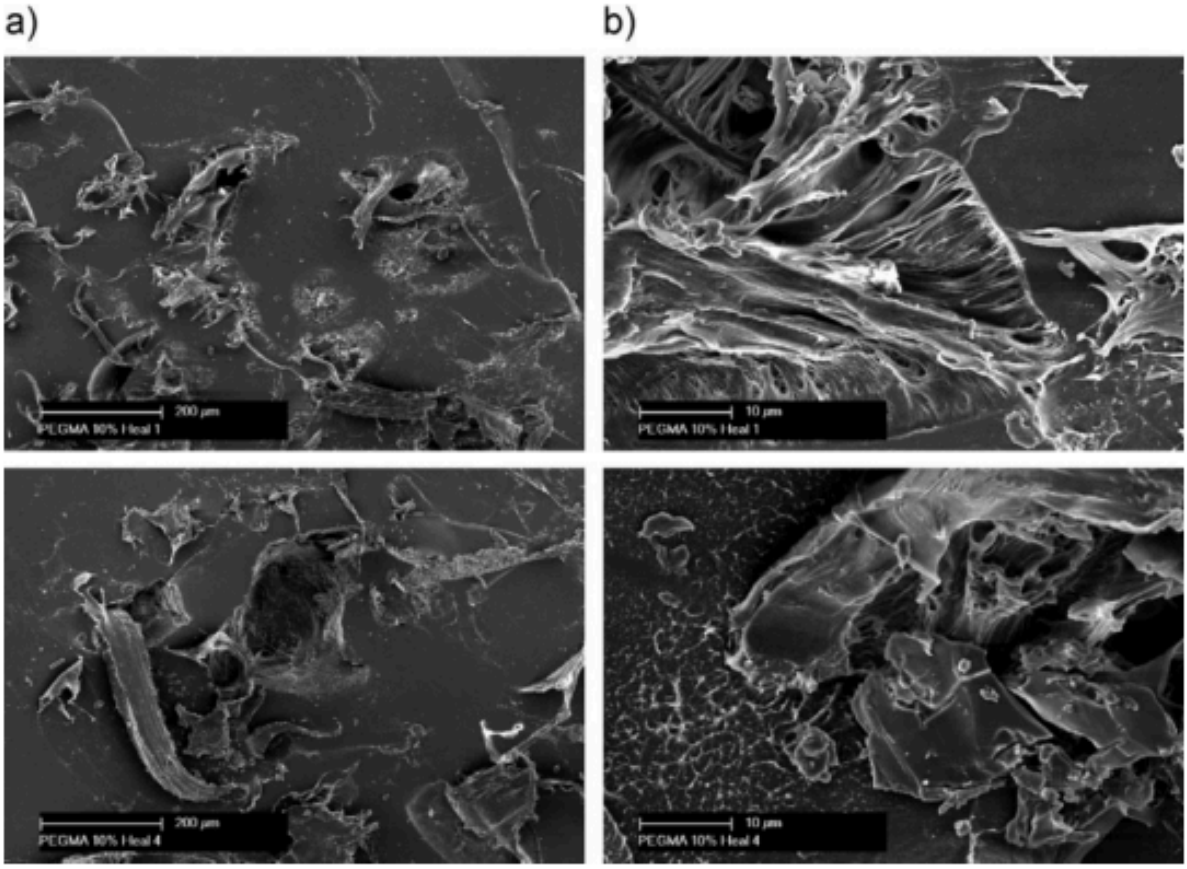

Figure 2. 34 - SEM images comparing cracking surfaces after 1 (top) and 4 (bottom) healing cycle for 10 wt% E-GMA modified epoxy resin systems at (a) low and (b) high magnifications [33].

In the following section, an overview of the most recent works will be addressed in order to discuss the main features to better understand healing processes and the pathway to select efficient healing agents.

2.2.4 Overview

It is very important to notice that not all thermoplastics can be employed as healing agents [38]. As mentioned in the previous sections, the thermoplastics must attend some requirements to be eligible as healing agent. One of the major properties thermoplastic healing agents must have is low melting temperature and viscosity, which allow them to flow efficiently into open cracks, while the thermoset matrix continues above the glass transition during the high temperature of healing process. Thus, healing temperature conventionally should be above of the thermoplastic melting point/glass transition temperature but below the glass transition of the thermoset matrix.

> *"In practice however, some mobility of the crosslinked matrix is required to facilitate adhesion of the thermoplastic to the epoxy matrix during healing and after cooling. Having some tackiness, flexibility or molecular mobility of the epoxy matrix during the healing process therefore, is likely to be beneficial to healing because of the increased propensity for diffusion between the thermoplastic and crosslinked network"* [33].

For this reason, it is acceptable that healing cycle occurs in a range of temperature just above the thermosetting glass transition, as long as no degradation in matrix is envisioned [33].

In two very insightful studies [33,38] dynamic mechanical thermal analyses (DMTA) were performed in order to verify changes in glass transition temperature of DGEBA/TETA samples containing 10 wt% of various thermoplastics.

In the first study [33] only polymer samples were analyzed, which typical curves are given in Figure 2. 35. Results show that the healing temperature of 150 ˚C was optimal once at this temperature all thermoplastics have melted and the epoxy matrix had just attained the rubbery plateau, according to the drop on storage moduli (Figure 2. 35(a)) and tan δ (Figure 2. 35(b)). Further, authors also mentioned that despite all thermoplastics agents did not present considerable miscibility with epoxy matrix, all mixtures exhibited a decrease in Tg values and a broadening of tan

δ compared to neat epoxy samples. This result indicates that the addition of thermoplastic restricted the thermosetting network formation, consequently creating a more heterogeneous network, which derive from an increase in the viscous part (loss moduli) and where possible, interfacial chemical reactions promoted by the adhesion of thermoplastic and epoxy matrix. Other relevant reason that could explain the changes in the DMTA curves is that "interfacial reactions would also be expected to alter epoxy amine stoichiometry further impacting network development" [33].

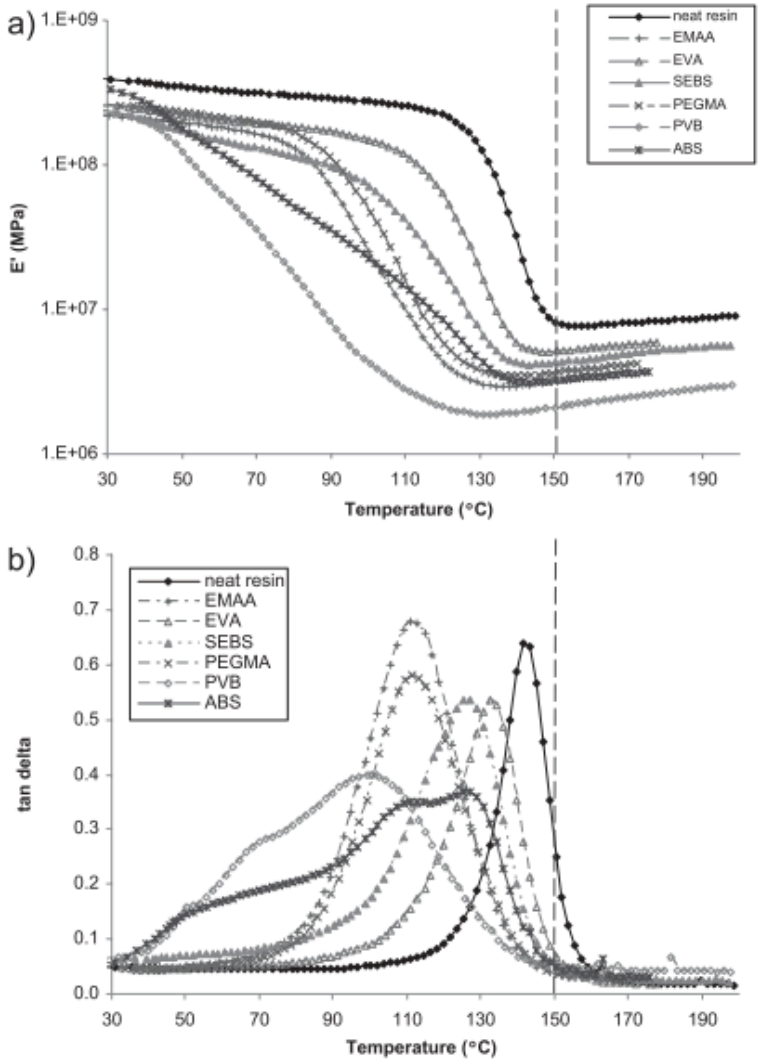

Figure 2. 35 - DMTA spectra of DGEBA/TETA cured resins modified with 10 wt% of the thermoplastic healing agents: (a) storage modulus, E' and (b) tan δ [33].

Other important information from these DMTA spectra lies on the ABS modified epoxy resin system, which presented a constant drop of its storage modulus (Figure 2. 35(a)). In this case, authors used a DGEBA/diethyl toluene diamine (DETDA) hardened epoxy system instead of DGEBA/TETA, as used in the

other thermoplastics. Authors observed that the ABS particles have dissolved in the epoxy matrix resulting in a 1-2 μm randomly dispersed particles into the cured sample, as shown in Figure 2. 36. The resulting morphology is entirely different from other thermoplastic one, which normally presented a 149-245 μm embedded particles size.

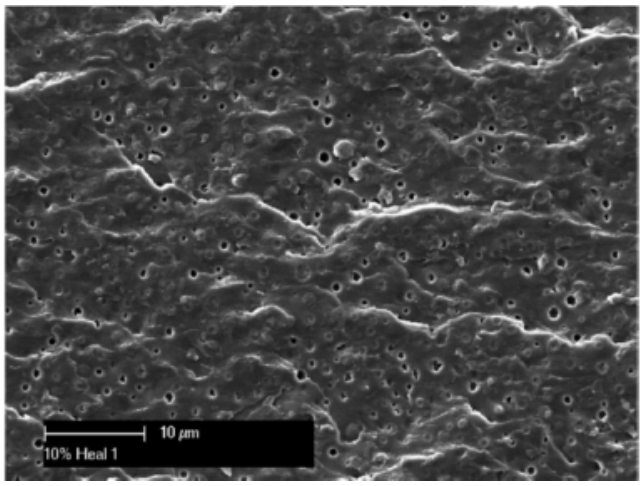

Figure 2. 36 - SEM images of fracture surface after one healing cycle for 10wt% ABS/DGEBA/DETDA resin system [33].

Further, as compared to other thermoplastic healing agents, mechanical tests revealed that DGEBA/DETDA epoxy modified with ABS presented no significant healing ability [33]. Authors suggest that this low level on healing is leaded by the reduced amount of thermoplastic available to heal and also by the poor adhesion of ABS to the thermosetting network. Furthermore, authors also mentioned that the pressure delivery mechanism depends on large thermoplastic particle size, which acts as dormant reservoirs of healing agents so smaller sized particles are incapable of delivering useful amounts of healing material to heal cracks [33].

In the second study [38], carbon fiber composite samples with containing a weight fraction of 10 % of thermoplastic healing agent were analyzed. Typical values of Tg, according to the onset drop on storage moduli (E') are given in Table 2. 6. Compared to glass transition temperature of unmodified resin systems (90 ˚C), it was observed that the effect of thermoplastic addition on Tg values was fluctuating. While E-GMA additions resulted in a decrease, E-MAA, EVA and ABS presented an increase in Tg. Authors mentioned however that the increasing and decreasing were modest if compared to neat resin Tg values. Other important observation is that as

compared to only polymer Tg values (Figure 2. 35(a)), it is evidenced that composite materials (Table 2. 6) are less influenced by the addition of thermoplastic healing agents.

Table 2. 6 - Thermal properties of carbon fiber composites containing 10 wt% of different thermoplastic healing agents [38].

Composite	Glass transition temperature, Tg (˚C)
Unmodified resin	90
E-GMA	83
E-MAA	97
EVA	97
ABS	92

As it was mentioned in the previous sections, it is crucial that the thermoplastic healing agent presents sufficient mobility to flow during healing process. For this reason, studying rheology of healing agents at elevated temperatures is decisive to predict and estimate its healing ability. In the study [33], rheological analysis were performed using several healing agents as shown in Figure 2. 37.

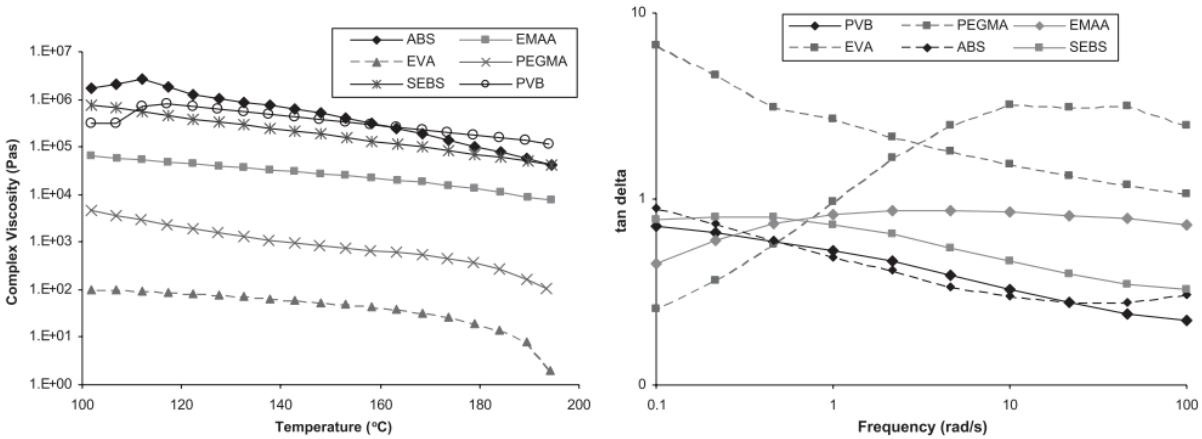

(a) (b)

Figure 2. 37 - Rheological analysis for different thermoplastics healing agents: (a) complex viscosity as a function of temperature; (b) tan δ as a function of frequency at the fixed temperature of 150 ˚C [33].

Rheological behavior along different temperatures (Figure 2. 37(a)) shows that thermoplastics may be categorized into two groups according to their viscosity.

The first group is represented by the high viscosity polymers composed by ABS, SEBS and PVB thermoplastics, which exhibited very similar and constant viscosity along all the temperature range. The second group is composed by the low viscosity polymers, which, in order of viscosity, are represented by E-MAA, E-GMA and EVA. Authors also pointed that “in the absence of a pressure delivery mechanism, low viscosity therefore is important for facilitating repeated healing” [33]. For this reason, EVA modified epoxy exhibited the highest degree of load recovery and repeatability among all the thermoplastics studied in the cited study [33]. In contrast to this result, ABS, SEBS and PVB which have the highest viscosities, presented the lowest degree of healing, specially after repeated healing cycles [33].

In addition to the viscosity profile along different temperatures, the viscoelastic response of the thermoplastic over different frequencies at a specific temperature are determining to support the use of a thermoplastic as healing agent. The viscoelastic behavior is determined by the tan δ values, which are defined as the fraction between elastic shear modulus, G”, and loss shear modulus, G’. Figure 2. 37(b) shows the tan δ spectra for different frequencies at 150 ˚C. Results show that ABS, SEBS and PVB have a solid-like behavior (i.e. tan $\delta < 1$) despite at this temperature they were already melted. On the other hand, E-MAA, E-GMA and EVA presented different viscoelastic behavior. E-MAA tan δ remained near of the unity along all the frequencies, indicating an equilibrium between the solid and liquid-like behavior at 150 ˚C. This property is interesting due to the advantageous balance for during and after healing process. E-GMA also presented a balance between solid and liquid-like behavior, attaining however a considerable increase in tan δ at higher frequencies, reiterating its ability to flow during healing. The EVA tan δ exhibited a liquid-like behavior under all frequencies conditions, confirming that its healing ability is mainly driven by its flow capacity [33]. Figure 2. 38 summarizes the major mechanisms of healing for the main thermoplastics abovementioned.

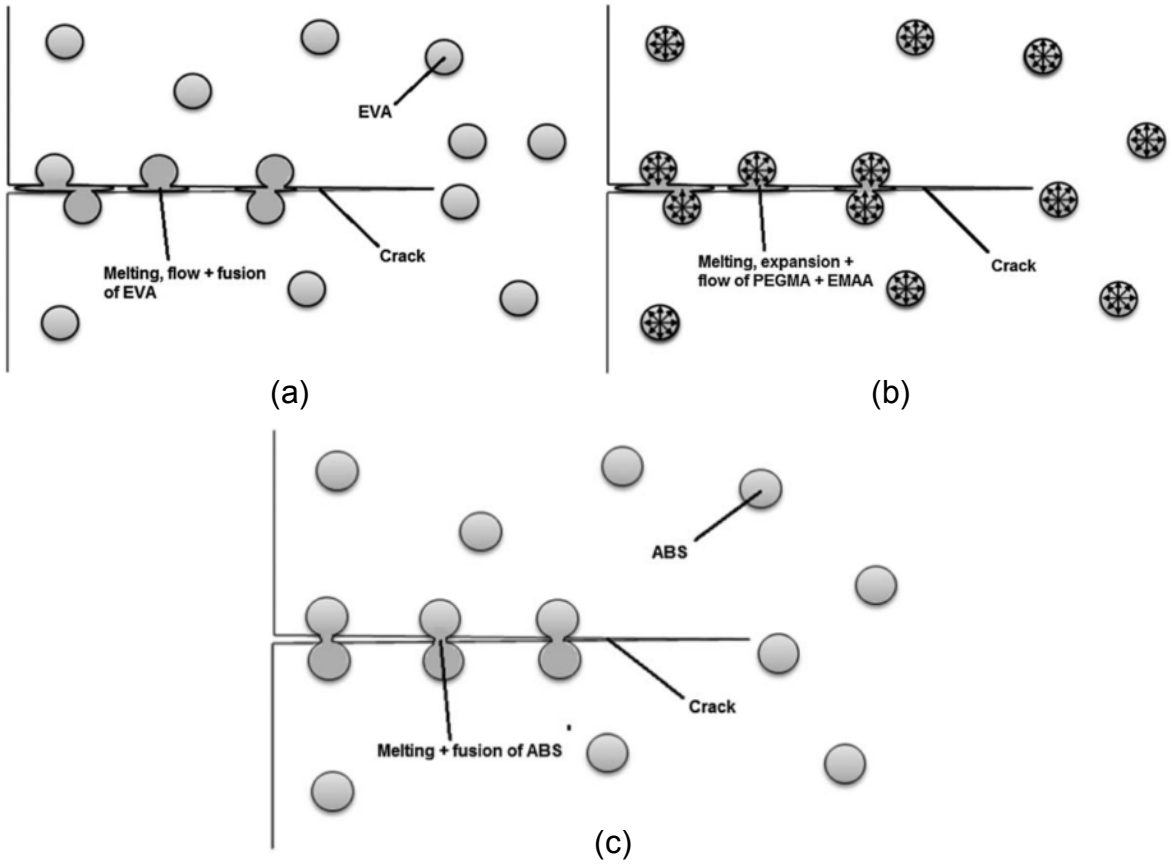

Figure 2. 38 - Schematic of healing mechanism for (a) EVA, (b) E-GMA or E-MAA and (c) ABS, SEBS and PVB thermoplastics [38].

Other relevant property thermoplastic healing agents should present is strong adherence to the epoxy matrix in order to provide strong binding ability after infilling open cracks [38]. Weak non-covalent bonds, as hydrogen bonds, are essential to ensure that the thermoplastic could melt and flow, as much as it remains strongly adhered to the crack surfaces when solid, therefore achieving good healing performance. Figure 2. 39 displays the effect of various thermoplastic additives in the delamination area of composite samples after healing.

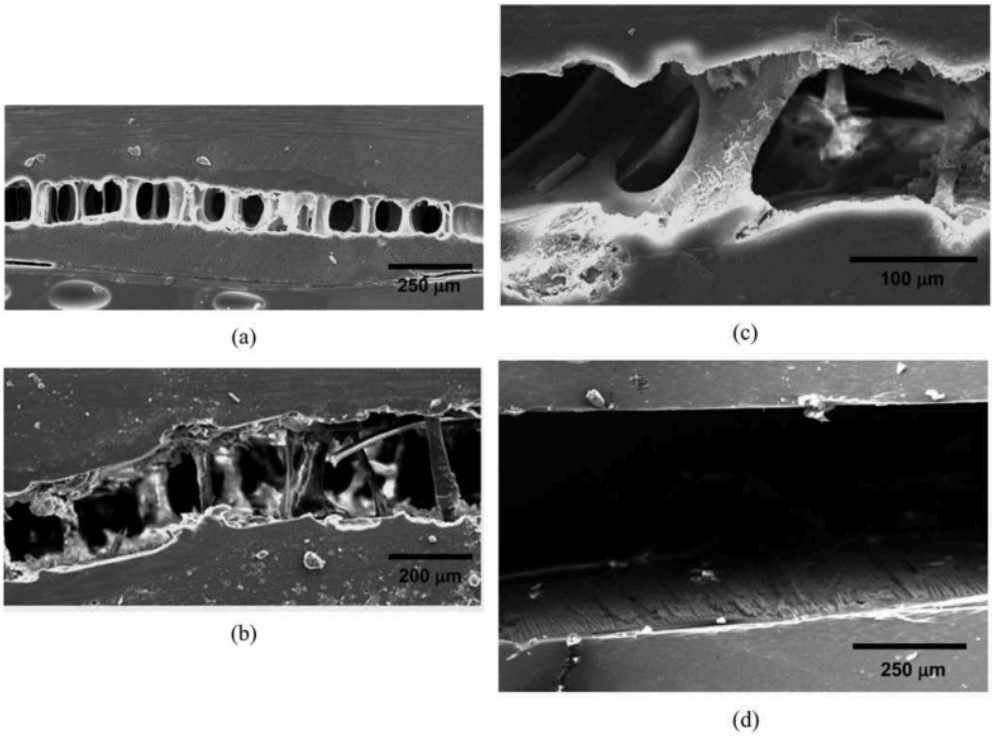

Figure 2. 39 - Delamination cracks in composites containing (a) EMAA, (b) PEGMA, (c) EVA and (d) ABS [38].

Table 2. 7 gives an overview of the main thermoplastic healing agents used in literature.

Table 2. 7 - Main thermoplastic found in literature used for self-healing purposes.

Mechanism of healing	Thermoplastic / prepolymer	Rheological properties	Melting / glass transition temperature (˚C)
Viscous flow	Epoxy particles	-	110-140 [25]
	EVA	Viscosity*: 3 x 10^3 Pa.s [33] MFI: 57 g/10 min (190˚C, 2.16kg) [46]	< 90 [33]
	ABS	Viscosity*: 8.3 x 10^4 Pa.s [33] MFI: 1-3 g/10 min (230˚C, 3.8kg) [47]	< 120 [33]
	SEBS	Viscosity*: 4.0 x 10^4 Pa.s [33] MFI: 10g/10min (200˚C, 5.0kg) [48]	< 90 [33]
	PVB	Viscosity*: 6.9 x 10^4 Pa.s [33]	
Molecular dissolution	PBE	-	Tg: 36˚C [49]
Thermally reactive	PCL	MFI: 9g/10min (80˚C, 2.16kg) [50]	55-60 [35]
	E-MAA	Viscosity*: 8.1 x 10^3 Pa.s [33] MFI: 60 g/10min (190˚C, 2.16kg) [51]	< 90 [33,41]
	E-MA	MFI: 2-6.0 g/10min [52,53]	81 [53]
	E-GMA	Viscosity*: 4.8 x 10^2 Pa.s [33] MFI: 5g/10min (190˚C, 2.16kg) [54]	< 100 [33,54]

* Complex viscosity at 147˚C.

Despite all the progress in the research of modified epoxy resins with thermoplastic healing agents, some issues are still needed to be further understood. As it was mentioned in previous studies [24,35], chemical changes on the polymer mixtures are determining to highlight mechanisms of interfacial bonding between thermoplastic and thermoset matrix. However, there is still a lack on studies on other thermoplastic healing agents, specially on those interfacial chemical reactions are expected, i.e. the thermally reactive thermoplastics, as E-GMA and E-MA. Further, the role that other epoxy matrices systems play is also a decisive feature that still need to be deeply appreciated.

For this work, the thermoplastic poly(ethylene-co-methyl acrylate-co-glycidyl methacrylate) (E-MA-GMA) was selected as healing agent due to its similar chemical structure to other thermoplastic healing agents discussed in literature, E-MA and E-GMA. Moreover, MFI (6g/10min, 190˚C, 2.16kg) [55,56] and melting point (65˚C) [55,56] of E-MA-GMA indicate that this material is a potential candidate for the use as self-healing agent in epoxy matrices.

3 Objectives

The objective of this work is to investigate the influence of the addition of the thermoplastic poly(ethylene-co-methyl acrylate-co-glycidyl methacrylate) (E-MA-GMA) to epoxy matrix for self-healing purposes in polymer matrix composites and assess the self-healing ability of modified material, as compared to neat epoxy. Influences of this addition of thermoplastic on processing, thermo-mechanical properties and chemical alterations in epoxy with two different hardeners types were analyzed.

4 Experimental

In this section the starting materials and the experimental procedures followed in the present work are addressed.

4.1 Starting materials

The epoxy resin systems used were diglycidyl ether of bisphenol A (DGEBA) based monomer (Araldite MY 750 and GY 260), diethyl toluene diamine (DETDA) and methyl tetrahydrophthalic anhydride (MTHPA) hardeners, and benzyl dimethylamine (BDMA) (Accelerator D 062), a tertiary amine that, in this case, acts as an accelerator for MTHPA hardener system. Chemical structures are shown in Figure 4. 1. Some of the main properties of the resin systems are given in Table 4. 1.

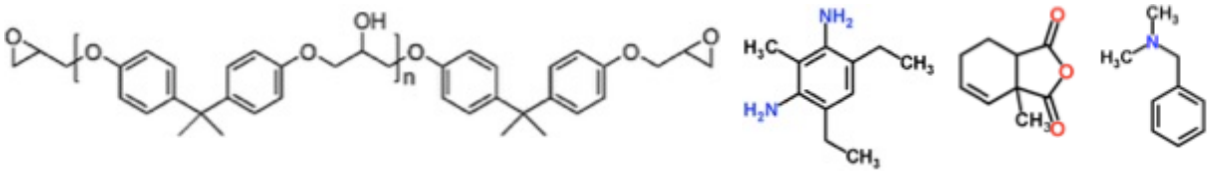

(a) (b) (c) (d)

Figure 4. 1 - Chemical structures of the constituents used in epoxy resin systems: (a) DGEBA epoxy monomer, (b) DETDA hardener, (c) MTHPA hardener and (d) BDMA accelerator.

Table 4. 1 - Physical properties of the epoxy resin systems reactants [57,58]

	DGEBA (MY 750)	**DGEBA (GY 260)**	**DETDA**	**MTHPA**	**BDMA**
Molecular weight	< 700	< 700	-	-	-
Aspect/color	Liquid and transparent	Liquid and transparent	Liquid yellowish to dark brown	Liquid yellowish	Liquid yellowish
Viscosity at 25˚C (mPa·s)	12,000 – 16,000	11,000 – 16,000	95 – 145	50 – 100	≤ 50
Density (g/cm^3)	1.13 – 1.19	1.10 – 1.20	0.99 – 1.02	1.16 – 1.20	0.85 – 0.95
Flash point (˚C)	> 160	185	121	> 140	92

The thermoplastic healing agent selected for this study was poly(ethylene-co-methyl acrylate-co-glycidyl methacrylate) (E-MA-GMA) copolymer from Sigma-

Aldrich Brazil. Its chemical structure is given in Figure 4. 2. It consists of an epoxy functional random acrylic copolymer (also named epoxy acrylate [19]), which carries on the chain an ethylene (E) group, a methyl acrylate (MA) group and an epoxy group (glycidyl methacrylate – GMA), in the proportion of 67, 25 and 8 wt%, respectively.

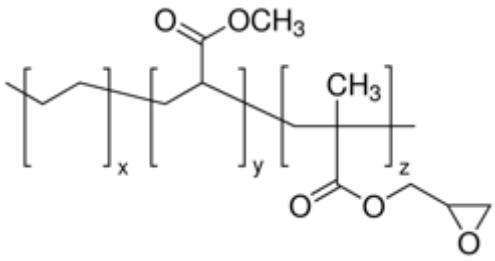

Figure 4. 2 - Chemical structure of E-MA-GMA copolymer.

Table 4. 2 summarizes some of the general properties of E-MA-GMA terpolymers used in industry. According to one of E-MA-GMA suppliers [55], the methyl acrylate functional group on the copolymer chain brings softness and polarity, while keeping high thermal stability during processing, whereas it also leads to high flexibility (low cristallinity) and, consequently, high impact absorption behavior. The glycidyl methacrylate group gives reactivity (between –OH, –COOH and $–NH_2$ groups), which leads to optimal dispersion during melt mixing with engineering thermoplastics.

Table 4. 2 - Typical properties of E-MA-GMA copolymer [55,56].

Properties	**Value**	**Unit**	**Test method**
Methyl acrylate content	25	wt%	
Glycidyl methacrylate content	8	wt%	
Melt index (190˚C/ 2.16 kg)	6	g/10min	ASTM D1238
Melting point	65	˚C	ISO 11357-3
Density	0.94	g/cm^3	ISO 1183
Vicat softening temperature	<40	˚C	ISO 306
Hardness Shore A	70		ASTM D2240

Considering E-MA-GMA chemical structure, which may most likely react with other epoxy hardener groups (as amine and anhydride) during the curing process, it is expected that interfacial chemical reactions between the two phases (thermoset-

thermoplastic) will be achieved. Furthermore, as previously reported in literature other acrylic copolymers, as poly(ethylene-co-glycidyl methacrylate), E-GMA [32,33,38], and poly(ethylene-co-methyl acrylate), E-MA [39], which chemical structure are very similar to E-MA-GMA, has also exhibited healing capabilities. Therefore, E-MA-GMA was chosen as the thermoplastic material employed in this study.

4.2 Sample preparation

Interactions between E-MA-GMA pellets and epoxy

In order to evaluate interactions between E-MA-GMA copolymer and epoxy liquid reactants, E-MA-GMA pellets were mixed for 1-2 h using a propeller stirrer 3-bladed under constant heating with: (i) diglycidyl ether of bisphenol-A (DGEBA) (Araldite MY 750) monomer, (ii) methyl tetrahydrophthalic anhydride (MTHPA) (Aradur HY 2918) and (iii) diethyl toluene diamine (DETDA) (XB 3473) hardeners.

During the blending process, when the temperature surpassed 90 ˚C (which is above the melting temperature of E-MA-GMA) pellets started to agglomerate forming a cluster. As no further homogenization was envisioned, the test was interrupted. Except by the E-MA-GMA agglomeration, no prominent changes were observed in the liquid systems. This indicates that no relevant chemical interactions occurred at those conditions.

Cryogenic grinding of E-MA-GMA pellets

As an attempt to improve homogeneous dispersion and, consequently, higher interactions with the resin system, cryogenic grinding of E-MA-GMA pellets was conducted using a hand blender in a liquid nitrogen cooled recipient. Liquid nitrogen was poured into the recipient containing E-MA-GMA pellets and the pellets remained submersed for about 10 minutes when the nitrogen was completely evaporated. After grinding, E-MA-GMA was sieved to obtain a particle size range of 200 to 400 μm (Figure 4. 3).

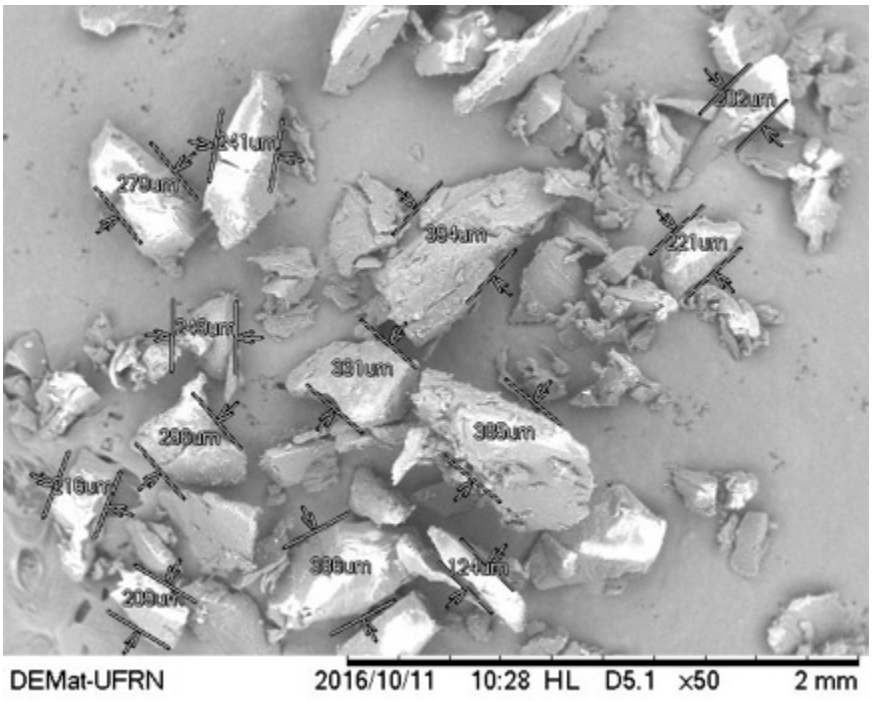

Figure 4. 3 - E-MA-GMA particles.

Mixture of E-MA-GMA particles with epoxy resin systems

Mixture of E-MA-GMA particles with epoxy resin systems was performed under constant agitation using a 3-bladed propeller stirrer and the temperature was monitored by a thermocouple. In all experiments, a content of 2.5 wt.% E-MA-GMA particles was added to the mixture. The constituent proportions of each resin system used are given in Table 4. 3.

Table 4. 3 - Proportions of each constituent used in the epoxy resin system.

Epoxy resin system	**Constituent**	**Weight (g)**
Anhydride hardener	DGEBA (MY 750)	100
	MTHPA (HY 2918)	85
	BDMA (DY 062)	2
Amine hardener	DGEBA (GY 260)	100
	DETDA (XB 3473)	23

The experiments were carried out in the following conditions:

i. **Room temperature mixtures**: Both DGEBA and MTHPA anhydride hardener were mixed together with E-MA-GMA particles for 15 minutes. After this procedure, the tertiary amine accelerator, BDMA, was added and mixed for 5 more minutes. The same procedure was taken for DGEBA and DETDA amine hardener mixtures, for which the same 20 minutes of total mix processing was accomplished. All samples were poured into a silicon mold and then cured.

ii. **Mixtures at 65˚C**: DGEBA, MTHPA anhydride hardener and E-MA-GMA particles were mixed together for 75 minutes. After this procedure, BDMA amine accelerator was added to the mixture and homogenization was carried out for 5 more minutes before the mixture was poured into a silicon mold for curing. The same procedure was adopted for the DETDA amine hardened epoxy resin. However, in this case, the mixture was homogenized for 80 minutes and degassed for 10 minutes before it was poured into the silicon mold.

In both experiments, samples of neat epoxy resin were processed using the same mixing conditions. Table 4. 4 summarizes the parameters used for sample processing.

Table 4. 4 - Parameters used for the sample processing for conditions (i) and (ii).

Epoxy resin system	**Mixing temperature (˚C)**	**Time under agitation (min)**	**Cure cycle**	**Post-cure cycle**
DETDA amine hardener	Room temp.	20	4 h at 120˚C	-
	65	80		
MTHPA anhydride hardener	Room temp.	20	2 h at 80˚C	2 h at 120˚C
	65	80		

4.3 Material characterization

Image photographs

Images of cured samples were obtained using an *EOS 6D Canon* digital camera equipped with a 100 mm macro lens and diffused flash at a fixed focal point.

Dynamical Mechanical Thermal Analysis (DMTA)

Dynamic mechanical thermal analysis (DMTA) was performed using a *Q800 Dynamic Mechanical Analyzer* (TA Instruments) with samples positioned in dual cantilever configuration. Samples with approximately 2.5 x 12.5 x 50 mm dimensions (thickness x width x length) were tested at a frequency of 1Hz and then ramped from room temperature to 160˚C at a heating rate of 2˚C/min. All tests were performed in duplicates of condition (ii) samples.

Fourier Transform Infrared (FTIR) Spectroscopy

In order to investigate the chemical reactions between E-MA-GMA particles and the two different epoxy systems (DETDA and MTHPA hardened), Fourier transform infrared (FTIR) spectroscopy was carried out on cured samples of approximately 3 mm thickness using a *Shimadzu IRTracer – 100 Spectrometer* in Attenuated Total Reflectance (ATR) mode. The analysis conditions were 32 scans, at a range of 750-4000 cm^{-1} and 4 cm^{-1} resolution. Rich and poor thermoplastic areas from cured epoxy samples mixed at 65˚C, rich thermoplastic area from cured epoxy samples mixed at room temperature, along to its respective neat epoxy systems and neat E-MA-GMA were analyzed. All FTIR spectra were obtained, at least, in duplicate.

Atomic Force Microscopy (AFM)

In order to investigate the microstructure of epoxy samples with and without thermoplastic addition, an atomic force microscope *Shimadzu SPM-9700* was used. The system was operated in tapping mode using a silicon probe. Topographic images were obtained using a resonance frequency of approximately 320 kHz. The

surface of the sample was prepared using an ultramicrotome with a diamond blade under liquid nitrogen cooling of approximately -80 ˚C. In order to verify microstructural changes into the bulk material, the microtomed fracture was performed in a central region of the thickness for all condition (ii) samples.

Self-healing effect assessment – Indentation method

Specimens of neat DETDA epoxy and also epoxy/E-MA-GMA mixture were cut with nominal dimensions of 64 x 13 x 3 mm (l x w x h) and subjected to a post-cure cycle in order to increase crosslink density. The indentation produces permanent damage on the surface of the brittle post-cured specimens. Considering post-cure cycles mentioned in literature [41], DETDA epoxy systems were subjected to 150 ˚C for 5h.

A damaged area was created on sample surface using a *WMP Leipzig HPO 250* Vickers hardness tester. A standard load-time of 30 kgf-10 s was applied on the sample surface.

After indentation, samples were placed in an air-circulated oven at 150 ˚C for 5 h. The healing cycle was defined taking into account the melt index of E-MAA (60 g/10min), which is 10 times the E-MA-GMA melt index (6 g/10 min), meaning that the time to E-MA-GMA will be *a priori* 10 times longer than the duration of E-MAA typical healing cycles (30 min at 150 ˚C). Changes in damaged area dimensions were observed using an *Nikon Eclipse MA200* inverted optical microscope at 50 x magnification. A schematic drawing showing the proposed healing effect assessment is shown in Figure 4. 4.

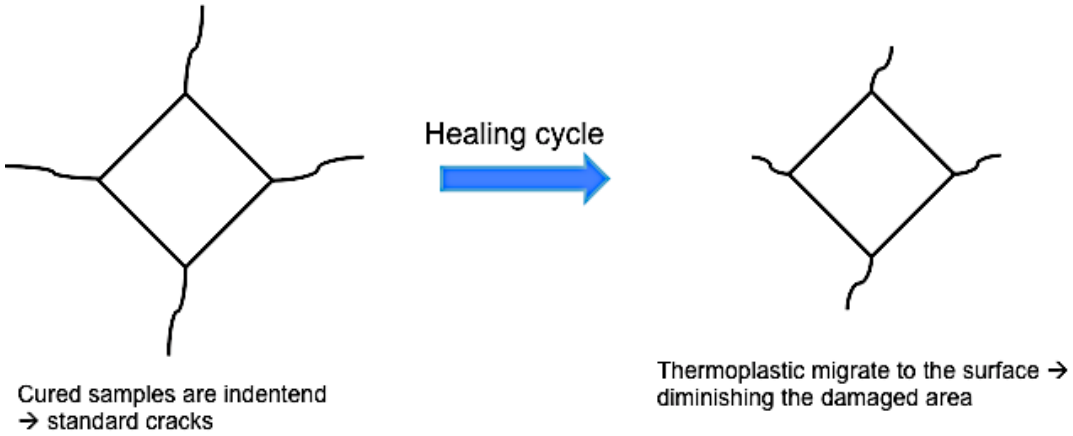

Figure 4. 4 - Schematic drawing of the assessment of healing effect using indentation method.

5 Results and discussion

5.1 General aspect

During processing at condition (i) (room temperature mixture) no apparent changes were observed in both amine DETDA and anhydride MTHPA hardened resin systems. As a consequence, all cured samples demonstrated a phase separation. A typical two phase image of the samples is given in Figure 5. 1. It can also be observed that MTHPA anhydride samples presented a more explicit E-MA-GMA phase separation (Figure 5. 1(a)) than the one observed in DETDA samples (Figure 5. 1(b)). As the same content of E-MA-GMA was used in both processing conditions, this result suggests that E-MA-GMA material dissolved more in the DETDA resin system than in the MTHPA resin system.

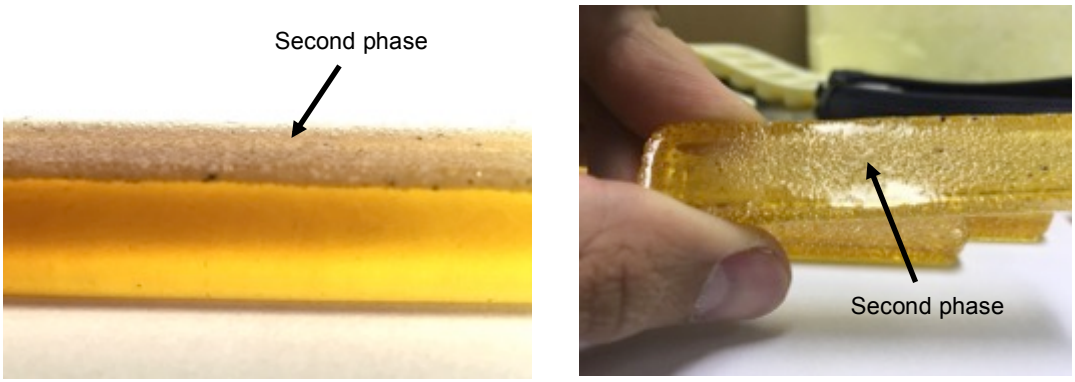

(a) (b)

Figure 5. 1 - Typical aspect of cured samples processed in condition (i): (a) MTHPA hardened and (b) DETDA hardened.

Under processing condition (ii) (65 ˚C mixture), DETDA amine hardened system did not present any visible change during mixture. For MTHPA anhydride hardened system, however, a considerable change occurred when BDMA amine accelerator was introduced. E-MA-GMA particles started to agglomerate in the first 2 minutes. Then, the mixture was immediately poured into the silicon mold to cure. In order to compare further results, neat MTHPA anhydride hardened samples were produced following the same processing route.

In both cured samples (DETDA amine and MTHPA anhydride hardened), thermoplastic phase separation has occurred. Figure 5. 2 shows all cured samples (neat and blended) for both heated DETDA and MTHPA hardened mixtures.

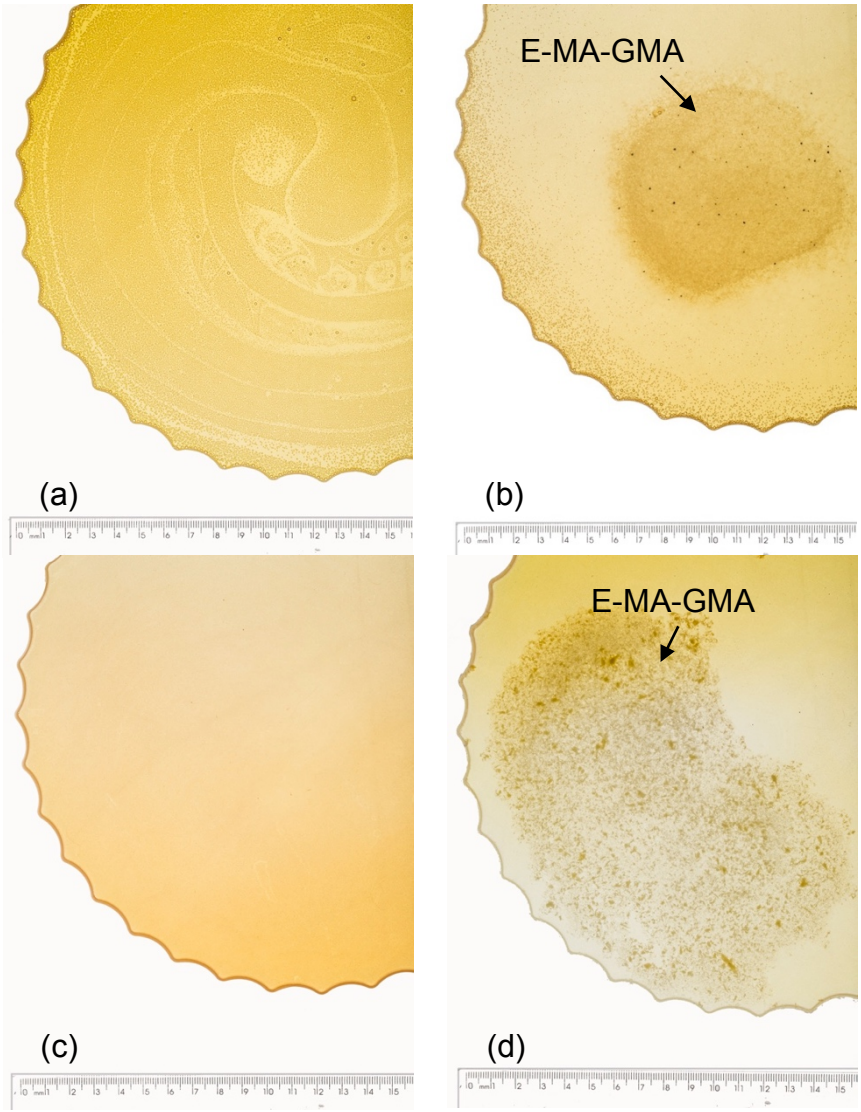

Figure 5. 2 - Photographs of the epoxy cured samples processed in heating mixture (condition (ii)): (a) neat DETDA hardened, (b) DETDA + E-MA-GMA blend, (c) neat MTHPA hardened and (d) MTHPA + E-MA-GMA blend.

In all E-MA-GMA mixtures it is possible to notice darker particles, which are believed to be contamination from the E-MA-GMA grinding process.

An explanation for the observations in MTHPA hardened mixtures (Figure 5. 2(c) and (d)) is that the accelerator introduced to the mixture reacted with the anhydride and epoxide ring in different rates, which leads to a quite complex sequence of competitive reactions [59], as shown schematically in Figure 5. 3. In this way, the reaction of tertiary amines with the epoxide ring from E-MA-GMA forming alkoxide anions (part A Figure 5. 3) may occur as a competitive reaction to DGEBA monomers (also part A Figure 5. 3) and the reaction with anhydride groups from the MTHPA hardener forming carboxylate anions (part B Figure 5. 3).

"*The chemistry of the cure process becomes complex because both step-growth and chain-growth mechanisms are operative in polymer formation, and the competition between both pathways depends on the cure temperature. However, the stoichiometry corresponding to the step growth reaction is usually not respected. Generally, a large excess of epoxy groups is initially introduced in the formulation, but the optimum for processing and properties is only obtained experimentally*" [19].

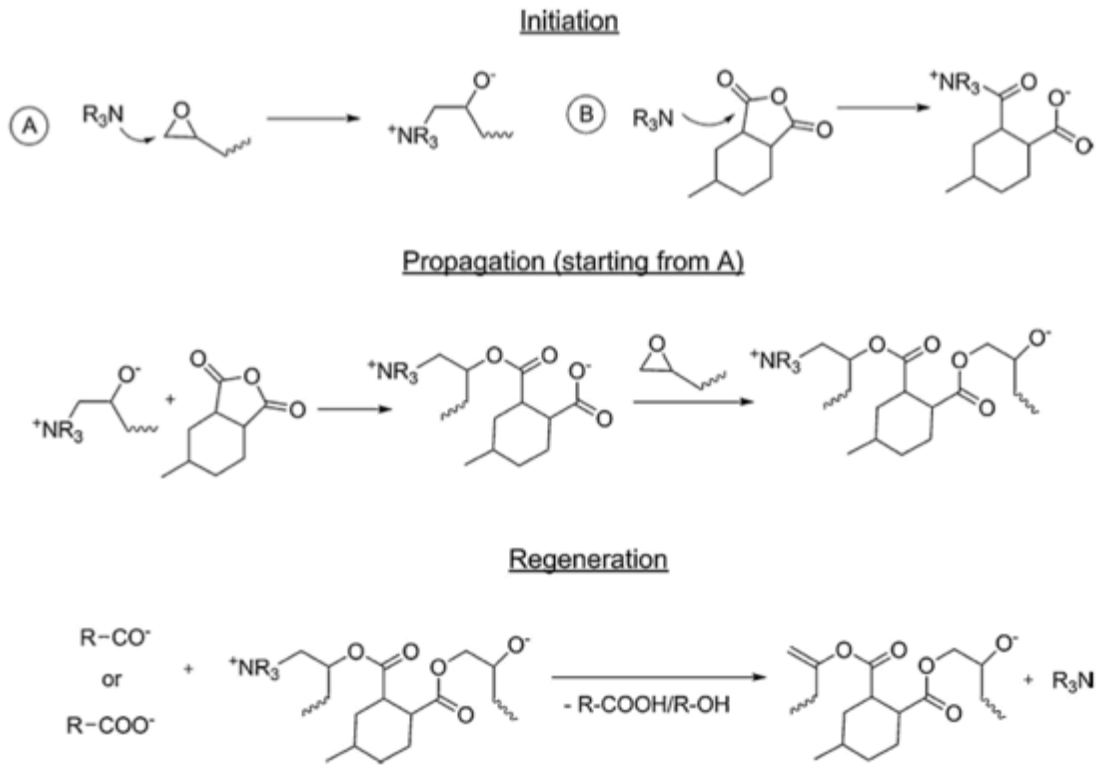

Figure 5. 3 - Curing mechanism of epoxy-anhydride formulation with tertiary amines [59].

Furthermore, the propagation reaction (chain-growth) starts with a nucleophilic attack on an anhydride by the alkoxide anion, resulting in the formation of a carboxyl anion, which is less reactive due to charge stabilization by resonance [59].

5.2 Dynamic mechanic thermal analysis (DMTA)

Typical curves obtained from dynamic mechanical thermal analysis of samples prepared in condition (ii) (65˚C mixtures) are shown in Figure 5. 4.

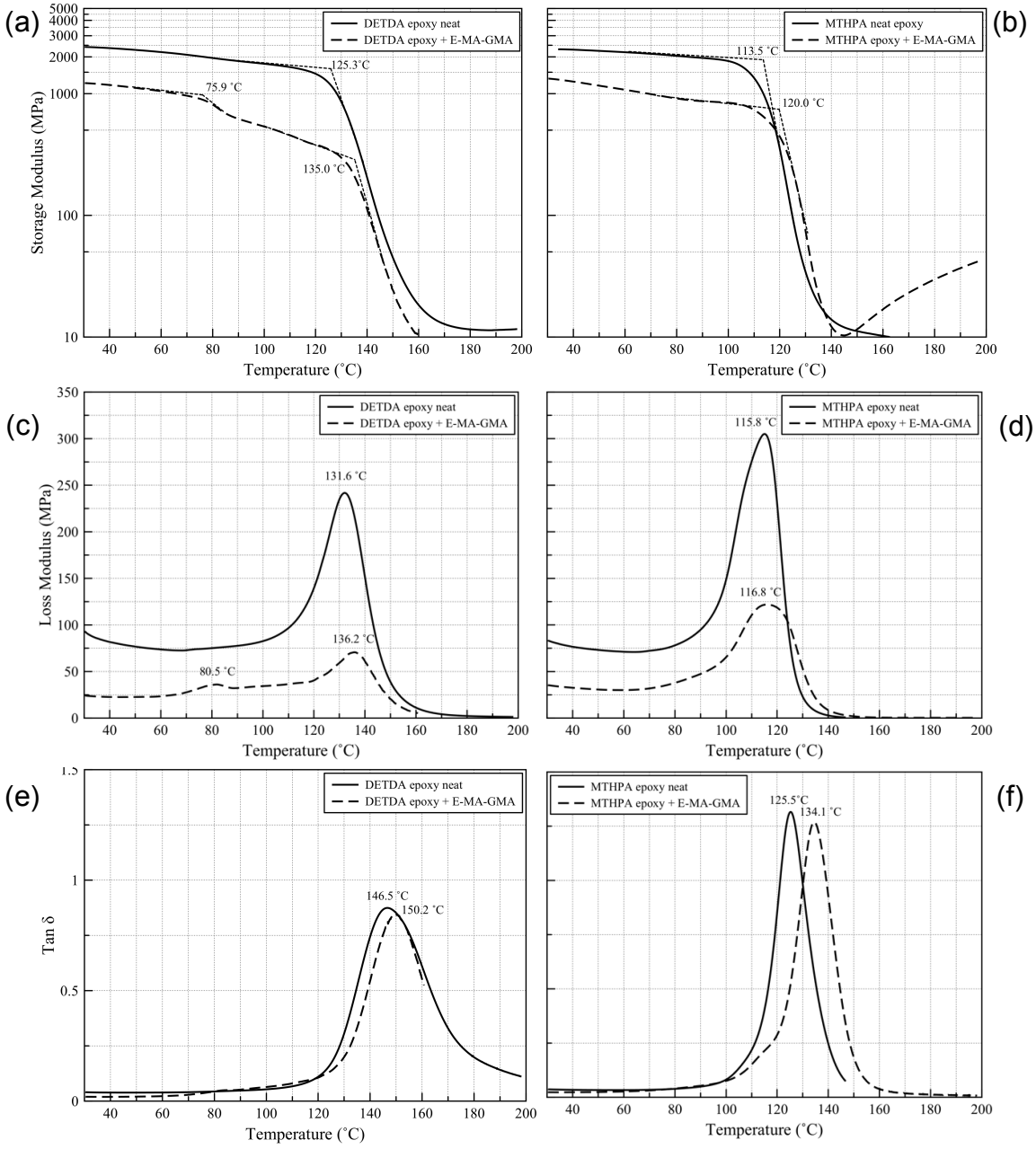

Figure 5. 4 - Typical DMTA curves for MTHPA and DETDA epoxy systems: (a-b) Storage modulus (E'), (c-d) Loss modulus (E'') and (e-f) Tan δ.

Considering the low amount of thermoplastic added (2.5 wt%) to epoxy, it was expected that the dispersed particles would not significant changes on storage

modulus (E'). However, the addition of E-MA-GMA to epoxy produced a considerable reduction on E' for both DETDA and MTHPA hardened epoxy systems (Figure 5. 4(a) and (b)). Compared to epoxy neat curves, a drop of nearly 1 GPa, which represents approximately 50% of the E', was observed in both DETDA and MTHPA hardened epoxy systems with addition of thermoplastic. One possible explanation for this observation is that some of the thermoplastic material reacted to the epoxy network during curing and, therefore, a less rigid material has been formed as compared to neat epoxy.

In the case of epoxy/DETDA/E-MA-GMA (Figure 5. 4(a)), as the temperature rises, there is a drop in E' at about 75˚C, which is related to the melting temperature of E-MA-GMA. Storage modulus continues to decrease with the increment of temperature at a similar rate until the glass transition region of epoxy is reached at 135 ˚C, given by the onset of E'.

In the case of epoxy/MTHPA/E-MA-GMA (Figure 5. 4(b)), no drop in E' is observed around 75˚C, but a slight reduction in the slope of the E' curve is observed after the melting point of E-MA-GMA at around 80˚C. This could suggest a greater interaction between the epoxy/MTHPA system and the E-MA-GMA thermoplastic. After that, the smaller slope of E' is due to the increased mobility of the epoxy produced by the increment of temperature.

The addition of E-MA-GMA to epoxy produced an increment in Tg for both epoxy systems studied. For the DETDA system, the increment in Tg on E' was about 10˚C (from 125 to 135˚C). For the MTHPA system, the increment was about 7˚C (from 113 to 120˚C). The same trend was also observed in Tg values of Tan δ curves (Figure 5. 4(e) and (f)). One possible reason for these observations is that chain mobility was reduced due to the reaction between thermoplastic molecules and the epoxy network, which produced longer molecules.

Regarding loss modulus (E") curves (Figure 5. 4(c) and (d)), characteristic peaks related to the Tg of the epoxy network are observed at 131˚C and 136˚C (Figure 5. 4(c)) and 115˚C and 116˚C (Figure 5. 4(d)). The modification of both studied epoxy systems with addition of thermoplastic led to a slight increase in Tg, as discussed above.

Further, for the loss modulus curve of epoxy/DETDA/E-MA-GMA, a small peak at 80˚C is observed (Figure 5. 4(c)), which is probably related to the melting of

the thermoplastic. The same E" peak however was not found for the epoxy/MTHPA/E-MA-GMA material. This is consistent with the idea that the interactions between epoxy/MTHPA and E-MA-GMA are more pronounced than in the epoxy/DETDA system.

In the case of epoxy/DETDA/E-MA-GMA, the normalized tan δ peak (Figure 5. 5(a)) is narrower as compared to the neat/DETDA. Thus, in this case the relaxations associated with the Tg happened not only at higher but also narrower temperature range. This effect is the opposite of that produced by plasticizers, which are known to lower the glass transition and broaden the tan δ peak. "The mechanism of antiplasticization can be formulated in terms of hindrance of the short- scale cooperative motions in the glassy state due to a dynamic coupling between the epoxy polymer and the antiplasticizer molecule" [60]. In addition to physical interactions, it is also possible that chemical reactions between E-MA-GMA and the epoxy resin network during curing has occurred. Thus, this chemical aggregation may have increased the length of polymer chains, which hindrance effect reduced its mobility.

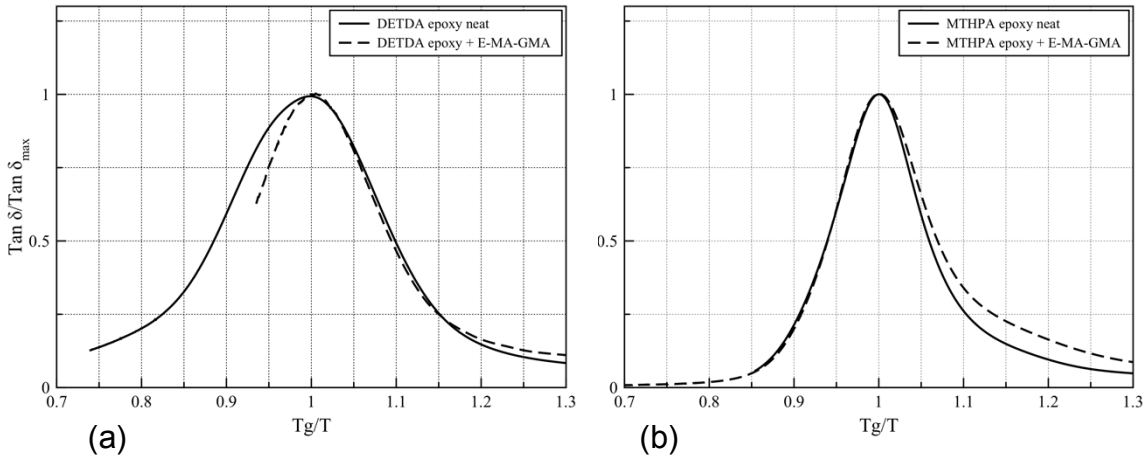

Figure 5. 5 - DMTA spectra of normalized tan δ for both epoxy resin systems (a) DETDA and (b) MTHPA hardened.

Figure 5. 6 shows the aspect of samples before and after DMTA testing. During the tests, all thermoplastic-thermosetting blend specimens adhered to the testing fixture, as it can be observed in the three clamp marks left in the samples (Figure 5. 6(b) and (d)). This confirms that the thermoplastic portion gains mobility during heating, as much as it maintains its adherence to the epoxy resin, supporting

its prospective use as healing agent. Further, it was observed that epoxy/DETDA/E-MA-GMA samples were more strongly adhered to the clamps than epoxy/MTHPA/E-MA-GMA ones.

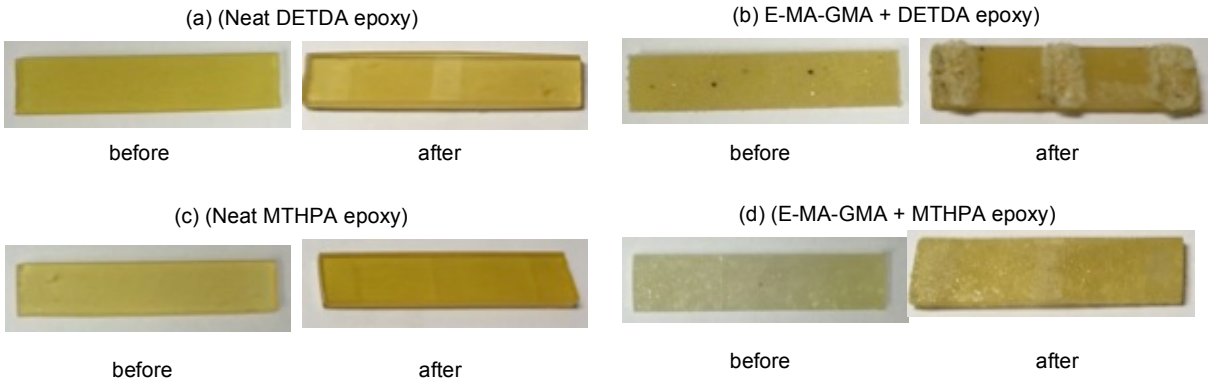

Figure 5. 6 - Aspect of DMTA samples before and after testing: (a) neat DETDA hardened epoxy; (b) E-MA-GMA + DETDA hardened epoxy; (c) neat MTHPA hardened epoxy and; (d) E-MA-GMA + MTHPA hardened epoxy.

5.3 Fourier Transform Infrared (FTIR) Spectroscopy

Table 5. 1, Table 5. 2 and Table 5. 3 show the main band assignments of FTIR spectra used in this study for E-MA-GMA terpolymer, DETDA and MTHPA hardened epoxy, respectively.

Table 5. 1 - Band assignments of FTIR spectra for functional groups from E-MA-GMA terpolymer.

Bond type	**Peak location**	**Ref.**
Epoxide ring (C–O) vibration	910 cm^{-1}	[61,62]
Ether (C–O) vibration	1114 and 1159 cm^{-1}	[62]
Ester (–C=O) vibration	1730 cm^{-1}	[61,62]
Alkane (C–H) vibration	2850 and 2921 cm^{-1}	[61,62]

Table 5. 2 - Band assignments of FTIR spectra for functional groups from DETDA hardened epoxy.

Bond type	**Peak location**	**Ref.**
Epoxide ring (C–O) vibration	915 cm^{-1}	[63,64]
Aliphatic Ether (C–O) vibration	1032 cm^{-1}	[64,65]
Aromatic Ether (C–O) vibration	1183 and 1234 cm^{-1}	[63,65]
Aromatic carbon (C=C) vibration	1608 cm^{-1}	[63–65]

Table 5. 3 - Band assignments of FTIR spectra for functional groups from MTHPA hardened epoxy.

Bond type	**Peak location**	**Ref.**
Epoxide ring (C–O) vibration	915 cm^{-1}	[63,64]
Aliphatic Ether (C–O) vibration	1042 cm^{-1}	[59,64]
Ester (O–C=O) vibration	1152 and 1739 cm^{-1}	[65]
Aromatic Ether (C–O) vibration	1240 cm^{-1}	[65]
Aromatic carbon (C=C) vibration	1608 cm^{-1}	[59,63,64]

FTIR spectra of MTHPA and DETDA epoxy mixtures, along with neat E-MA-GMA FTIR spectrum, are presented in Figure 5. 7 and Figure 5. 8, respectively. Since no relevant changes were observed in all neat epoxy spectra for both room temperature and 65 ˚C mixture conditions, a representative spectrum was adopted for each pure epoxy sample. A reference peak of 1608 cm^{-1} corresponding to the aromatic core of DGEBA monomers was adopted, from which all epoxy samples (neat or thermoplastic blended) peaks were set (as referenced in [63,66]).

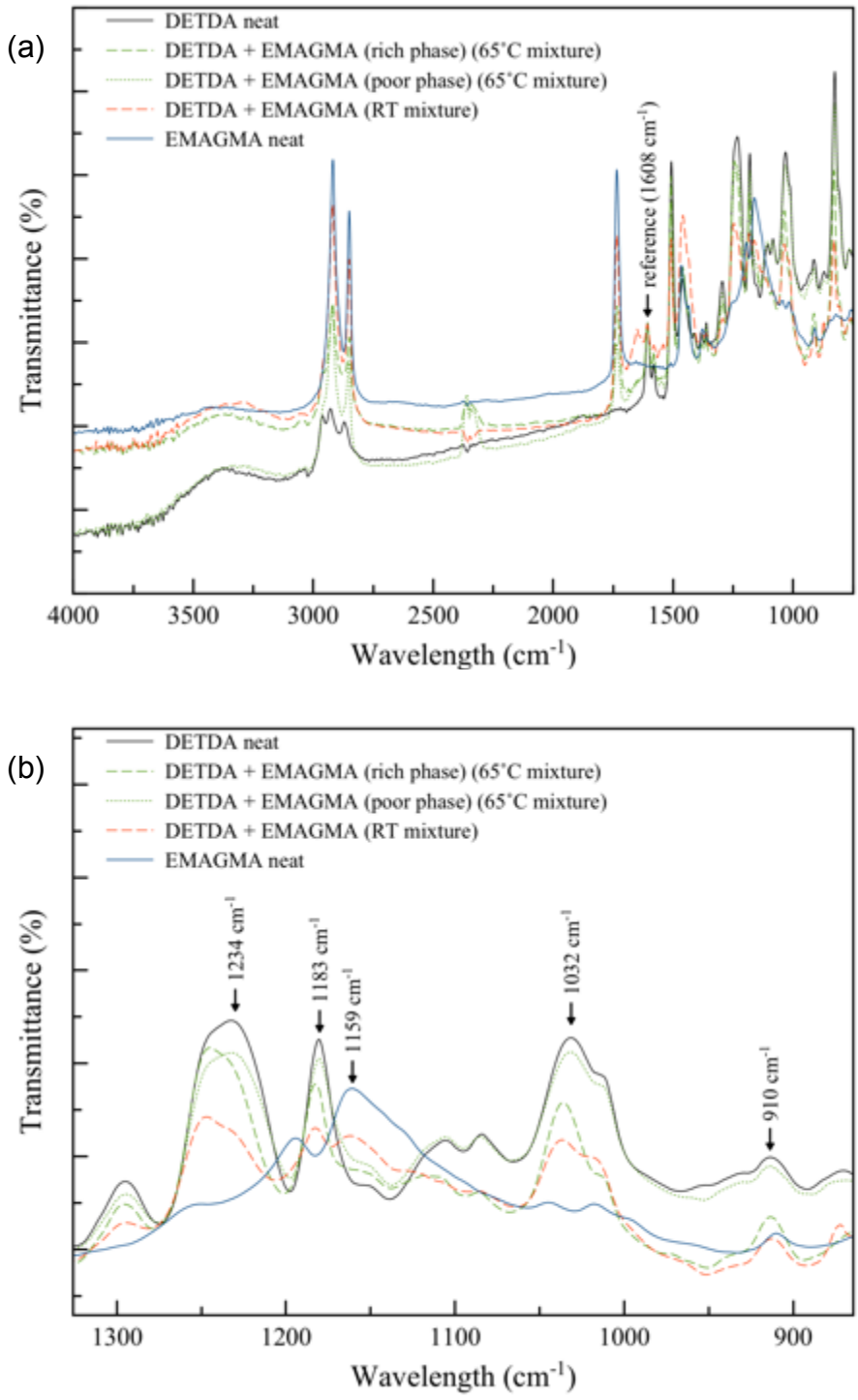

Figure 5. 7 - FTIR spectra of DETDA hardened epoxy systems with and without addition of E-MA-GMA under room temperature and 65 ˚C mixing conditions, along with spectra of neat E-MA-GMA terpolymer. FTIR spectra of overall (a); (b) 1300-900 cm-1; (c) 1800-1500 cm-1; and (d) 3000-2800 cm-1 ranges.

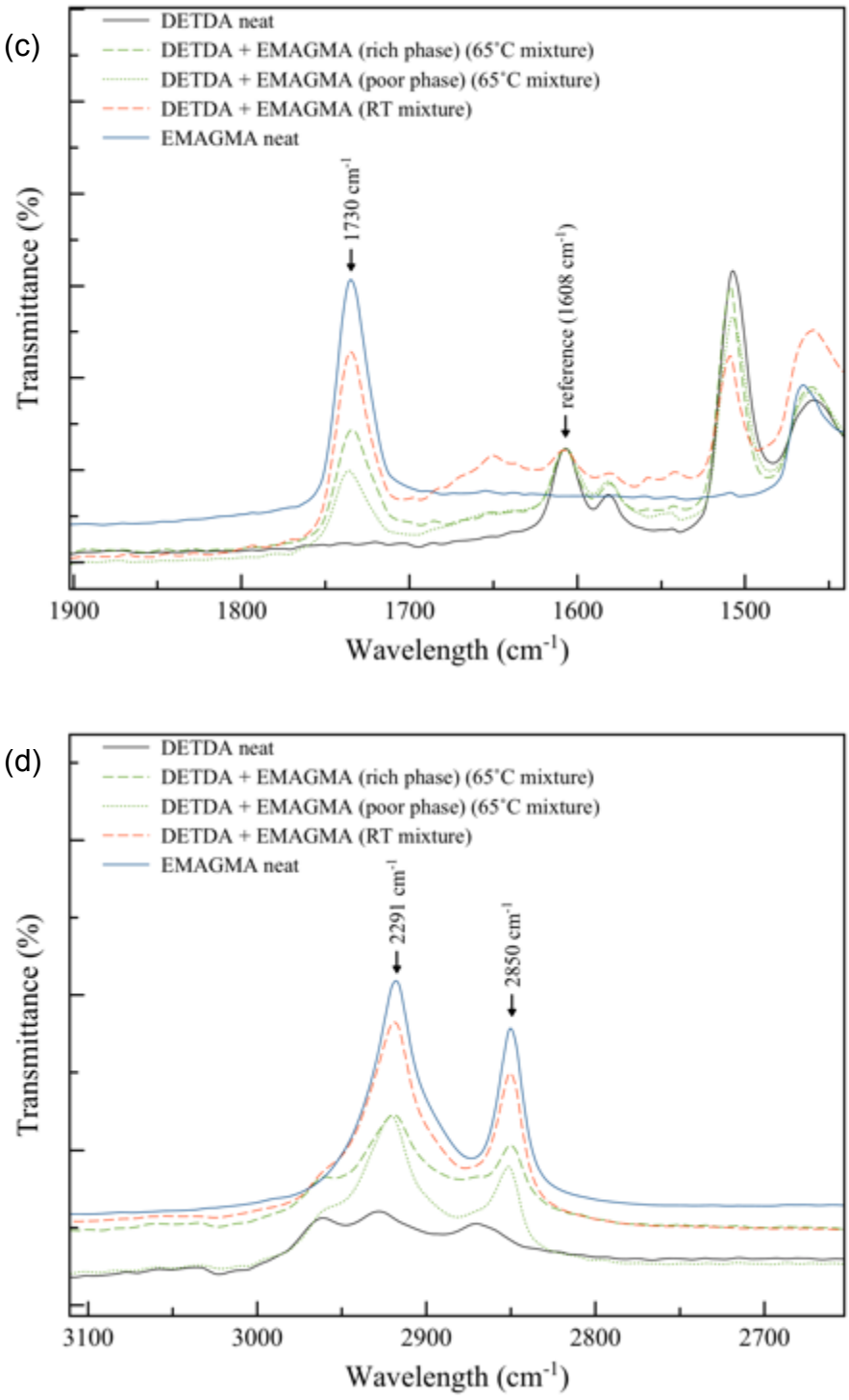

Figure 5. 7 - continuation.

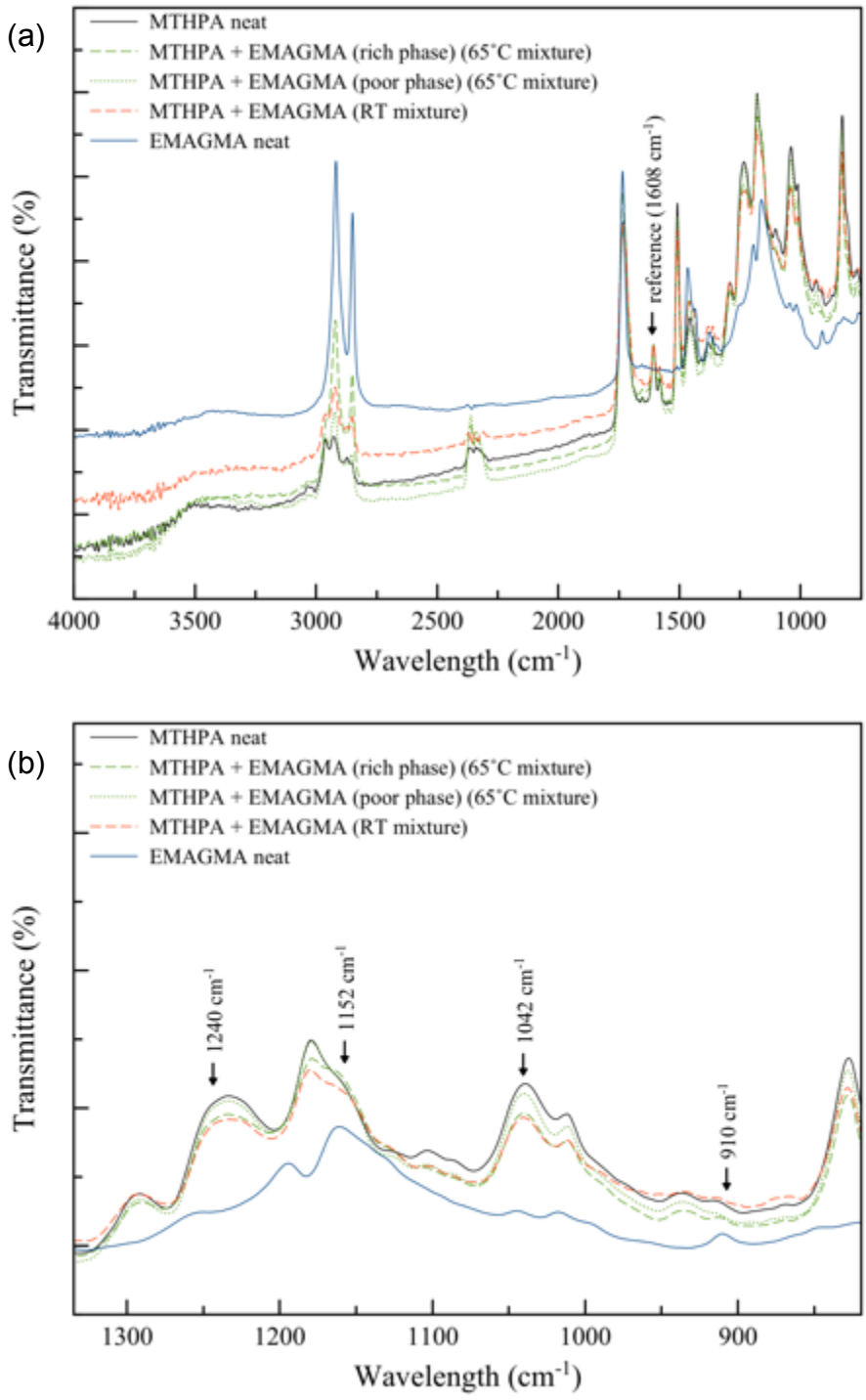

Figure 5. 8 - FTIR spectra of MTHPA hardened epoxy systems with and without addition of E-MA-GMA under room temperature and 65 ˚C mixing conditions, along with spectra of neat E-MA-GMA terpolymer. FTIR spectra of overall (a); (b) 1300-900 cm^{-1}; (c) 1800-1500 cm^{-1}; and (d) 3000-2800 cm^{-1} ranges.

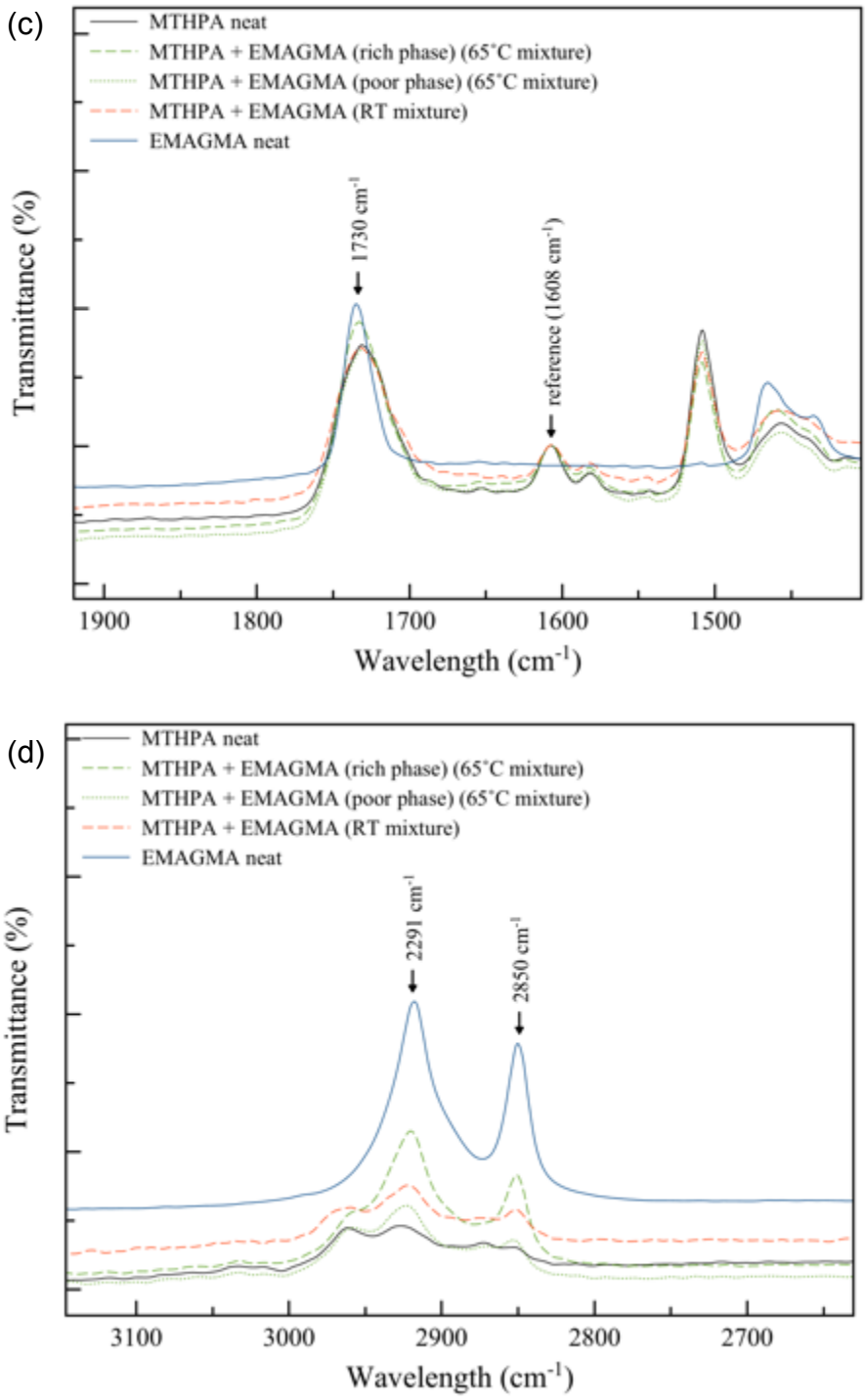

Figure 5. 8 - continuation.

Discussion of DETDA hardened mixtures

A decrease in all peak intensity corresponding to ether bands of epoxy network (1032, 1183 and 1234 cm^{-1}) was observed for all E-MA-GMA-epoxy mixtures (Figure 5. 7(b)). This result suggests that E-MA-GMA terpolymer affects the degree of crosslinking, since ether formation may be attributed to side reactions occurring during curing of epoxy amine hardened systems [19,67]. This result also suggests that in the same manner other thermoplastic/epoxy reactive blends, it is believed that a phase separation may have occurred, once "as the curing reaction proceeds, the thermoplastic component undergoes a phase separation. The separated thermoplastic can retard the curing reaction." [60].

Comparing peak intensity changes between ether groups types (Figure 5. 7(b)), a more pronounced change in peak intensity of aliphatic ether (1032 cm^{-1}) was observed. This is consistent to the alteration of etherification reaction rate, once aromatic ether (1183 and 1234 cm^{-1} peaks) is not chemically bonded to the epoxide ring, as it can be seen in DGEBA structure (Figure 4. 1(a)). It is still noteworthy that the thermoplastic mixing temperature may affect the etherification reaction rate, as it can be noticed in peak shifts between room temperature and 65 ˚C mixing conditions. Nevertheless, the same trend was not found in neat DETDA epoxy resin mixed at room temperature. This result suggests that when E-MA-GMA is in a state of greater energy (65 ˚C mixture), it gains mobility and it is allowed to react within the epoxy system in a different manner of E-MA-GMA under a lower state of energy. Therefore, "unreacted" E-MA-GMA is believed to preferentially affect the etherification reaction rate.

An evident decrease in peak intensity corresponding to ether vibration of E-MA-GMA terpolymer (1159 cm^{-1}) was observed for all E-MA-GMA-epoxy mixtures (Figure 5. 7(b)). This change suggests a consumption of E-MA-GMA ether groups by the epoxy system. Further, 65 ˚C thermoplastic mixture reveal an almost completely disappearance of the ether peak, which leads to believe that the consumption is a thermally activated mechanism.

Two different observations concerning to epoxide ring vibration (910 cm^{-1}) peaks (Figure 5. 7(b)) can be described:

I. Peaks of neat E-MA-GMA and DETDA epoxy resin and poor E-MA-GMA phase are more intense than neat E-MA-GMA and rich E-MA-GMA phase (for both room temperature and 65 ˚C mixtures). It suggests that the epoxide ring band from epoxy network presents a different shape and intensity than the other from E-MA-GMA based spectra, which authors [63,64] named “fingerprint” band of the molecule. Therefore, the decrease in epoxide ring peak is not necessarily related to a consumption of this functional group. Further, considering that E-MA-GMA rich phases present the same fingerprint band, it suggests that in those samples the epoxide ring is an E-MA-GMA chemically dominated area. In addition, epoxide ring peaks from epoxy resin specimens (Table 5. 2) are slightly dislocated (915 cm^{-1}) if compared to peaks from E-MA-GMA (910 cm^{-1}).

II. Comparing both E-MA-GMA rich phases mixed at 65˚ C and at room temperature, a slight change in epoxide ring band (915 cm^{-1}) was observed. It suggests that more epoxide ring groups are available at 65 ˚C epoxy-E-MA-GMA blend samples. One possible cause of this lies on the adsorption of E-MA-GMA by epoxy resin network dispersive forces, which brings upward the 65 ˚C mixture baseline. Other possible cause is that “unreacted” E-MA-GMA from room temperature mixture showed a bigger consumption of epoxide ring during curing. However, the most likely cause of this event is related to a bond cleavage of epoxide ring part from E-MA-GMA backbone chain (Figure 5. 9) due to ester reactions (which will be discussed below).

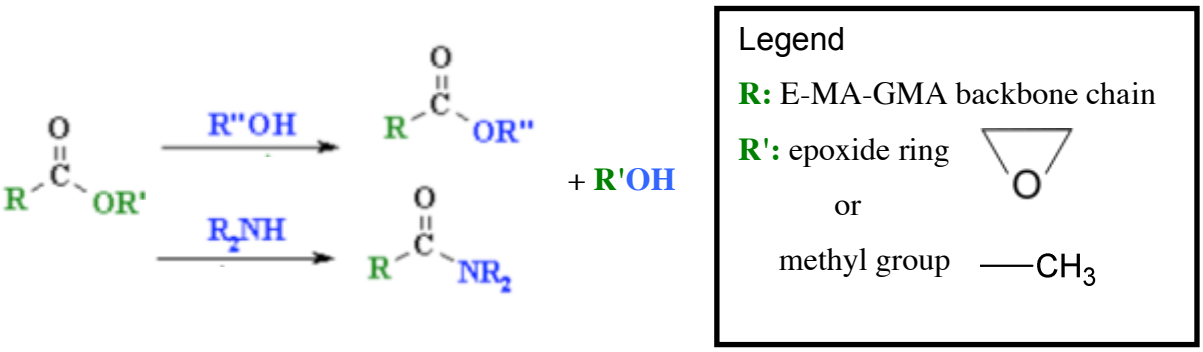

Figure 5. 9 - Ester reactions with hydroxyl and amine groups (Adapted [68]).

A downward tendency on ester peak intensity (1730 cm^{-1}) from neat E-MA-GMA was noticed in all thermoplastic mixtures (Figure 5. 7(c)). It suggests that this functional group has been consumed during curing. This result is believed due to inherent ability of ester groups to react with hydroxyl and amine groups [68] (Figure 5. 9), respectively deriving from epoxy network and DETDA hardener. Further, heated thermoplastic mixtures showed a sharper shift on intensity peak than that from room temperature thermoplastic mixture, which indicates that greater ester consumption is achieved in more energetic conditions. This result is consistent to the alterations on epoxide ring band vibrations observed above, once in “unreacted” E-MA-GMA the less ester groups are consumed the less epoxide ring groups are available. In contrast, “reacted” E-MA-GMA presents the analog behavior: the more ester groups are consumed the more epoxide rings are available, indicating that the bond cleavage has occurred.

Alterations on band regions related to the ethylene core (2850 and 2291 cm^{-1}) of E-MA-GMA were also noticed (Figure 5. 7 (d)). In this case, due to its inherent non-reactivity it is believed that only dispersive forces act to promote C–H adsorption into the resin network. Therefore, room temperature E-MA-GMA mixtures presented more pronounced peaks related to C–H vibrations than mixtures at 65 ˚C, suggesting that “unreacted” E-MA-GMA specimens attain a higher adsorption level than “reacted” ones. Furthermore, the presence of C–H vibration in similar intensity of both rich and poor phase spectra indicates that the E-MA-GMA adsorption into epoxy network has been promoted for the whole thermoplastic blend.

Discussion of MTHPA hardened mixtures

A slight decrease in peak intensity corresponding to ether band of epoxy network (1240 and 1042 cm^{-1}) was observed in all thermoplastic mixtures (Figure 5. 8 (b)). It suggests that dominated dispersive forces from the E-MA-GMA structure are bringing downwards the peak baseline. No relevant chemical reactions hence are envisioned. Further, due to the very similar aspect of the peak for both 65 ˚C and room temperature mixing conditions it is believed that mixing conditions, in this case, does not develop a significant role on the E-MA-GMA adsorption into the epoxy network. This may be justified by the lower reactivity of epoxy curing before the

addition of the tertiary amine (BDMA), i.e. as the tertiary amine was introduced only in the final part of both mixing conditions, the curing rate for both mixing condition is believed to be close.

Alterations in intensity peak from epoxide ring band (910 cm^{-1}) were also noticed (Figure 5. 8(b)). A decrease in the epoxide ring peak intensity from E-MA-GMA room temperature in comparison to 65˚C mixture indicates a higher consumption of this functional group at higher temperatures mixing conditions. This result is consistent to the visible changes observed during 65 ˚C mixing conditions (Figure 5. 2(d)).

Slight changes on peak intensity of ester group (1739 and 1152 cm^{-1}) were observed (Figure 5. 8(b) and (c)). In this case, it is believed that both E-MA-GMA adsorption and chemical reactions has been promoted. Peak intensity of E-MA-GMA-epoxy mixtures at 65 ˚C shows a slight increase in comparison to room temperature mixtures. Further, a peak dislocation from 1739 to 1730 cm^{-1} and the appearance of a small shoulder at 1152 cm^{-1} also suggest that chemical interactions have been promoted, hence indicating that more ester groups have reacted with epoxy resin system. This result is consistent, once ester reactions likely took place in the presence of tertiary amine (Figure 5. 3). It is important to notice that, in this case, ester reaction is not necessarily related to a bond cleavage.

Significant changes on peak intensity related to ethylene core (2850 and 2921 cm^{-1}) of E-MA-GMA were observed (Figure 5. 8(d)). As mentioned in DETDA mixture discussion, due to its inherent non-reactivity it is believed that only dispersive forces act to promote C–H adsorption into the resin network. All E-MA-GMA mixtures presented peaks at this band range, which indicates that E-MA-GMA has been adsorbed into epoxy network. In contrast to DETDA results, 65 ˚C mixtures presented more intense peaks than room temperature mixtures. It suggests that the effect of heating mixture increases E-MA-GMA adsorption into MTHPA hardened epoxy systems.

5.4 Atomic Force Microscopy

Topographic images of DETDA and MTHPA hardened epoxy systems are given in Figure 5. 10 and Figure 5. 11, respectively. In all images, descending striation marks indicate the direction of the blade cutting. Lighter raised discrepancies observed in some images are believed to represent a sort of sample contamination. These presumed contamination peaks are more evidenced at neat DETDA epoxy (Figure 5. 10 (a-b)), neat MTHPA epoxy (Figure 5. 11 (a-b)) and E-MA-GMA-MTHPA epoxy (Figure 5. 11(c-d)).

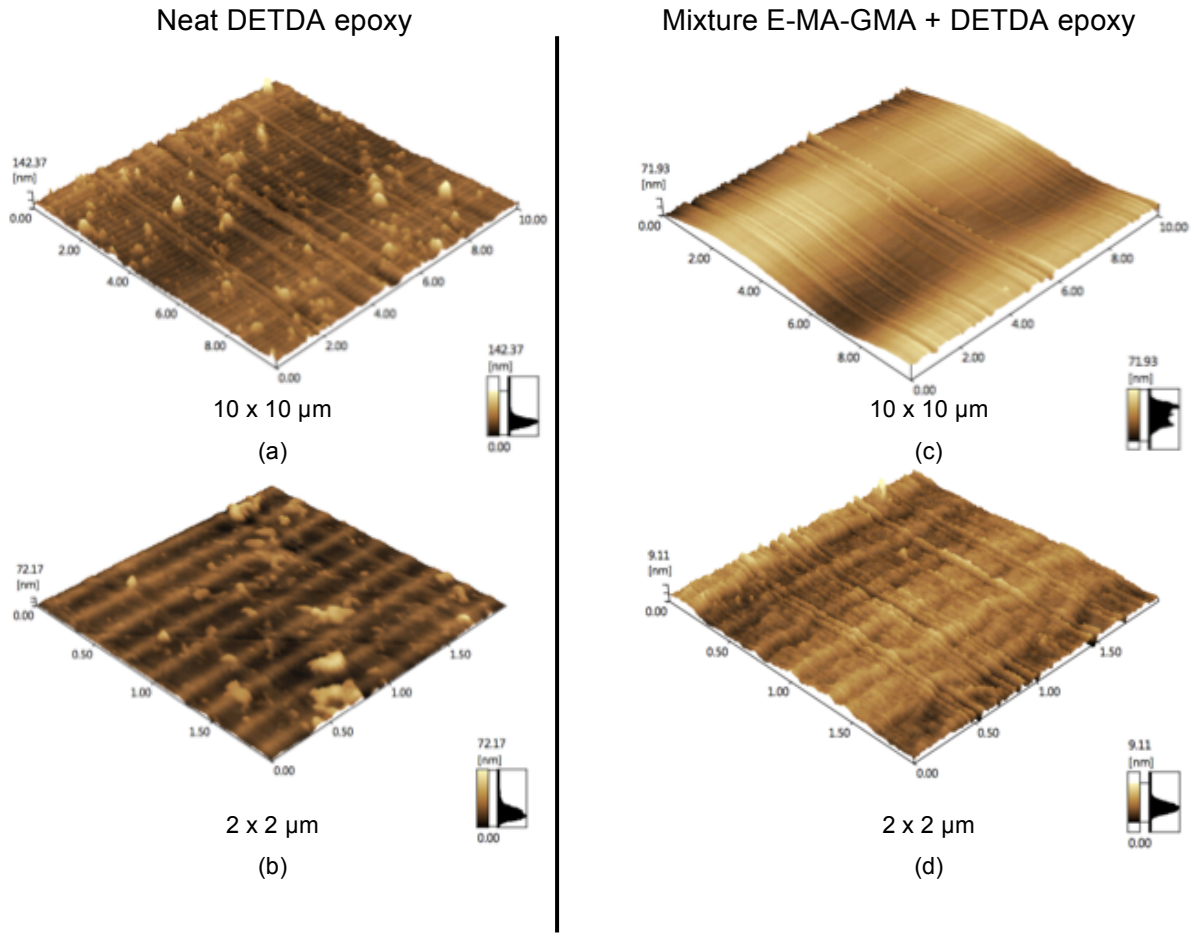

Figure 5. 10 - AFM topographic images of (a-b) neat DETDA hardened epoxy and (c-d) DETDA hardened epoxy with E-MA-GMA addition under different magnification.

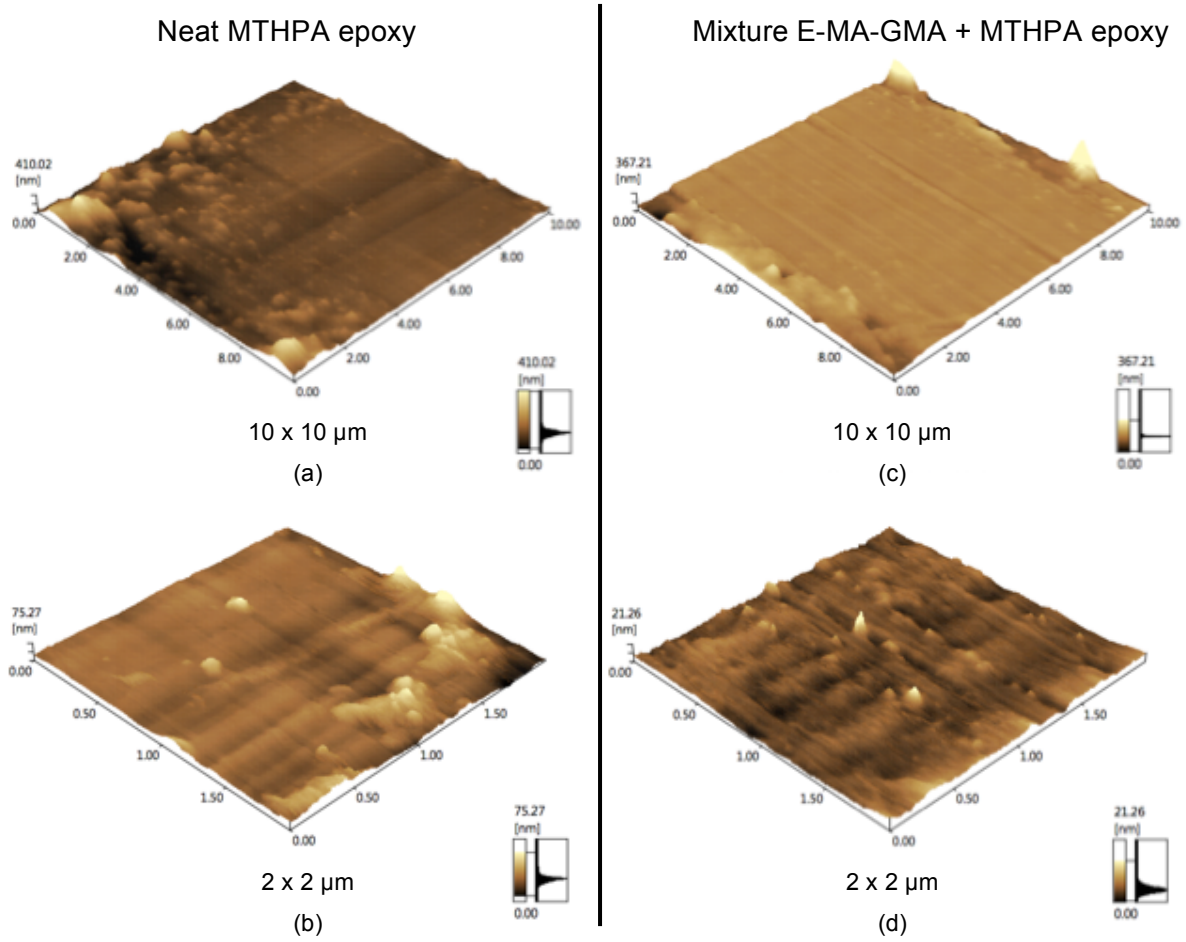

Figure 5. 11 - AFM topographic images of (a-b) neat MTHPA hardened epoxy and (c-d) MTHPA hardened epoxy with E-MA-GMA addition under different magnification.

Characteristic river lines from epoxy resin systems [69,70] are found in both neat epoxy DETDA (Figure 5. 10(a-b)) and MTHPA (Figure 5. 11) systems.

Comparing the roughness pattern of the surface specimens, it is believed that the E-MA-GMA mixture specimen showed a more ductile fracture profile, once it presented a larger and more irregular fractured surface.

AFM images from other epoxy studies [69,70] (Figure 5. 12) suggest that a similar nanostructure has been formed due to E-MA-GMA addition. This indicates that, despite E-MA-GMA macroscopically has demonstrated to be immiscible with epoxy resin system, in a molecular level a nanostructured phase has problably been formed.

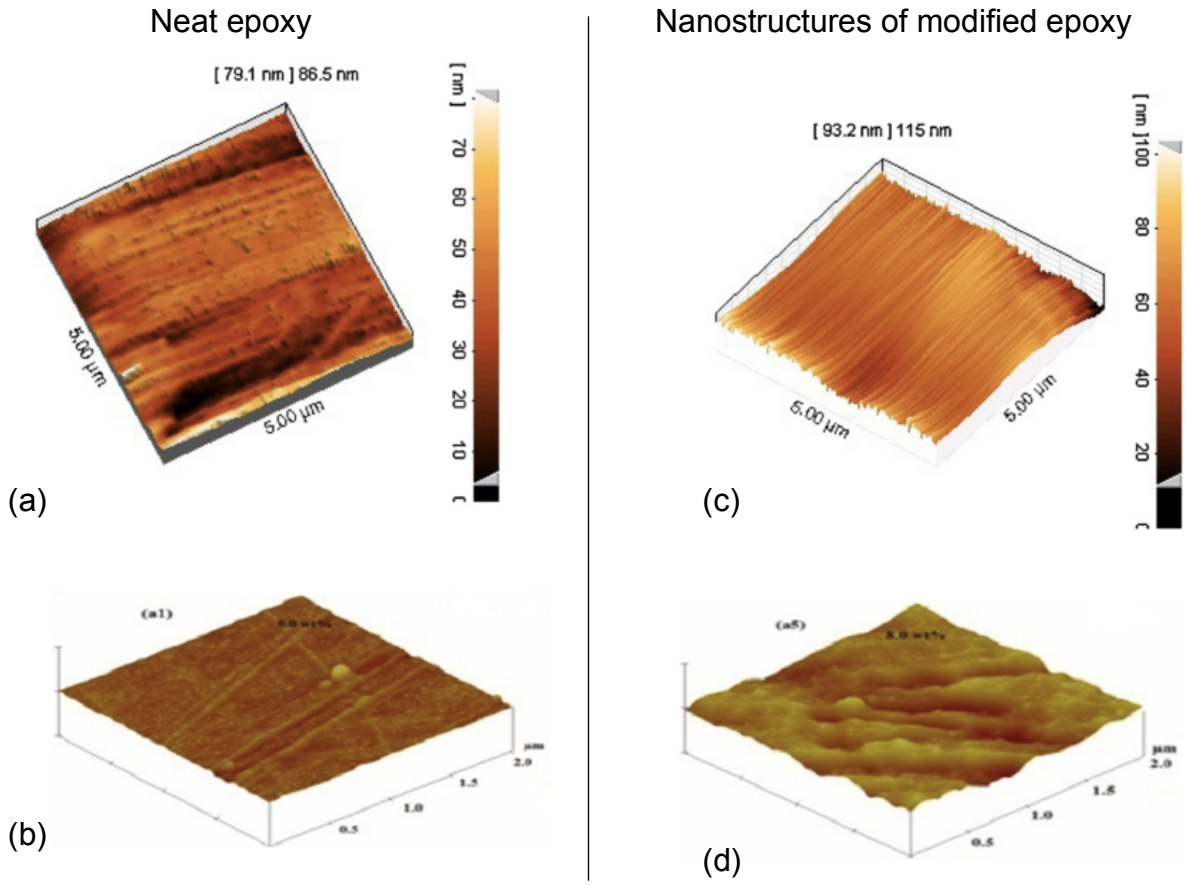

Figure 5. 12 - AFM images showing examples of nanostructures in epoxy network: (a-b) neat epoxy, (c-d) nanostructures of modified epoxy [69,70].

Comparing the structure of both DETDA and MTHPA epoxy systems, it is possible to infer that DETDA system structures presented more significant changes when E-MA-GMA is added, revealing that E-MA-GMA addition affects more DETDA than MTHPA epoxy systems.

5.5 Assessment of self-healing effect

Typical optical microscope images of indentations areas before and after healing cycle at 150 ˚C for 5 hours are shown in Figure 5. 13.

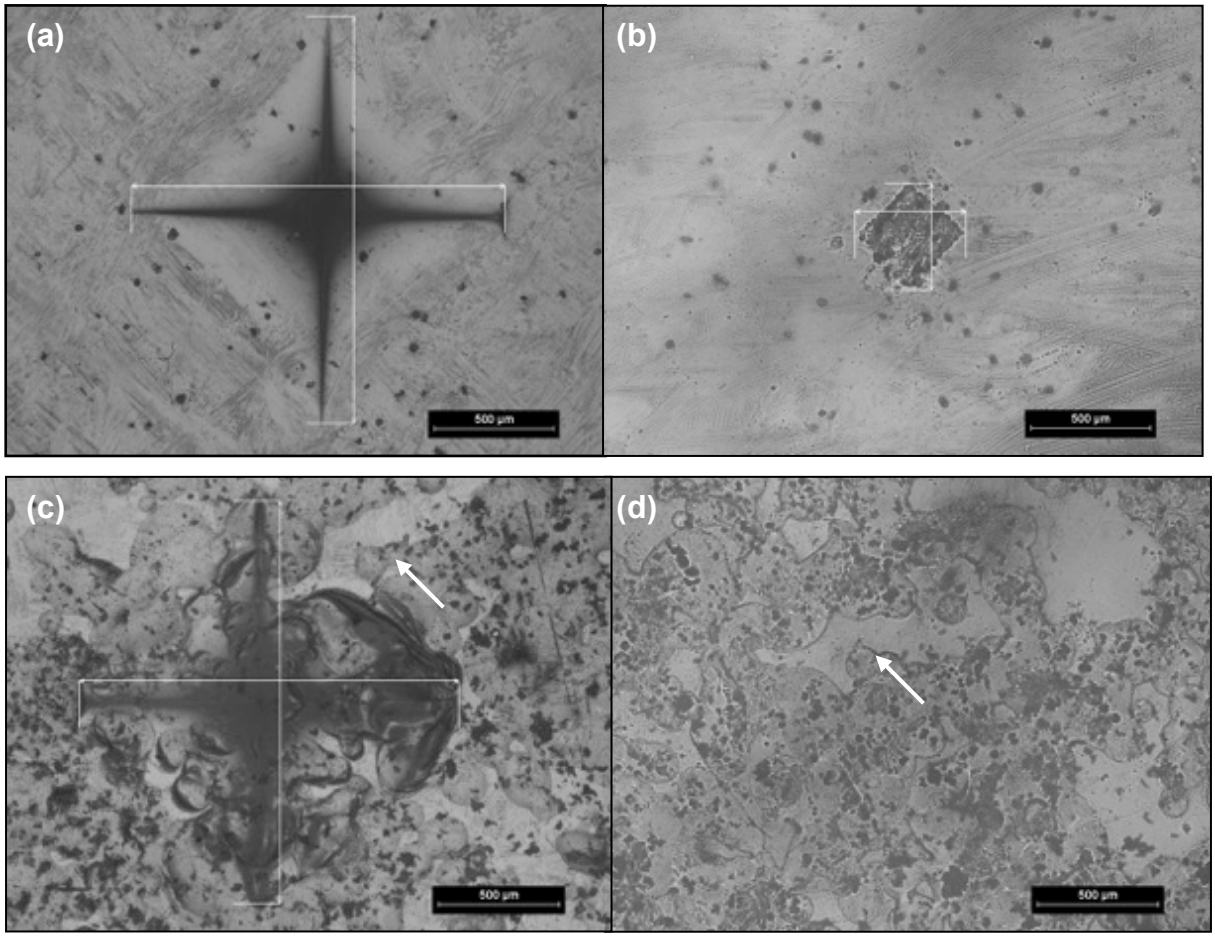

Figure 5. 13 - Typical optical microscope images of indentations areas of neat DETDA epoxy (a) before and (b) after healing cycle and E-MA-GMA mixture (c) before and (d) after healing cycle.

It is possible to notice that neat epoxy samples presented sharper indentations (Figure 5. 13(a)) than those observed in E-MA-GMA mixtures (Figure 5. 13(c)). This result suggests that E-MA-GMA additions affect the fracture toughness of samples.

A considerable diminishing on the indentation area of approximately 70% was noticed on neat epoxy system (Figure 5. 13 (a-b)). This result is consistent to literature, once “after a healing event, the unmodified system also exhibited a modest healing response, highlighting the ability of residual functional groups within

the epoxy network to react and form linkages across fractured interfaces" [33]. Nevertheless, the indentation mark completely disappeared on E-MA-GMA mixture (Figure 5. 13 (c-d)) after a healing cycle. This result reveals that the E-MA-GMA addition enhances the ability of repair of damage in epoxy.

In regard to the self-healing effect test method, results also suggest that healing assessment cycle employed was likely inadequate to assess properly the gradual changes occurring during healing, as much as it showed an unexpected healing ability to non-modified epoxy systems. Still, no rising microcrack were observed on indented samples – even under high mechanical loads or using other hardness testers configuration (Brinell F or Vickers microindentation).

Analyzing the healing effect on E-MA-GMA mixture (Figure 5. 13 (c-d)) it is possible to identify some neighboring particles (indicated by arrows in the Figure 5. 13 (c-d)), which after healing cycle remained at the same position. This result also supports the use of E-MA-GMA as a healing agent, since, in addition to showing damage closure, the particles remained strongly adhered to the epoxy matrix.

6 Conclusions

The goal of this work was to study the effects of the addition of a thermoplastic material poly(ethylene-co-methyl acrylate-co-glycidyl methacrylate) (E-MA-GMA) as a healing agent to epoxy resins. Its influence on thermo-mechanical, chemical and microstructural properties was evaluated.

All formulations of epoxy resins with addition of E-MA-GMA showed an expected macroscopic phase separation in both heated and room temperature mixing conditions, although Fourier transform infrared (FTIR) spectra and atomic force microscopy (AFM) reveal the presence of E-MA-GMA in the epoxy even in thermoplastic poor areas.

A considerable change during mixing was only observed in heated epoxy/MTHPA/E-MA-GMA mixtures. This change was related to the tertiary amine (BDMA) accelerator, which opens the epoxide ring from E-MA-GMA chain and epoxy monomers in different rates.

Dynamic mechanical thermal analyses (DMTA) of E-MA-GMA mixtures revealed an increment in glass transition temperature (Tg) for all specimens tested in comparison to Tg values of unmodified resins. Despite this rise in Tg may indicate an increase in crosslink density, it is believed that the presence of the thermoplastic has unfavorably affected curing rate reactions, specially in aromatic amine hardened (DETDA) epoxy mixtures. Two explanations may describe what occurred. Firstly, this upward tendency in Tg may be related to the fact that the E-MA-GMA part from mixture samples have flowed due to clamp pressure of DMTA equipment, diminishing the clamp pressure on the sample, hence masking the results. Secondly, chemical reactions between thermoplastic and epoxy matrix may have diminished the polymer chain mobility. Therefore, differential scanning calorimetry (DSC) is suggested to assess changes in Tg values on these samples.

DMTA of epoxy-E-MA-GMA mixture samples also revealed a considerable drop of approximately 50% on storage modulus in comparison to unmodified epoxy systems. This reduction on storage modulus suggests a likewise loss on elastic modulus, which suggest that the thermoplastic has interfered on the curing reaction.

FTIR spectra revealed that more pronounced chemical changes were observed in amine (DETDA) hardened mixtures than anhydride (MTHPA) mixtures. Comparing DETDA mixture FTIR spectra, it was observed that chemical and

adsorption governed interactions occurred, suggesting bonds between particles and epoxy matrix. On the other hand, MTHPA revealed an overall adsorption-governed interactions, suggesting a more advantageous bonding than in DETDA mixtures.

Atomic force microscopy (AFM) images showed that less regular structures on E-MA-GMA modified epoxy systems were created in contrast to neat epoxy resin, suggesting that E-MA-GMA addition leads to a formation of a nanostructure phase. Thus, despite E-MA-GMA macroscopically has demonstrated to be immiscible with epoxy resin system, in a molecular level a new nanostructured phase has been formed.

Modified epoxy resin system DETDA shows that damage caused by indents disappears after a healing cycle. These results indicate the potential of the use of E-MA-GMA a healing agent in polymer matrix composites.

Suggestion for future works

In order to investigate the role each individual resin reactant (hardener, monomer and accelerator) play in chemical interactions, FTIR spectra of E-MA-GMA films with addition to DETDA/MTHPA, DGEBA and BDMA is suggested.

Further works focused on changes in thermal properties of the systems assessed by differential scanning calorimetry (DSC) runnings are suggested.

Assess of healing efficiency in modified resins with different contents of E-MA-GMA and times of healing cycles by single edge notch beam (SENB) tests are also suggested.

Assess of healing efficiency in carbon laminates and prepreg composites with different addition contents by comparing results on interlaminar shear strength (ILSS) are also suggested.

In order to investigate the influence of other hardener types, the same tests mentioned above will be carried out with aliphatic amines and anhydrides.

Imaging of fracture surface will also be addressed in order to investigate the mechanism of healing.

Further studies regarding alternative processing routes and varying amounts of thermoplastic material are also suggested in order to assess alterations in chemical interactions between thermoplastic and epoxy, alterations in dynamic mechanical properties and in the self-healing effect.

References

[1] **R. F. Gibson**, *Principles of Composite Material Mechanics*. McGraw-Hill, Inc., 1994.

[2] **D. R. Askeland, P. P. Fulay, and W. J. Wright**, *The science and engineering of materials*, 6th ed. Cengage Learning, 2011.

[3] **W. D. Callister and D. G. Rethwisch**, *Materials science and engineering: an introduction*, 8th ed. John Wiley and Sons, 2009.

[4] **D. Hull**, *An introduction to composite materials*. Cambridge University Press, 1981.

[5] **B. Harris**, "Engineering Composite Materials," p. 344, 1999.

[6] **F. L. Matthews and R. D. Rawlings**, *Composite materials: science and engineering*. 1999.

[7] **K. K. Chawla**, *Composite Materials*. 2012.

[8] **A. P. Cysne Barbosa *et al.***, "Accelerated aging effects on carbon fiber/epoxy composites," *Composites Part B: Engineering*.

[9] **G. M. Odegard and A. Bandyopadhyay**, "Physical aging of epoxy polymers and their composites," *Journal of Polymer Science, Part B: Polymer Physics*, vol. 49, no. 24, pp. 1695–1716, 2011.

[10] **B. Dao, J. Hodgkin, J. Krstina, J. Mardel, and W. Tian**, "Accelerated aging versus realistic aging in aerospace composite materials. V. The effects of hot/wet aging in a structural epoxy composite," *Journal of Applied Polymer Science*, vol. 115, no. 2, pp. 901–910, 2010.

[11] **R. S. Trask, H. R. Williams, and I. P. Bond**, "Self-healing polymer composites: mimicking nature to enhance performance.," *Bioinspiration & biomimetics*, vol. 2, no. 1, pp. 1–9, 2007.

[12] **M. R. Kessler**, "Self-healing: a new paradigm in materials design," *Proceedings of the Institution of Mechanical Engineers, Part G: Journal of Aerospace Engineering*, vol. 221, no. 4, pp. 479–495, 2007.

[13] **S. D. Bergman and F. Wudl**, "Mendable polymers," *Journal of Materials Chemistry*, vol. 18, p. 41, 2008.

[14] **J. L. Mercy and S. Prakash**, "Self Healing Composite Materials : A Review," *International Journal of ChemTech Research*, vol. 9, no. 3, pp. 316–324, 2016.

[15] **Y. C. Yuan, T. Yin, M. Z. Rong, and M. Q. Zhang**, "Self healing in polymers

and polymer composites. Concepts, realization and outlook: A review," *Express Polymer Letters*, vol. 2, no. 4, pp. 238–250, 2008.

[16] **I. L. Hia, V. Vahedi, and P. Pasbakhsh**, "Self-Healing Polymer Composites: Prospects, Challenges, and Applications," *Polymer Reviews*, vol. 56, no. 2, pp. 225–261, 2016.

[17] **M. Q. Zhang and M. Z. Rong**, *Self-healing Polymers and Polymer Composites*. John Wiley & Sons, Inc., 2011.

[18] **V. Authors**, *Self-healig Polymers: From Principles to Applications*. 2013.

[19] **V. Authors**, *Epoxy polymers*. Wiley-VCH, 2010.

[20] **D. Y. Wu, S. Meure, and D. Solomon**, "Self-healing polymeric materials: A review of recent developments," *Progress in Polymer Science*, vol. 33, no. 5, pp. 479–522, 2008.

[21] **C. E. Diesendruck, N. R. Sottos, J. S. Moore, and S. R. White**, "Biomimetic Self-Healing," *Angewandte Chemie - International Edition*, vol. 54, no. 36, pp. 10428–10447, 2015.

[22] **S. A. Hayes, F. R. Jones, K. Marshiya, and W. Zhang**, "A self-healing thermosetting composite material," *Composites Part A: Applied Science and Manufacturing*, vol. 38, no. 4, pp. 1116–1120, 2007.

[23] **S. R. White, B. J. Blaiszik, S. L. B. Kramer, S. C. Olugebefola, J. S. Moore, and N. R. Sottos**, "Self-healing polymers and composites," *American Scientist*, vol. 99, no. 5, pp. 392–399, 2011.

[24] **S. Meure, D. Y. Wu, and S. A. Furman**, "FTIR study of bonding between a thermoplastic healing agent and a mendable epoxy resin," *Vibrational Spectroscopy*, vol. 52, no. 1, pp. 10–15, 2010.

[25] **M. Zako and N. Takano**, "Intelligent material systems using epoxy particles to repair microcracks and delamination damage in GFRP," *Journal of Intelligent Material Systems and Structures*, vol. 10, pp. 836–841, 1999.

[26] **S. A. Hayes, W. Zhang, M. Branthwaite, and F. R. Jones**, "Self-healing of damage in fibre-reinforced polymer-matrix composites," *Journal of The Royal Society Interface*, vol. 4, no. 13, pp. 381–387, 2007.

[27] **W. Zhang, F. Jones, and S. Hayes**, "Self-Healing Thermosetting Epoxy Resins," in *Extras.Springer.Com*, 2007, no. April, pp. 1–6.

[28] **S. Meure, D. Y. Wu, and S. Furman**, "Polyethylene-co-methacrylic acid healing agents for mendable epoxy resins," *Acta Materialia*, vol. 57, no. 14, pp.

4312–4320, 2009.

[29] **S. Meure, S. Furman, and S. Khor**, “Poly[ethylene-co-(methacrylic acid)] healing agents for mendable carbon fiber laminates,” *Macromolecular Materials and Engineering*, vol. 295, no. 5, pp. 420–424, 2010.

[30] **S. Meure, R. J. Varley, D. Y. Wu, S. Mayo, K. Nairn, and S. Furman**, “Confirmation of the healing mechanism in a mendable EMAA-epoxy resin,” *European Polymer Journal*, vol. 48, no. 3, pp. 524–531, 2012.

[31] **X. Luo, R. Ou, D. E. Eberly, A. Singhal, W. Viratyaporn, and P. T. Mather**, “A thermoplastic/thermoset blend exhibiting thermal mending and reversible adhesion,” *ACS Applied Materials and Interfaces*, vol. 1, no. 3, pp. 612–620, 2009.

[32] **K. Pingkarawat, T. Bhat, D. A. Craze, C. H. Wang, R. J. Varley, and A. P. Mouritz**, “Healing of carbon fibre–epoxy composites using thermoplastic additives,” *Polymer Chemistry*, vol. 4, pp. 5007–5015, 2013.

[33] **R. J. Varley, D. A. Craze, A. P. Mouritz, and C. H. Wang**, “Thermoplastic healing in epoxy networks: Exploring performance and mechanism of alternative healing agents,” *Macromolecular Materials and Engineering*, vol. 298, no. 11, pp. 1232–1242, 2013.

[34] **R. P. Wool and K. M. O’Connor**, “Time Dependence of Crack Healing,” *Polymer letters edition*, vol. 20, no. 13, pp. 7–16, 1982.

[35] **A. Cohades, E. Manfredi, J.-C. Plummer, and V. Michaud**, “Thermal mending in phase-separated Poly(ε-caprolactone)/epoxy blends-SUBMITED,” *European Polymer Journal*, vol. 81, pp. 114–128, 2016.

[36] **J. Chen and F. Chang**, “Phase Separation Process in Poly (ε -caprolactone) - Epoxy Blends,” *Macromolecules*, vol. 32, no. 2, pp. 5348–5356, 1999.

[37] **K. Pingkarawat, C. H. Wang, R. J. Varley, and A. P. Mouritz**, “Self-healing of delamination fatigue cracks in carbon fibre-epoxy laminate using mendable thermoplastic,” *Journal of Materials Science*, vol. 47, no. 10, pp. 4449–4456, 2012.

[38] **K. Pingkarawat, C. H. Wang, R. J. Varley, and A. P. Mouritz**, “Mechanical properties of mendable composites containing self-healing thermoplastic agents,” *Composites Part A: Applied Science and Manufacturing*, vol. 65, pp. 10–18, 2014.

[39] **C. H. Wang, K. Sidhu, T. Yang, J. Zhang, and R. Shanks**, “Interlayer self-

healing and toughening of carbon fibre/epoxy composites using copolymer films," *Composites Part A: Applied Science and Manufacturing*, vol. 43, no. 3, pp. 512–518, 2012.

[40] **T. Yang, C. H. Wang, J. Zhang, S. He, and A. P. Mouritz**, "Toughening and self-healing of epoxy matrix laminates using mendable polymer stitching," *Composites Science and Technology*, vol. 72, no. 12, pp. 1396–1401, 2012.

[41] **R. J. Varley and F. Charve**, "EMAA as a healing agent for mendable high temperature epoxy amine thermosets," *Composites Part A: Applied Science and Manufacturing*, vol. 43, no. 7, pp. 1073–1080, 2012.

[42] **C. D. Olio, Q. Yuan, and R. J. Varley**, "Epoxy / Poly (ethylene- co - methacrylic acid) Blends as Thermally Activated Healing Agents in an Epoxy / Amine Network," *Macromolecular Materials and Engineering*, vol. 300, pp. 70–79, 2014.

[43] **V. Janarthanan and G. Thyagarajant**, "Miscibility studies in blends of poly (N-vinyl pyrrolidone) and poly (methyl methacrylate) with epoxy resin : a comparison," vol. 33, no. 17, pp. 3593–3597, 1992.

[44] **E. M. Woo and M. N. Wu**, "Blends of a diglycidylether epoxy with bisphenol-A polycarbonate or poly(methyl methacrylate): Cases of miscibility with or without specific interactions," *Polymer*, vol. 37, no. 12, pp. 2485–2492, 1996.

[45] **D. Olmos, K. Bagdi, J. Mózcó, B. Pukánszky, and J. González-Benito**, "Morphology and interphase formation in epoxy/PMMA/glass fiber composites: Effect of the molecular weight of the PMMA," *Journal of Colloid and Interface Science*, vol. 360, no. 1, pp. 289–299, 2011.

[46] "Sigma-Aldrich Product Specification: Poly(ethylene-co-vinyl acetate)." [Online]. Available: http://www.sigmaaldrich.com/Graphics/COfAInfo/SigmaSAPQM/SPEC/34/340502/340502-BULK_____ALDRICH__.pdf. [Accessed: 18-Jul-2017].

[47] "Sigma-Aldrich Product Specification: Poly(acrylonitrile-co-butadiene-co-styrene)." [Online]. Available: http://www.sigmaaldrich.com/catalog/product/aldrich/430129?lang=pt&region=BR. [Accessed: 18-Jul-2017].

[48] "Sigma-Aldrich Product Specification: Poly(styrene-block-polybutadiene-block-polystyrene)." [Online]. Available: http://www.sigmaaldrich.com/catalog/product/aldrich/432490?lang=pt&region=

BR. [Accessed: 18-Jul-2017].

[49] **A. M. Rocco, D. P. Moreira, and R. P. Pereira**, “Specific interactions in blends of poly(ethylene oxide) and poly(bisphenol A-co-epichlorohydrin): FTIR and thermal study,” *European Polymer Journal*, vol. 39, no. 9, pp. 1925–1934, 2003.

[50] “Scientific Polymer Products, INC. Material Safety Datasheet: Polycaprolactone.” [Online]. Available: http://scientificpolymer.com/wp-content/uploads/2013/12/1030.pdf. [Accessed: 26-Jul-2017].

[51] “Sigma-Aldrich Product Specification: Poly(ethylene-co-methacrylic acid).” [Online]. Available: http://www.sigmaaldrich.com/Graphics/COfAInfo/SigmaSAPQM/SPEC/42/426628/426628-BULK_____ALDRICH__.pdf. [Accessed: 18-Jul-2017].

[52] “Sigma-Aldrich Product Specification: Poly(ethylene-co-methyl acrylate).” [Online]. Available: http://www.sigmaaldrich.com/catalog/product/aldrich/430757?lang=pt&region=BR . [Accessed: 18-Jul-2017].

[53] **R. N. Santra, T. K. Chaki, S. Roy, and G. B. Nando**, “Studies on miscibility of blends of thermoplastic polyurethane and poly(ethylene-co-methyl acrylate),” vol. 213, no. 3784, pp. 7–13, 1993.

[54] “Sigma-Aldrich Product Specification: Poly(ethylene-co-glycidyl methacrylate).” [Online]. Available: http://www.sigmaaldrich.com/catalog/product/aldrich/430862?lang=pt&region=BR. [Accessed: 18-Jul-2017].

[55] “Arkema Product Specification: Lotader ® AX8900.” [Online]. Available: http://www.lotader.com/export/shared/.content/media/downloads/products-documentations/altuglas-international/pof/lotader/tds-lotader-ax8900.pdf. [Accessed: 18-Jul-2017].

[56] “Sigma-Aldrich Product Specification: Poly(ethylene-co-methyl acrylate-co-glycidyl methacrylate).” [Online]. Available: http://www.sigmaaldrich.com/Graphics/COfAInfo/SigmaSAPQM/SPEC/43/433640/433640-BULK_____ALDRICH__.pdf. [Accessed: 18-Jul-2017].

[57] “Huntsman Product Specification: Araldite MY 750, Aradur HY 2918, Acelerador DY 062.” .

[58] “Huntsman Product Specification: Araldite GY 260, Hardener XB 3473.” .

[59] **E. Duemichen *et al.***, “Analyzing the network formation and curing kinetics of epoxy resins by in situ near-infrared measurements with variable heating rates,” *Thermochimica Acta*, vol. 616, pp. 49–60, 2015.

[60] **J. K. Fink**, *Reactive Polymers Fundamentals and Applications: Epoxy Resins*. 2013.

[61] **S. K. Dogan, S. Gumus, A. Aytac, and G. Ozkoc**, “Properties of modified ethylene terpolymer/poly(lactic acid) blends based films,” *Fibers and Polymers*, vol. 14, no. 9, pp. 1422–1431, 2013.

[62] **S. T. Cholake *et al.***, “Quantitative analysis of curing mechanisms of epoxy resin by mid- and near-fourier transform infra red spectroscopy,” *Defence Science Journal*, vol. 64, no. 3, pp. 314–321, 2014.

[63] **M. González-González, J. C. Cabanelas, and J. Baselga**, “Applications of FTIR on Epoxy Resins - Identification, Monitoring the Curing Process, Phase Separation and Water Uptake,” *University Carlos III of Madrid*, vol. 2, pp. 261–284, 2012.

[64] **S. R. Brownlow, A. P. Moravsky, N. G. Kalugin, and B. S. Majumdar**, “Probing deformation of double-walled carbon nanotube (DWNT)/epoxy composites using FTIR and Raman techniques,” *Composites Science and Technology*, vol. 70, no. 10, pp. 1460–1468, 2010.

[65] **V. Ollier-Dureault and B. Gosse**, “Photooxidation of anhydride-cured epoxies: FTIR study of the modifications of the chemical structure,” *Journal of applied polymer*, vol. 70, pp. 1221–1287, 1998.

[66] **X. Fernández-Francos, A. Rybak, R. Sekula, X. Ramis, and A. Serra**, “Modification of epoxy-anhydride thermosets using a hyperbranched poly(ester-amide): I. Kinetic study,” *Polymer International*, vol. 61, no. 12, pp. 1710–1725, 2012.

[67] **J. Mijovic and J. Wijaya**, “Etherification reaction in epoxy-amine systems at high temperature,” *Polymer*, vol. 35, no. 12, pp. 2683–2686, 1994.

[68] **The McGraw-Hill Companies**, “Chapter 20: Carboxylic Acid Derivatives. Nucleophilic Acyl Substitution,” *Organic Chemistry 4e Carey - Online Learning Center*, 2000. [Online]. Available: http://www.mhhe.com/physsci/chemistry/carey/student/olc/ch20reactionsesters.html. [Accessed: 15-Apr-2017].

[69] **A. Motahari, A. Omrani, A. A. Rostami, and M. Ehsani**, “Preparation and

characterization of a novel epoxy based nanocomposite using tryptophan as an eco-friendly curing agent," *Thermochimica Acta*, vol. 574, pp. 38–46, 2013.

[70] **A. Bouzidi, K. Omri, L. El Mir, and H. Guermazi**, "Preparation, structural and optical investigations of ITO nanopowder and ITO/epoxy nanocomposites," *Materials Science in Semiconductor Processing*, vol. 39, pp. 536–543, 2015.